2023 Fall

"Phase Transformation *in* Materials"

10.09.2023

Eun Soo Park

Office: 33-313
Telephone: 880-7221
Email: espark@snu.ac.kr
Office hours: by an appointment

Contents for today's class

- **Atomic Mobility** $D_B = M_B RTF$

Thermodynamic factor

$$F = (1 + \frac{d \ln \gamma_B}{d \ln X_B})$$

- **Tracer Diffusion in Binary Alloys** $\tilde{D} = X_B D_A + X_A D_B = F(X_B D_A^* + X_A D_B^*)$

D*$_{Au}$ gives the rate at which Au* (or Au) atoms diffuse in a **chemically homogeneous** alloy, whereas **D$_{Au}$** gives the diffusion rate of Au when **concentration gradient** is present.

- **High-Diffusivity Paths** $D_s > D_b > D_l \iff A_l > A_b > A_S$

    1. Diffusion along Grain Boundaries and Free Surface

    Grain boundary diffusion makes a significant contribution $D_{app} = D_l + D_b \frac{\delta}{d}$

    only when D$_b$δ > D$_l$d.   (*T* < 0.75~0.8 *T*$_m$)

    2. Diffusion Along Dislocation

    At low temperatures, (*T* < ~0.5 *T*$_m$)
    gD$_p$/D$_l$ can become so large that the apparent diffusivity is entirely due to diffusion along dislocation.

- **Diffusion in Multiphase Binary Systems**

$$v = \frac{dx}{dt} = \frac{1}{(C_B^\beta - C_B^\alpha)} \{\tilde{D}(\alpha)\frac{\partial C_B^\alpha}{\partial x} - \tilde{D}(\beta)\frac{\partial C_B^\beta}{\partial x}\}$$ (velocity of the α/β interface)

2

Q: What conditions high-diffusivity paths' (grain boundary, dislocation) diffusion is important?

$$D_s > D_b > D_l \quad \Longleftrightarrow \quad A_l > A_b > A_S$$

1. Diffusion along Grain Boundaries and Free Surface

Grain boundary diffusion makes a significant contribution

only when $D_b\delta > D_l d.$ ($T < 0.75\sim0.8\ T_m$)

$$D_{app} = D_l + D_b \frac{\delta}{d}$$

2. Diffusion Along Dislocation

At low temperatures, ($T < \sim0.5\ T_m$)
gD_p/D_l can become so large that the apparent diffusivity is entirely due to diffusion along dislocation.
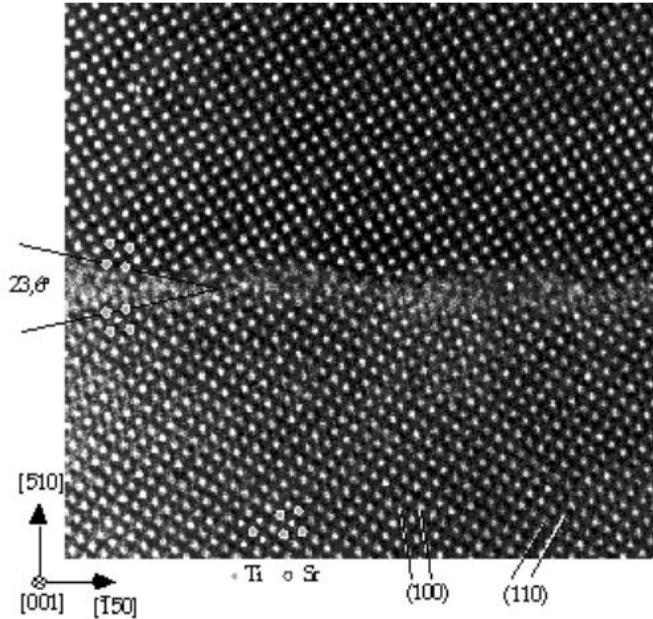
3

2.7. High-diffusivity paths
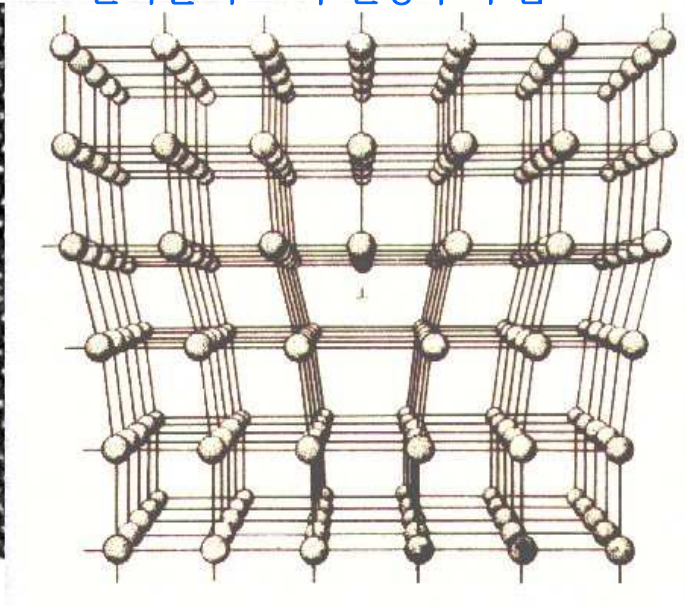
Real materials contain <u>**defects.**</u>
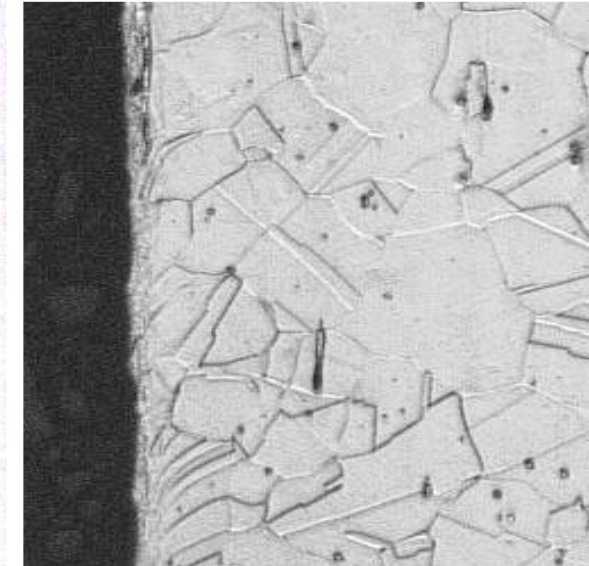
= **more open structure** ⟹ **fast diffusion path.**

원자들의 도약 진동수가 큼   확산의 주요한 행로

Grain boundary   **dislocation**   **surface**

Diff. along lattice

$$D_l = D_{lo} \exp(-\frac{Q_l}{RT})$$

$$\boxed{D_s > D_b > D_l}$$ Diff. along grain boundary

$$D_b = D_{bo} \exp(-\frac{Q_b}{RT})$$

Diff. along free surface

$$D_s = D_{so} \exp(-\frac{Q_s}{RT})$$

**But area fraction → *lattice* > *grain boundary* > *surface***   **4**

2.7.1 Diffusion along grain boundaries

Atoms diffusing along the boundary will be able to penetrate much deeper than atoms which only diffuse through the lattice.

In addition, as the concentration of solute builds up in the boundaries, atoms will also diffuse from the boundary into the lattice.

Metal A   Metal B

Weld interface

dx
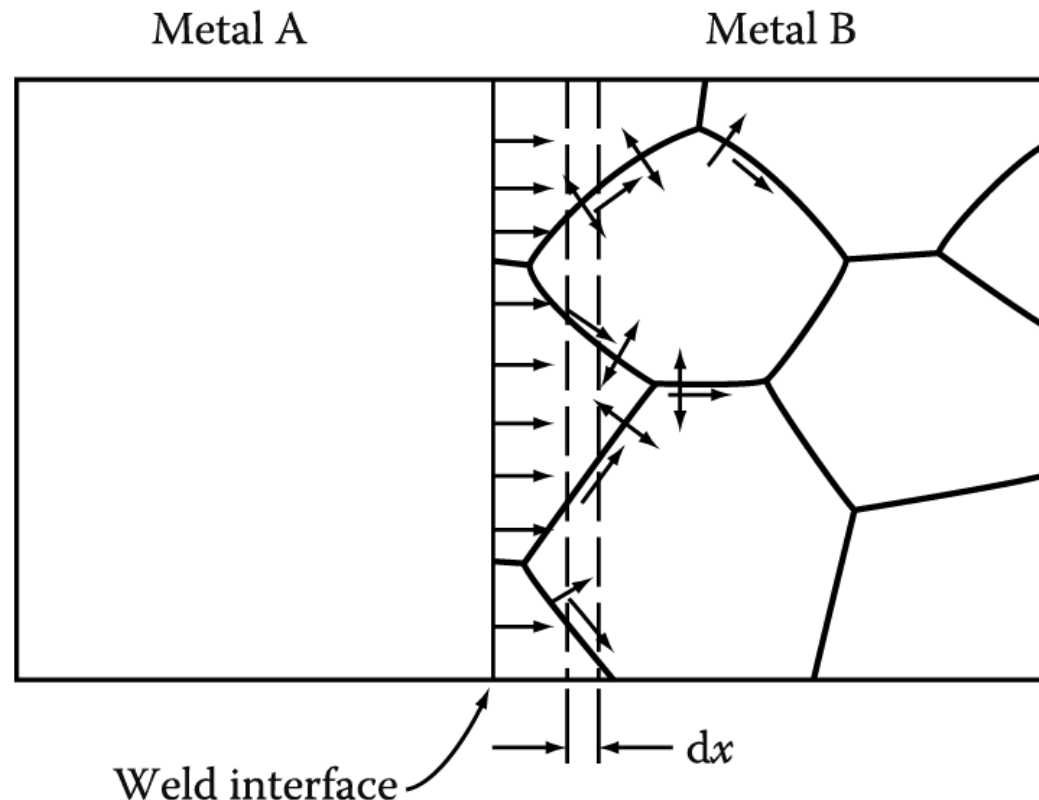
Composite between plastic matrix and a continuous network of Al sheets

* The effect of grain boundary diffusion combined with volume diffusion.

: Rapid diffusion along the grain boundaries
→ increase in the apparent diffusivity in the materials as a whole

5

2.7.1 Diffusion along grain boundaries

$$D_l = D_{lo} \exp(-\frac{Q_l}{RT})$$ **VS** $$D_b = D_{bo} \exp(-\frac{Q_b}{RT})$$

more open structure $Q_b \sim \tfrac{1}{2} Q_l$

TABLE 2.3

Crystal Structure	$D_{b0}\,\mathrm{mm^2\ s^{-1}}$	Q_b'/RT_m
Fcc	18.9	10.0
Bcc	670	11.7
Hcp	54.8	10.8

$\dfrac{Q_l}{RT} \sim$ **18** in fcc and hcp metals

Temperature dependence

1) $D_{liq} \approx D_b \ near\ T_m$

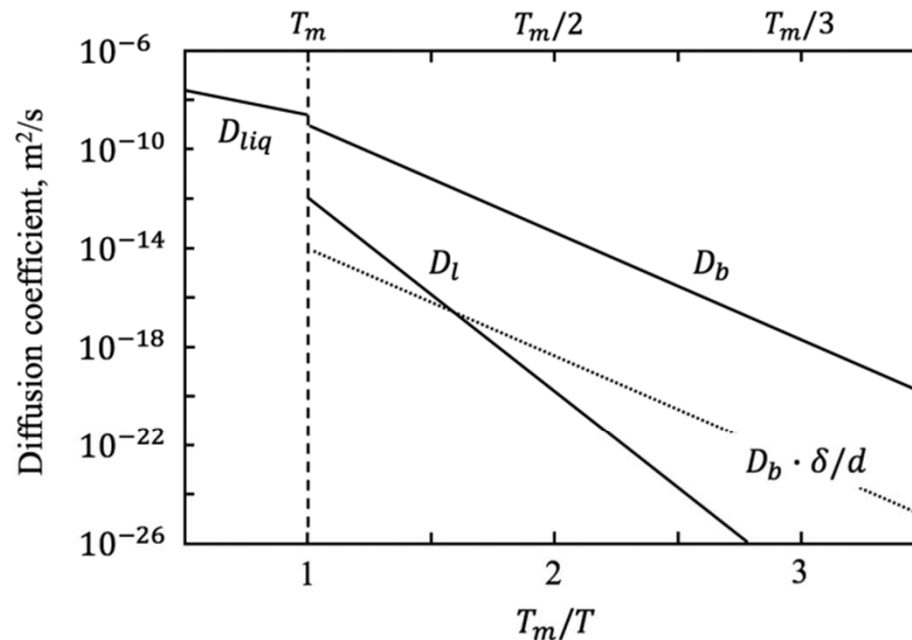2) With decreasing T ,

D_l/D_b ↓

FIGURE 2.25 Temperature dependence of typical lattice and grain boundary self-diffusion coefficients for fcc metals. T_m is the melting temperature. (Based on data in A.M. Brown and M.F. Ashby, *Acta Metall.*, **28**:1085 (1980) assuming grain boundary thickness, $\delta = 0.5\,\mathrm{nm}$. Dotted line drawn for $d = 50\,\mu m$. Data for diffusion in the liquid is from N.A. Gjostein, Diffusion, Amer. Soc. Metals, Metals Park, OH, p. 241 (1974).)

6

2.7.1 Diffusion along grain boundaries

Impurities and solutes in dilute solid solution tend to segregate to grain boundaries

1) at equilibrium, the mole fraction of solute in the solute on the boundary, X_S^b, is greater than the mole fraction in the adjacent α grain, X_S^α
$$(X_S^b > X_S^\alpha)$$

2) As the temperature decreases, the ratio X_S^b / X_S^α increases.

⇒ Segregation (concentration gradient)

Segregation ratio, s, $s = C_b / C_{l(b)}$

in terms of concentrations expressed as amounts per unit volume.
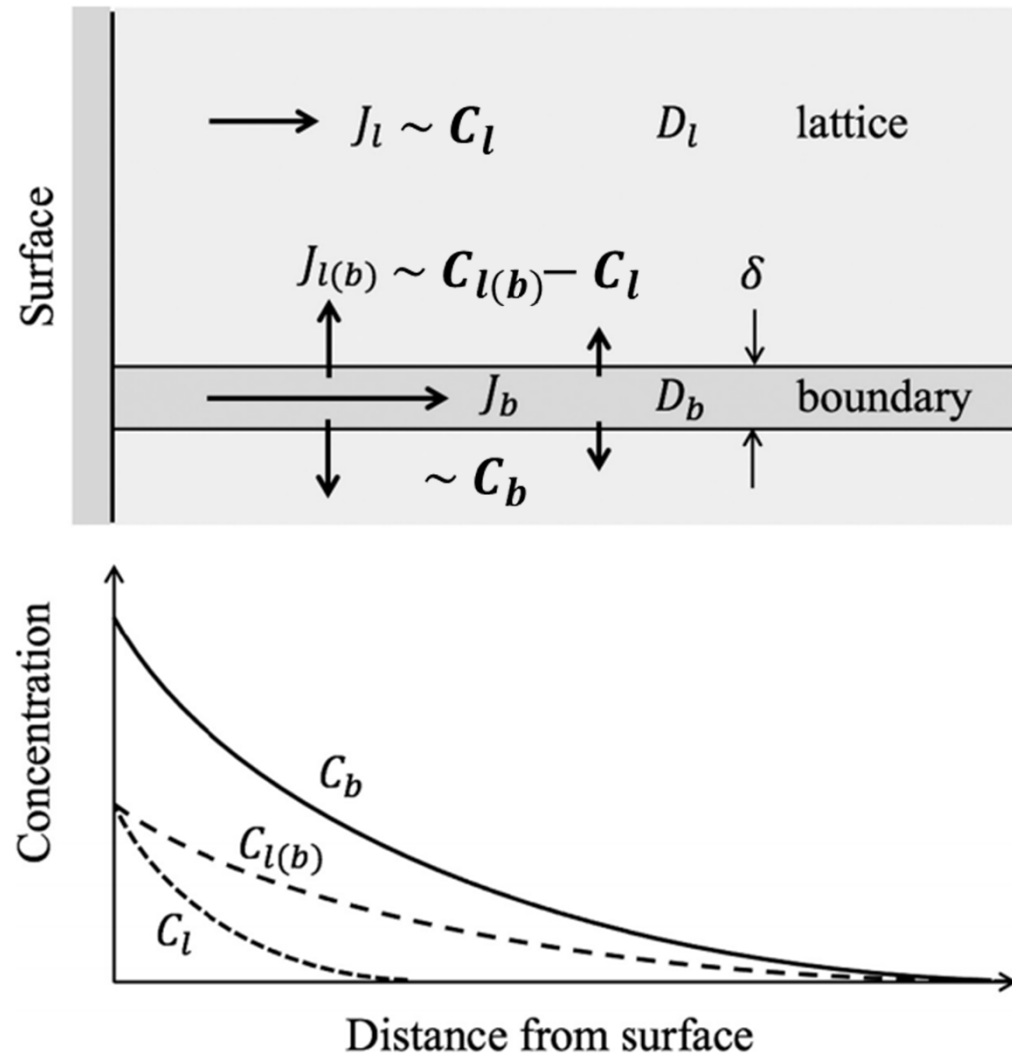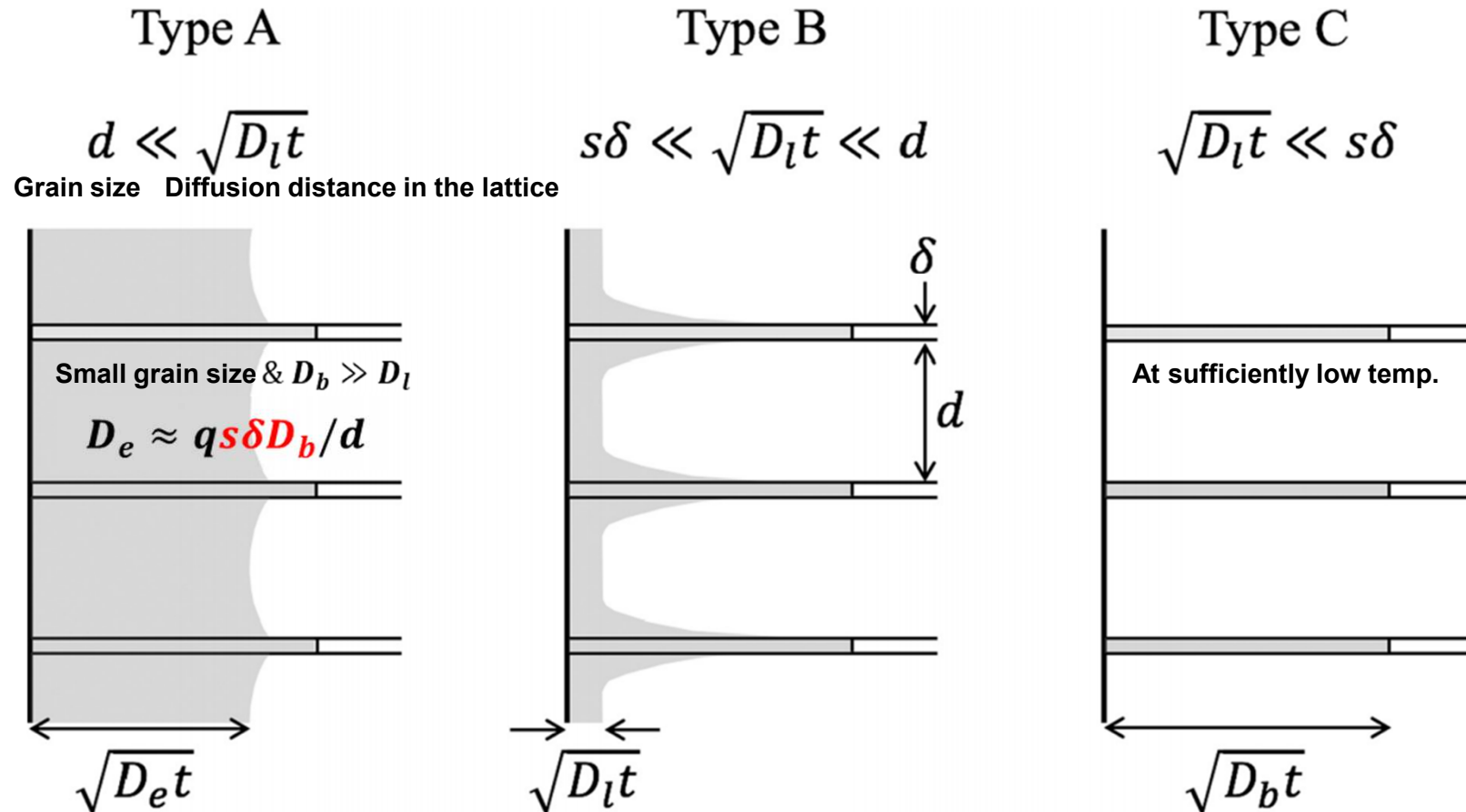
In the case of self − diffusion, $S = 1$

FIGURE 2.26 Model for diffusion of a surface deposit into a metal or alloy through the grain and along a grain boundary. Grain boundary considered to be a film of thickness δ in which the diffusion coefficient is D_b. Line C_b shows the concentration of the diffusing species in the boundary, line $C_{l(b)}$ the concentration in the lattice adjacent to the boundary, and C_l the concentration in the lattice far from the boundary. $C_b / C_l = s$, the segregation factor.

2.7.1 Diffusion along grain boundaries

FIGURE 2.27 Types of grain boundary vs. lattice diffusion kinetics.

depending on grain size, temperature and segregation factor

Type A	Type B	Type C
$d \ll \sqrt{D_l t}$	$s\delta \ll \sqrt{D_l t} \ll d$	$\sqrt{D_l t} \ll s\delta$

Grain size   Diffusion distance in the lattice

Type A: Small grain size & $D_b \gg D_l$

$$D_e \approx q s\delta D_b / d$$

$\sqrt{D_e t}$

Type B: δ, d

$\sqrt{D_l t}$

Type C: At sufficiently low temp.

$\sqrt{D_b t}$

Poly crystalline metal behaves macroscopically like a single crystal having an effective diffusion coefficient equal to the weighted average of the boundary and lattice diffusivities:

$$D_e = sfD_b + (1 - sf)D_l$$

f: volume fraction of GB $= q\delta / d$

q: geometrical factor related to grain shape

Leakage from the grain boundaries only affects a very small fraction of the grain volume. The effects of lattice diffusion are limited to the near-surface region.

Diffusion distance in the lattice can be so small that leakage from the GB is essentially nonexistent. The GB phase is effectively isolated from the adjacent lattice.

8

2.7.1 Diffusion along grain boundaries

$D_e \approx qs\delta D_b / d \rightarrow$ when $s = 1$ (self-diffusion), δD_b can be obtained from 3 different conditions.

For impurity diffusion, $S > 1$ and, like D_b itself, it also varies exponentially with Temp. Usually, the temp dependence of S will be unknown, which makes it impossible to determine D_b for impurity diffusion from experiments in the A and B regimes alone. But, measurement at various temp in the C regime allow the determination of $\delta D_b \rightarrow$ extrapolation $\rightarrow$ temp dependence of S

S varies over the range ~2-1000 as the temperature decreases over the range studied (see Excercise 2.11).
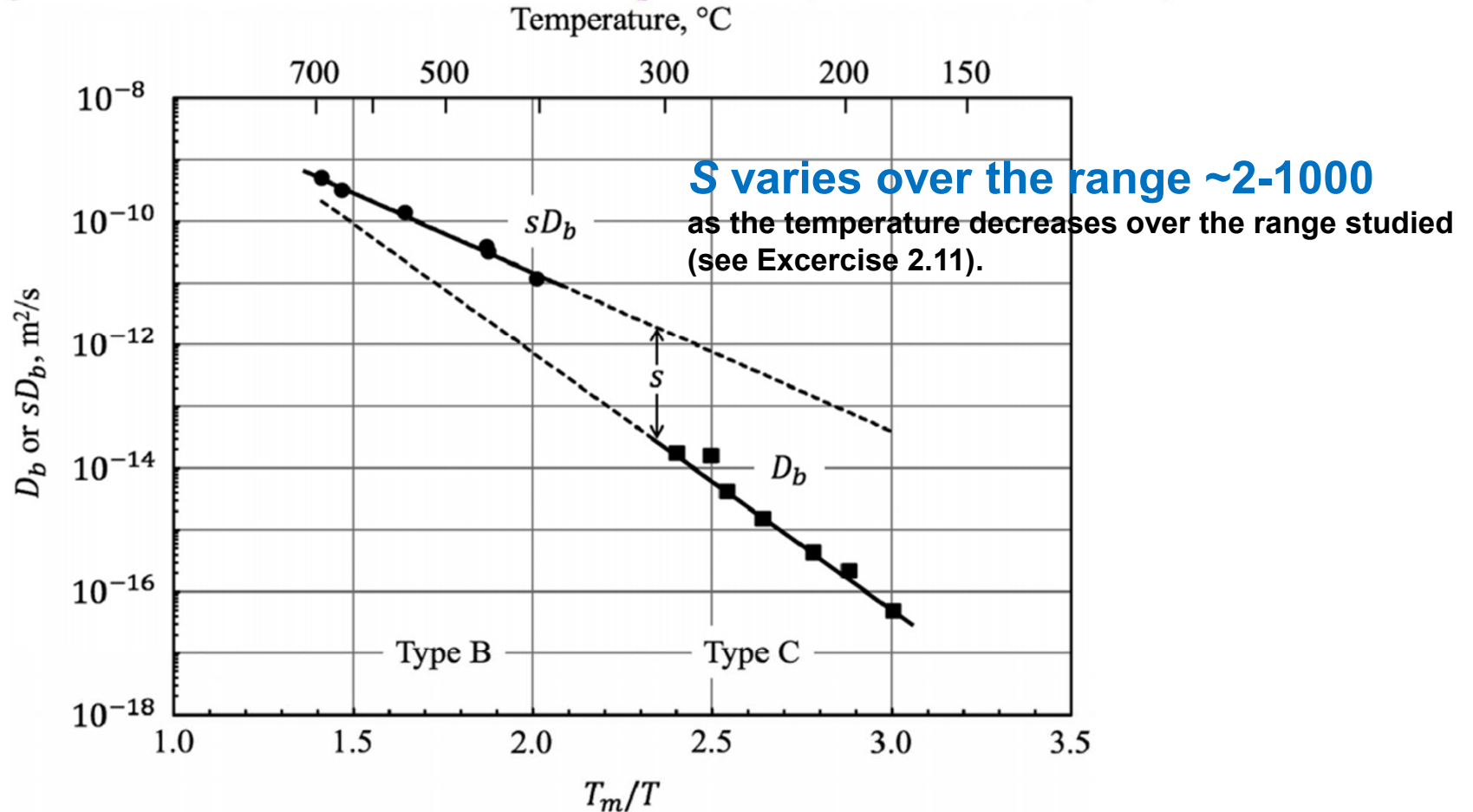
FIGURE 2.28 Results of tracer impurity diffusion of silver in copper grain boundaries assuming $\delta = 0.5$ nm. $T_m = 1085°C$ (1358 K). (Data from tables in S. V. Divinski, M. Lohmann and Chr. Herzig: *Acta Mater.* **49**:249–261 (2001).)

9

Combined diffusion of grain boundary and lattice
: What conditions grain boundary diffusion is important?

Assumption: GBs are perpendicular tot the sheet, steady-state diffusion, Concentration gradients in the lattice and along the GB are identical,
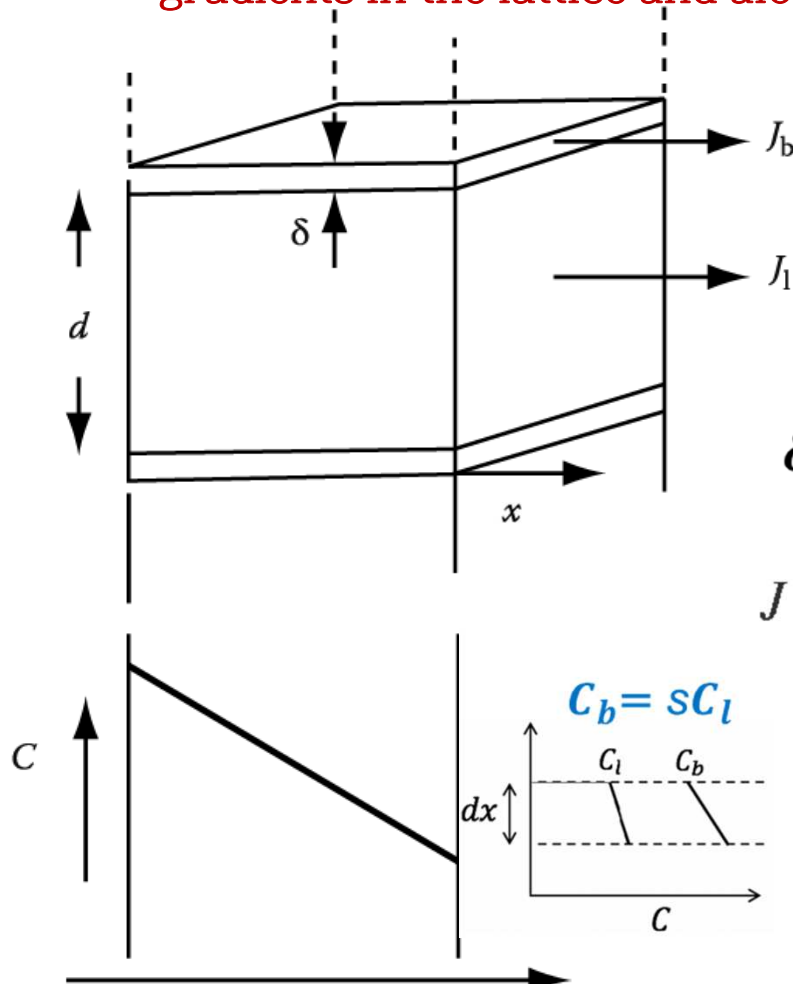
$$J_l = -D_l \frac{dC_l}{dx}$$

$$J_b = -D_b \frac{dC_b}{dx} = -sD_b \frac{dC_l}{dx}$$

$\delta \ll d \rightarrow \delta + d \approx d$ & for unit depth,

$$J = (J_b \delta \cdot 1 + J_l d \cdot 1)/(d + \delta) \approx -\left(\frac{sD_b\delta + D_l d}{d}\right)\frac{dC_l}{dx}$$

$$C_b = sC_l$$

$$D_{app} = D_l + sD_b\delta/d \quad \text{or} \quad \frac{D_{app}}{D_l} = 1 + \frac{sD_b\delta}{D_l d}$$

δ : grain boundary thickness ≈ 0.5nm

d : grain size

D_{app} : apparant diffusivity

Thus, grain boundary diffusion makes a significant contribution only when $sD_b\delta > D_l d$.

Fig. 2.29 Combined lattice and boundary fluxes during steady-state diffusion through a thin slab of material.

The relative magnitudes of $sD_b\delta$ and D_ld are most sensitive to temperature.

$$D_b = D_{bo}\exp(-\frac{Q_b}{RT}) \quad D_l = D_{lo}\exp(-\frac{Q_l}{RT})$$

Decreasing temperature →

$-Q/2.3R$

$sD_{b'}$

($T < 0.75\sim0.8\ T_m$)

D_{app}

$sD_b(\delta/d)$

D_l

$\log D$

$1/T$

Fig. 2.27 Diffusion in a polycrystalline metal.

GB diffusion is dominant increases a sδ/d increases.
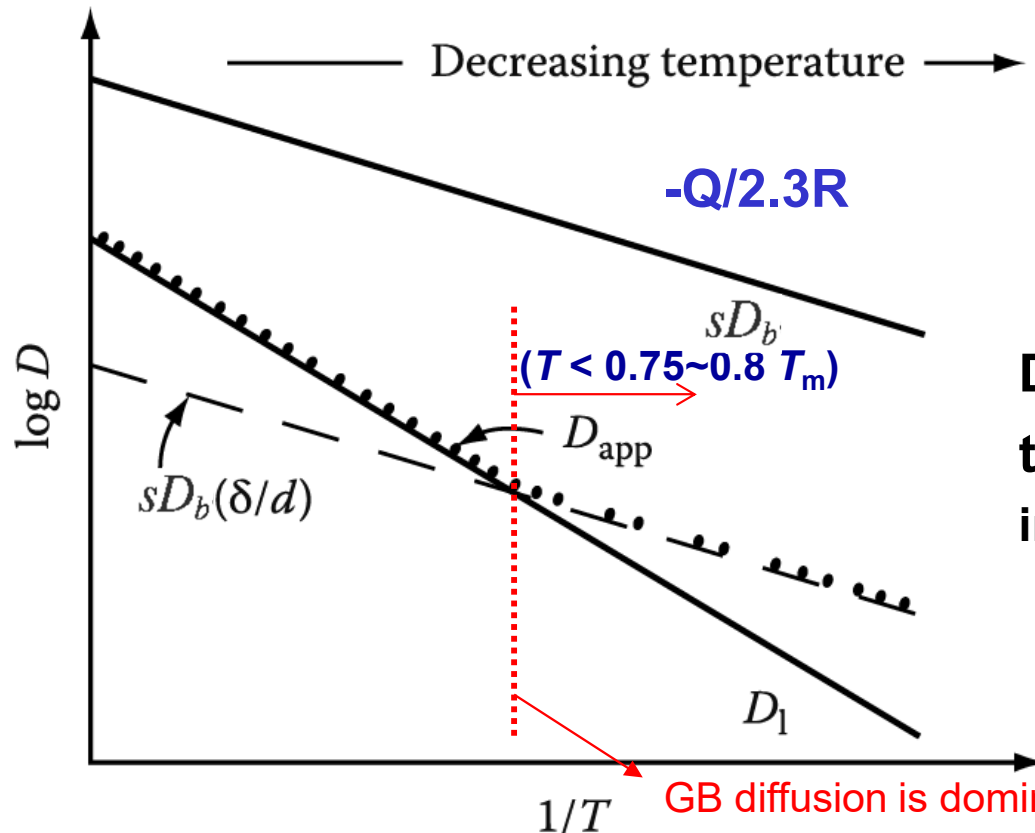
$D_b > D_l$ at all temp.

Due to $Q_b < Q_l$, ($Q_b = 0.5Q_l$)
the curves for D_l and $sD_b\delta/d$ cross
in the coordinate system of ln$D$ versus 1/T.

➡ **Therefore, the grain boundary diffusion becomes predominant at temperatures lower than the crossing temperature.**

($T < 0.75\sim0.8\ T_m$)

The diffusion rate depends on the atomic structure of the individual boundary = orientation of the adjoining crystals and the plane of the boundary. Also, the diffusion coefficient can vary with direction within a given boundary plane.

11

The dotted line in the following Figure indicates that for self-diffusion (s=1) in an fcc metal with a grain size of 50 μm (=$10^5\delta$) this would be the case below about 0.6 T_m).
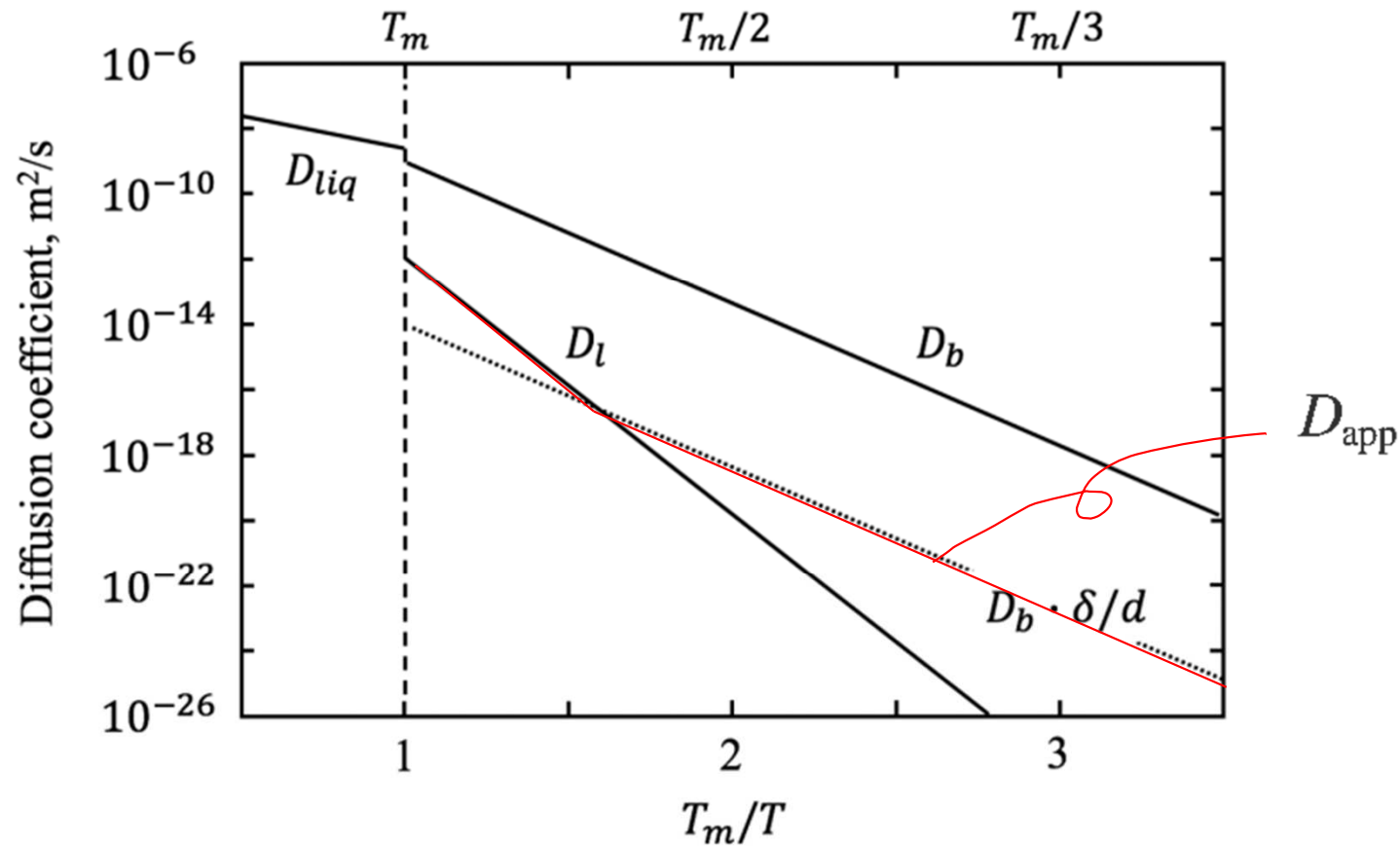

FIGURE 2.25 Temperature dependence of typical lattice and grain boundary self-diffusion coefficients for fcc metals. T_m is the melting temperature. (Based on data in A.M. Brown and M.F. Ashby, *Acta Metall.*, **28**:1085 (1980) assuming grain boundary thickness, $\delta = 0.5$ nm. Dotted line drawn for $d = 50$ μm. Data for diffusion in the liquid is from N.A. Gjostein, Diffusion, Amer. Soc. Metals, Metals Park, OH, p. 241 (1974).)

2.7.2 Diffusion along dislocations

Total area of
pipe = g per unit area
of lattice

D_p

D_l

Dislocation
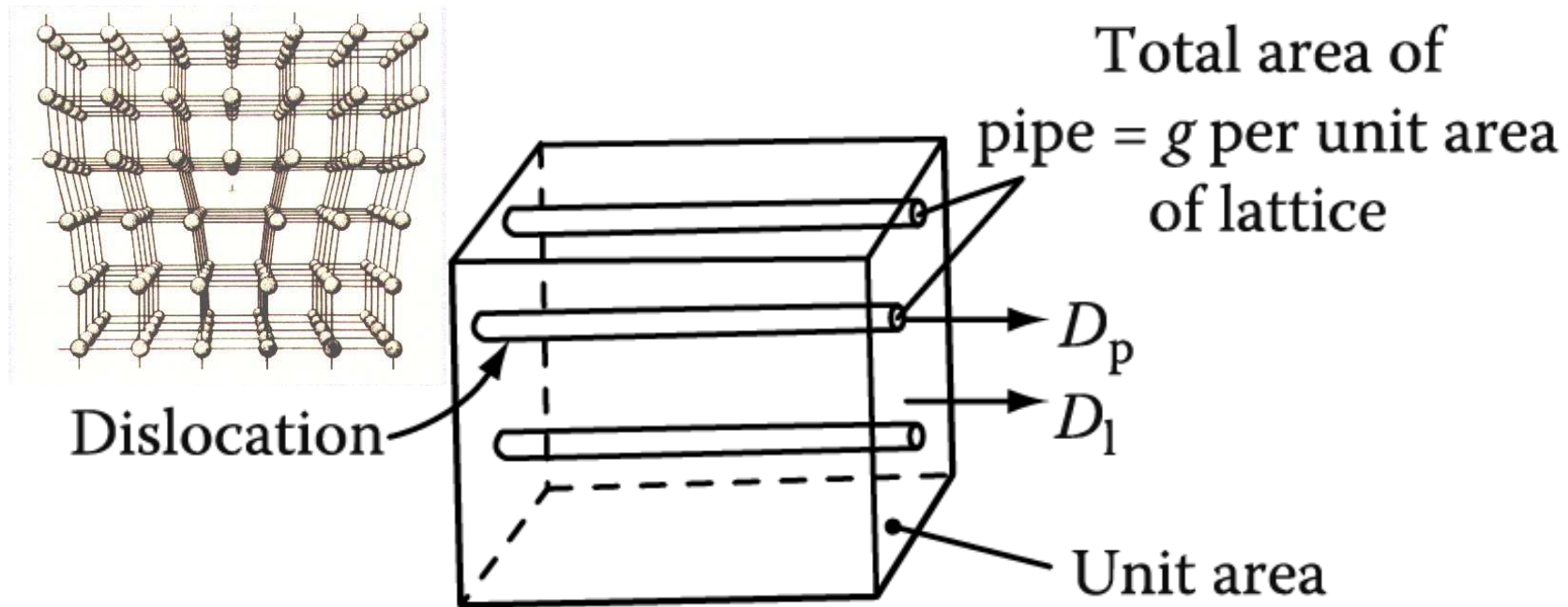
Unit area

Composite between plastic matrix and Al wires

Fig. 2.30. Dislocations act as a high conductivity path through the lattice.

D_{app} = ?   hint) 'g' is the cross-sectional area of 'pipe' per unit area of matrix.

파이프와 기지의 횡단면적

$$D_{app} = D_l + g \cdot D_p$$ ➡ $$\frac{D_{app}}{D_l} = 1 + g \cdot \frac{D_p}{D_l}$$

ex) annealed metal ~ 10^5 disl/mm^2; one dislocation($\perp$) accommodates 10 atoms in the cross-section; matrix contains 10^{13} atoms/mm^2.

$$g = \frac{10^5 * 10}{10^{13}} = \frac{10^6}{10^{13}} = 10^{-7}$$

g = cross-sectional area of 'pipe' per unit area of matrix

At high temperatures,
diffusion through the lattice is rapid and gD_p/D_l is very small
so that the dislocation contribution to the total flux of atoms is very small.

Due to $Q_p < Q_l$,
the curves for D_l and gD_p/D_l cross in the coordinate system of lnD versus 1/T.

At low temperatures, **($T < \sim 0.5\ T_m$)**
gD_p/D_l can become so large that the apparent diffusivity is entirely
due to diffusion along dislocation.

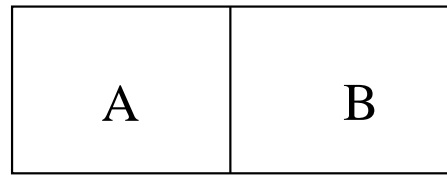**Q: How can we formulate the interface (α/β, β/γ) velocity in multiphase binary systems?**

$$v = \frac{dx}{dt} = \frac{1}{(C_B^\beta - C_B^\alpha)}\{\tilde{D}(\alpha)\frac{\partial C_B^\alpha}{\partial x} - \tilde{D}(\beta)\frac{\partial C_B^\beta}{\partial x}\}$$

(velocity of the α/β interface)
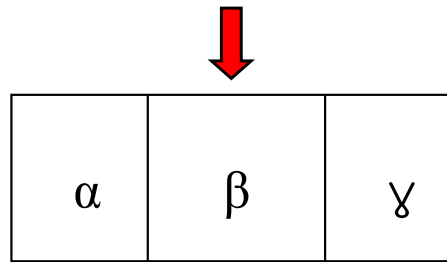
2.8 Diffusion in multiphase binary systems (다상 2원계의 확산)
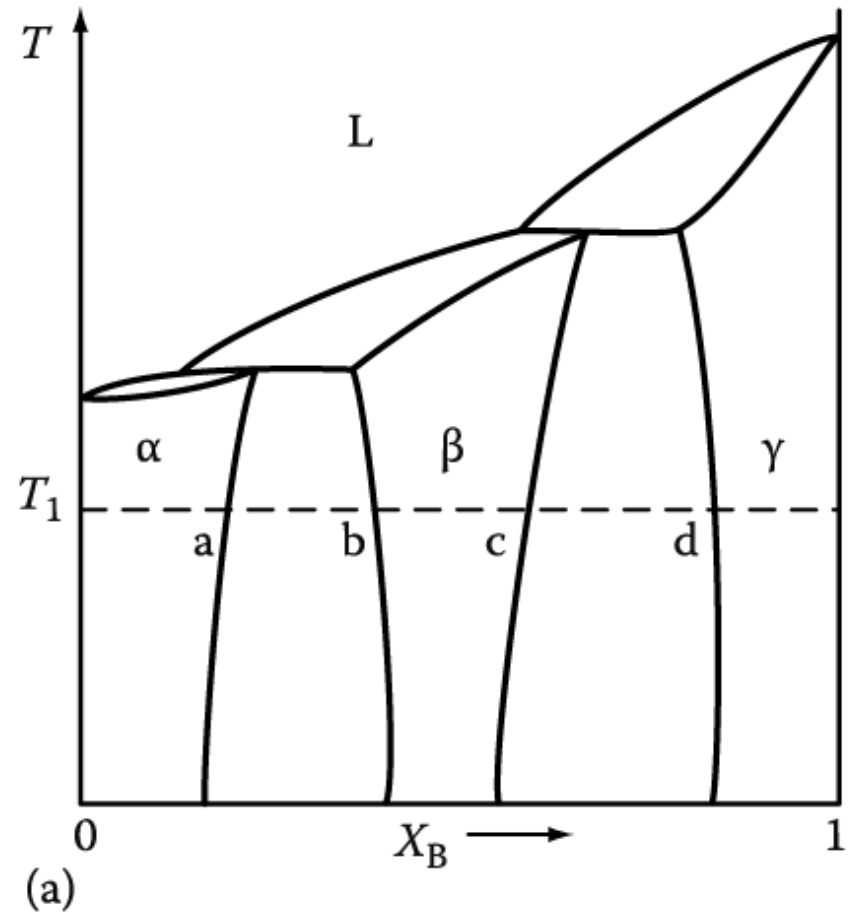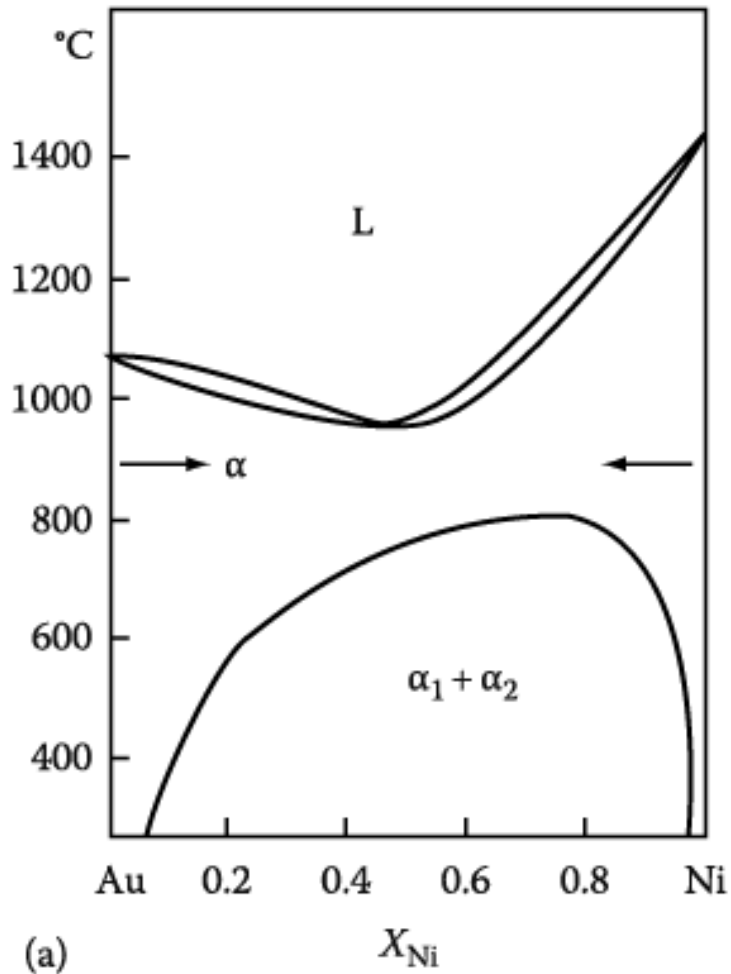
2.8 Diffusion in multiple binary system

A diffusion couple made by welding together pure A and pure B

What would be the microstructure evolved after annealing at T_1 ?

→ **a layered structure**

  containing α, β & γ.

Draw a phase distribution and composition profile in the plot of distance vs. X_B after annealing at T_1.
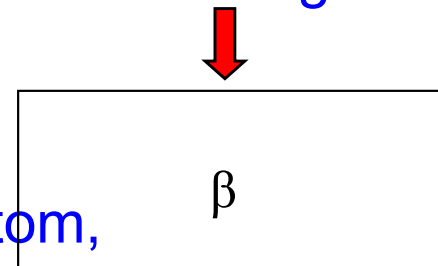
Draw a profile of activity of B atom, in the plot of distance vs. a_B after annealing at T_1.

A or B atom → easy to jump interface (local equil.)

→ $\mu_A{}^{\alpha} = \mu_A{}^{\beta}, \; \mu_A{}^{\beta} = \mu_A{}^{\gamma}$ at interface

  $(a_A{}^{\alpha} = a_A{}^{\beta}, \; a_A{}^{\beta} = a_A{}^{\gamma})$
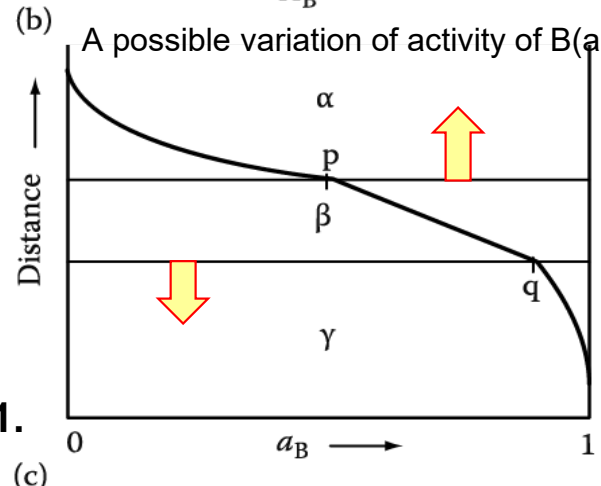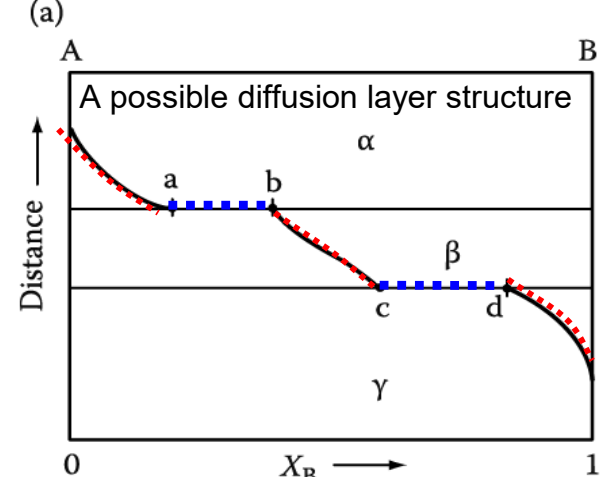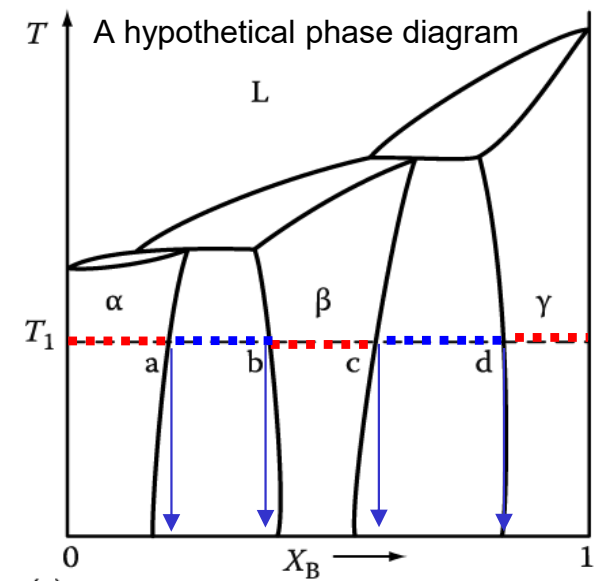
Fig. 2.31.

(a) A hypothetical phase diagram

(b) A possible diffusion layer structure

(c) A possible variation of activity of B(a_B)

How can we formulate the interface (α/β, β/γ) velocity?

If unit area of the interface moves a distance dx,
a volume (dx·1) will be converted
from α containing C_B^α atoms/m³
to β containing C_B^β atoms/m³.

$C_B^\alpha \ < \ C_B^\beta$

$\left(C_B^\beta - C_B^\alpha\right)dx \rightarrow shaded\ area$

$\alpha \rightarrow \beta$ transformation

$\left(C_B^\beta - C_B^\alpha\right)dx\ equal\ to$
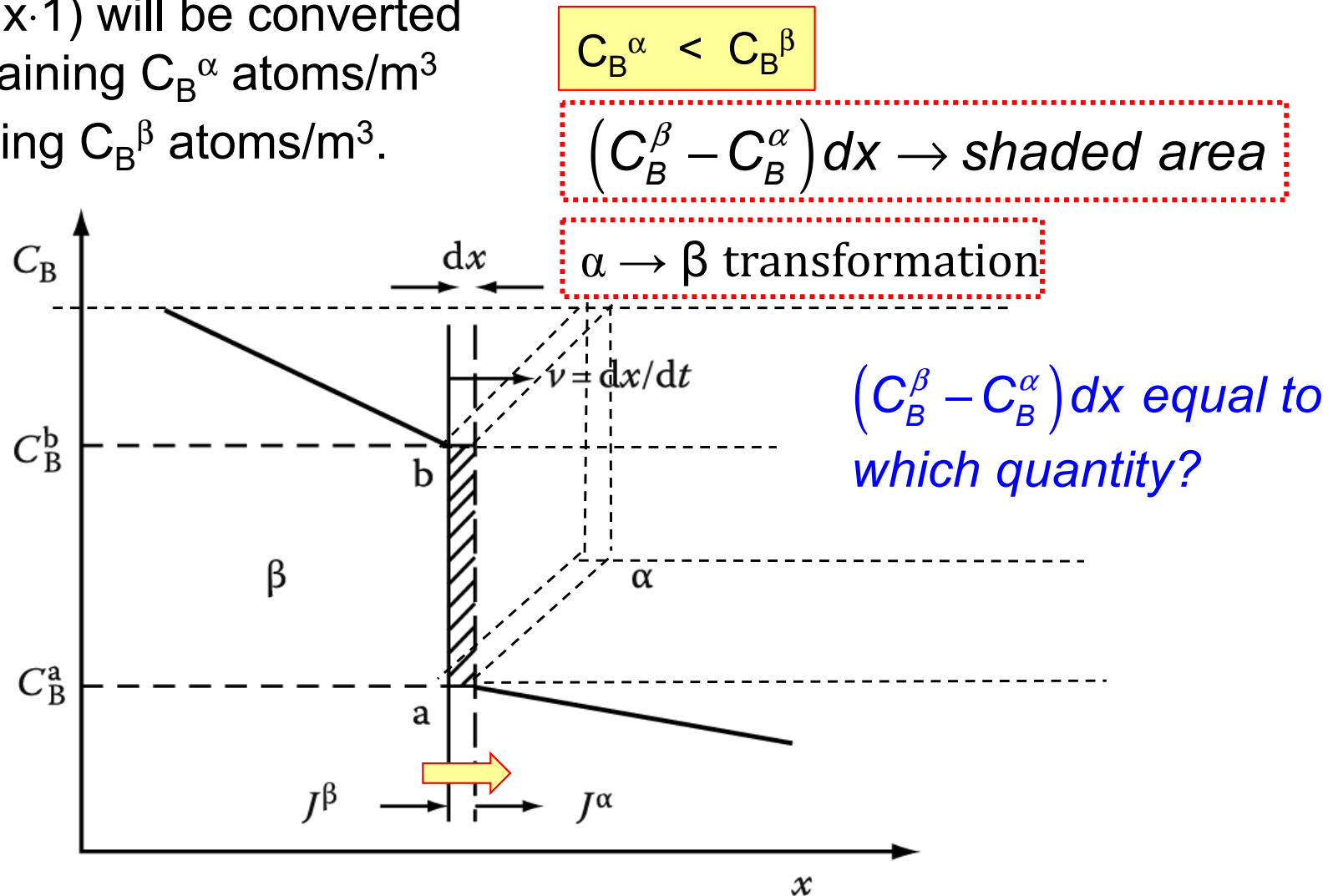$which\ quantity?$

Fig. 2.32. Concentration profile across the α/β interface and its associated movement assuming diffusion control.

18

Local equilibrium is assumed.

a flux of B towards the interface from the β phase

$$J_B^{\beta} = -\tilde{D}(\beta)\frac{\partial C_B^{\beta}}{\partial x}$$

a flux of B away from the interface into the α phase

$$J_B^{\alpha} = -\tilde{D}(\alpha)\frac{\partial C_B^{\alpha}}{\partial x}$$

In a time dt, there will be an accumulation of B atoms given by

$$\frac{\partial C}{\partial t} = -D\frac{\partial^2 C}{\partial x^2}$$
$\Rightarrow$
$$\frac{\partial C}{\partial t} = -\frac{\partial J}{\partial x}$$

$- [J_B - J_A]\, dt$

$dCdx$

$$\left\{ -\left(\tilde{D}(\beta)\frac{\partial C_B^b}{\partial x}\right) - \left(-\tilde{D}(\alpha)\frac{\partial C_B^a}{\partial x}\right) \right\} dt = (C_B^b - C_B^a)dx$$

Accumulation of B atoms during dt

$$v = \frac{dx}{dt} = \frac{1}{(C_B^b - C_B^a)}\left\{ \tilde{D}(\alpha)\frac{\partial C_B^a}{\partial x} - \tilde{D}(\beta)\frac{\partial C_B^b}{\partial x} \right\}$$

(velocity of the α/β interface)

19

Contents for today's class

- **Atomic Mobility** $\boxed{\boxed{D_B} = \boxed{M_B} RTF}$

$$F = (1 + \frac{d \ln \gamma_B}{d \ln X_B})$$

- **Tracer Diffusion in Binary Alloys** $\tilde{D} = X_B D_A + X_A D_B = F\left(X_B D_A^* + X_A D_B^*\right)$

 D*$_{Au}$ gives the rate at which **Au*** (or Au) atoms diffuse in a **chemically homogeneous** alloy, whereas **D$_{Au}$** gives the diffusion rate of Au when **concentration gradient** is present.

- **High-Diffusivity Paths** $\quad D_s > D_b > D_l \quad \Longleftrightarrow \quad A_l > A_b > A_S$

 1. Diffusion along Grain Boundaries and Free Surface

 Grain boundary diffusion makes a significant contribution

 $$D_{app} = D_l + sD_b \frac{\delta}{d}$$

 only when D$_b$δ > D$_l$d. ($T < 0.75 \sim 0.8\ T_m$)

 2. Diffusion Along Dislocation

 At low temperatures, ($T < \sim0.5\ T_m$)
 gD$_p$/D$_l$ can become so large that the apparent diffusivity is entirely due to diffusion along dislocation.

- **Diffusion in Multiphase Binary Systems**

$$v = \frac{dx}{dt} = \frac{1}{(C_B^\beta - C_B^\alpha)}\{\tilde{D}(\alpha)\frac{\partial C_B^\alpha}{\partial x} - \tilde{D}(\beta)\frac{\partial C_B^\beta}{\partial x}\}$$ **(velocity of the α/β interface)**

* Homework 2 : Exercises 2 (pages 108-111)

until 18th Ooctober, 2023

Contents in Phase Transformation

Background to understand phase transformation

(Ch1) Thermodynamics and Phase Diagrams

(Ch2) Diffusion: Kinetics

(Ch3) Crystal Interface and Microstructure

Representative Phase transformation

(Ch4) Solidification: Liquid → Solid

(Ch5) Diffusional Transformations in Solid: Solid → Solid

(Ch6) Diffusionless Transformations: Solid → Solid

Contents for today's class

Chapter 3 Crystal Interfaces and Microstructure

1) **Interfacial Free Energy**

2) **Solid/Vapor Interfaces**

3) **Solid/Liquid Interfaces**

4) Boundaries in Single-Phase Solids

5) Interphase Interfaces in Solid (α/β)

6) Interface migration

Q: Types of interface in metallic system?

• Types of Interface

Basically, three different types of interface are important in metallic system:

1. Free surface (solid/vapor interface)

vapor

solid
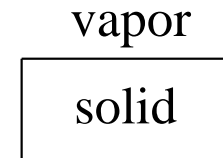
: Important in vaporization and condensation transformations

2. Grain boundary (α/ α interfaces)

> **same composition, same crystal structure**

> **different orientation**

: Important in recrystallization, i.e. the transformation of a highly deformed grain structure into new undeformed grains, and following grain coarsening and grain growth

3. inter-phase boundary (α/β interfaces) : "Important role in determining the kinetics of phase transformation/ complex"

> **different composition & crystal structure**

α

β
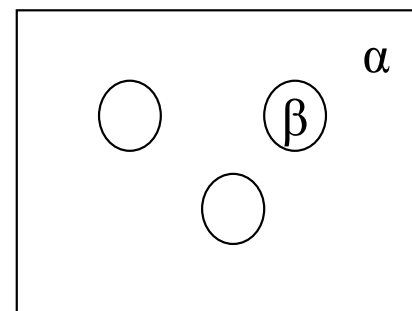
$\Longrightarrow$ defect
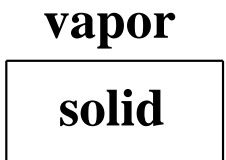
$\Longrightarrow$ energy ↑

→ First, consider simple interfaces, (1) and (2) in this chapter

Q: Interfacial free energy, γ vs Surface tension, F?

3.1. Interfacial free energy

Interfacial energy (γ : J/m^2)

→ **Gibbs free energy of a system containing an interface of area A**

→ $G_{bulk} + G_{interface}$

vapor

solid

→ $G = G_0 + \boxed{\gamma\,A}$ (excess free E arising from the fact that some material lies in or close to the interface)

3.1. Interfacial free energy

Interfacial energy (γ : J/m^2)

$\rightarrow$ **Gibbs free energy of a system containing an interface of area A**

$\rightarrow$ **$G_{bulk} + G_{interface}$**

vapor
solid

$\rightarrow$ **$G = G_0 + \gamma A$** (excess free E arising from the fact that some material lies in or close to the interface)

Interfacial energy (γ) vs. surface tension (F: a force per unit length)

1) work done : F dA = dG

2) dG = γ dA + A dγ

$\rightarrow$ **F = γ + A dγ /dA**

In case of a liq. film, dγ /dA = 0, F = γ (N/m = J/m^2)

Ex) liq. : dγ /dA = 0 *Why?* **Maintain a constant surface structure by rearrangement**
(independent of A)

sol. : dγ /dA $\neq$ 0, but, very small value
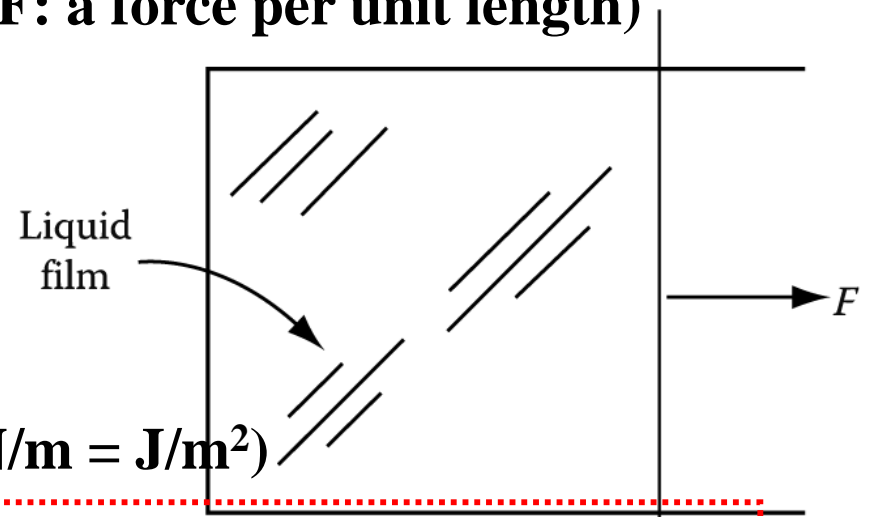
Liquid film $\rightarrow$ F

Fig. 3.1 A liquid film on a wire frame.

At near melting temperature dγ /dA = 0 $\rightarrow$ F = γ (N/m = J/m^2)
(high enough atomic mobility)

Q: Free surface (solid/vapor interface)?

(a) E_{SV} vs γ ?

Extra energy per atom on surface: 표면 에너지

- The measured γ values for pure metals near the melting temperature

$E_{SV} = 3 \, \varepsilon/2 = 0.25 \, L_S /N_a$ $\Longrightarrow$ $\gamma_{SV} = 0.15 \, L_S /N_a$ J / surface atom

($\because$ surface free E averaged over many surface plane, S effect at high T)

(b) Equilibrium shape: Wulff surface

: Polyhedron with the largest facets having the lowest interfacial free energy

3.2 Solid / Vapor Interfaces

* Assumption: S/V interface → Hard sphere model/ uncontaminated surface

(In real systems surfaces will reduce their free energies by the adsorption of impurities.)

- Fcc : density of atoms in these planes decreases as $(h^2+k^2+l^2)$ increases
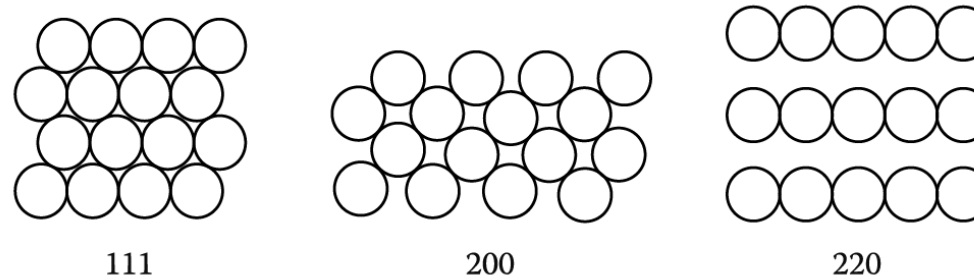
Fig. 3.2 Atomic configurations on the three closest-packed planes in fcc crystals; (111), (200), and (220).

(notation {200} and {220} plane has been used instead of {100} and {110} because the spacing of equivalent atom planes is than given by $a/(h^2+k^2+l^2)^{1/2}$ where a is the lattice parameter.)

For (111) plane   CN=12   [111]
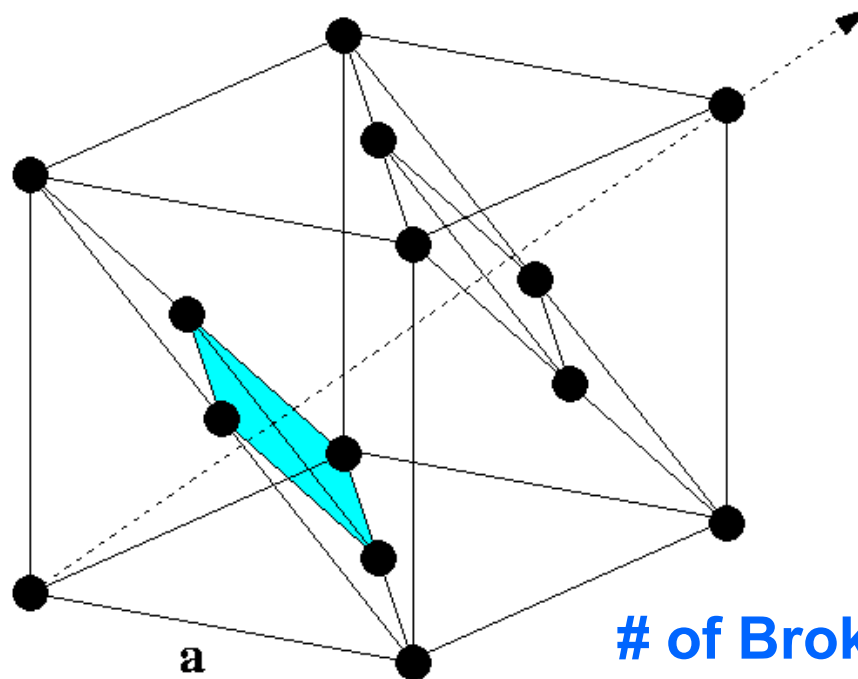
# of Broken Bonds per atom at surface?

# of Broken Bonds per atom at surface? → **3 per atom**

2005 - S.G. Podkolzin

For (111) plane

  # of broken bond at surface : 3 broken bonds

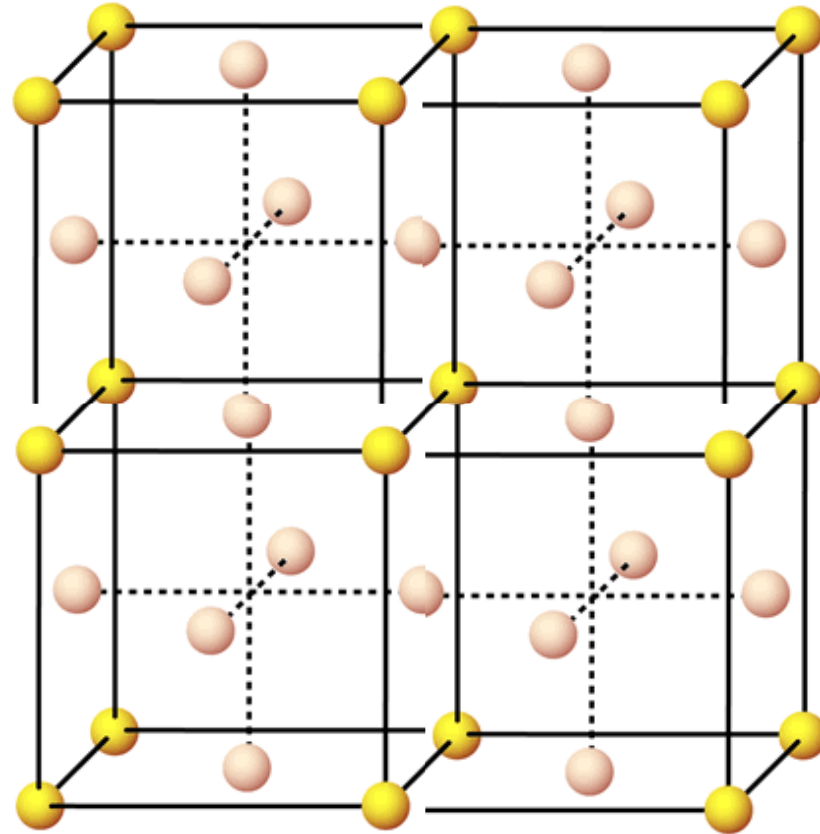 Bond Strength: ε ⟶ for each atom : $\varepsilon/2$

  Excess internal energy over that of the atoms in the bulk: $3\varepsilon/2$ ↑

For (200) plane   CN=12
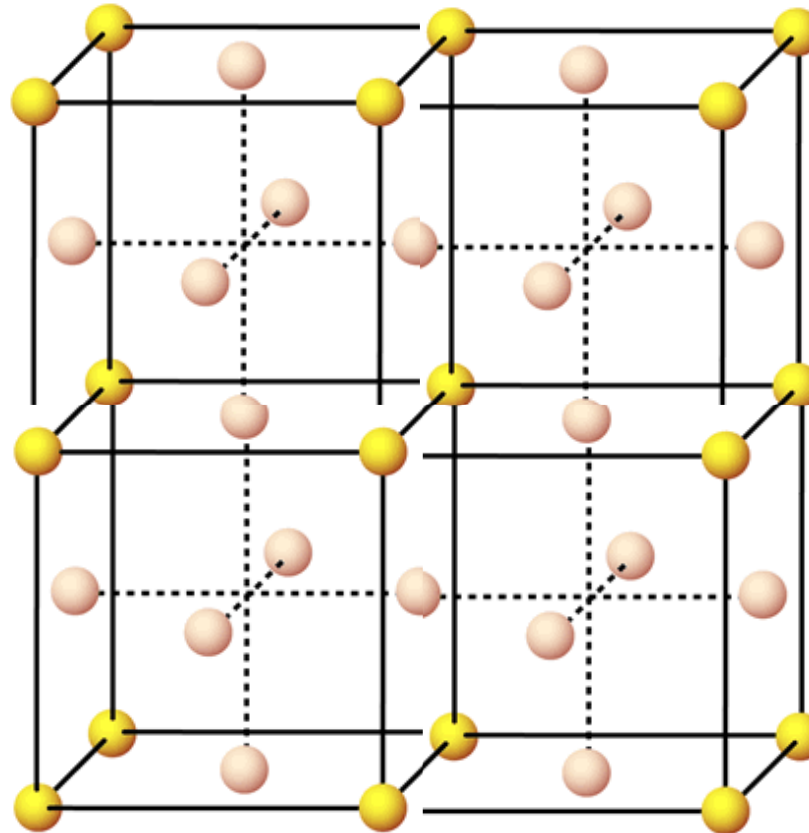
# of Broken Bonds per atom at surface?

For (200) plane   CN=12

# of Broken Bonds per atom at surface?

# of broken bond at surface : 4 broken bonds

Bond Strength: ε ⟶ for each atom : $\varepsilon/2$

Excess internal energy over that of the atoms in the bulk: $4\varepsilon/2$ ↑

(excess internal energy of $4\varepsilon/2$ over that of the atoms in the bulk)

For (111) plane

# of broken bond at surface : 3 broken bonds

Bond Strength: $\varepsilon \longrightarrow$ for each atom : $\varepsilon/2$

Extra energy per atom on surface: $3\varepsilon/2$

Heat of Sublimation (승화) in terms of ε? $\rightarrow$ $L_S = 12\,N_a\,\varepsilon/2$
(Latent heat of melting + vaporization)

(1 mole of solid = 12 N_a)

Energy per atom of a {111} Surface?

$E_{SV} = 3\,\varepsilon/2 = 0.25\,L_S\,/N_a$ (¼ of L_s/N_a) $\Rightarrow$ **E_{SV} vs γ ?**

"Approximated value" due to assumptions, 1) 2nd nearest neighbors have been ignored and 2) strengths of the remaining bonds in the surface are unchanged from the bulk values.

γ interfacial energy = surface free energy $\leftarrow$ Gibb's free energy (J/m^2)

$\rightarrow \gamma = G = H - TS$

$= E + PV - TS$ (if PV is ignored)   ($E_{SV} \uparrow \rightarrow \gamma \uparrow$)

$\rightarrow \gamma = E_{sv} - TS_{sv}$ (S_{sv} thermal entropy, configurational entropy)

surface>bulk   Extra configurational entropy due to vacancies

$\rightarrow \partial\gamma /\partial T = -S$: surface free energy decreases with increasing T

$0 < S < 3$ (mJ/m^{-2}K^{-1}) due to increased contribution of entropy

34

* E_{SV} vs γ ?

 • The measured γ values for pure metals near the melting temperature

$E_{SV} = 3\,\varepsilon/2 = 0.25\;L_S\,/N_a$ ⟹ $\gamma_{SV} = 0.15\;L_S\,/N_a$ J / surface atom

($\because$ surface free E averaged over many surface plane, S effect at high T)

TABLE 3.1 **Average Surface Free Energies of Selected Metals**

Crystal	T_m (°C)	γ_{sv} (mJ m^{-2})
Sn	232	680
Al	660	1080
Ag	961	1120
Au	1063	1390
Cu	1084	1720
δ-Fe	1536	2080
Pt	1769	2280
W	3407	2650

측정 어려움, **near T_m**

γ of Sn : 680 mJ/m^2 (T_m : 232ºC)
γ of Cu : 1720 mJ/m^2 (T_m : 1083ºC)

cf) G.B. energy γ_{gb} is about one third of γ_{sv}

* Higher T_m → stronger bond (large L_s) → larger surface free energy (γ_{SV})

$$high\;T_m \rightarrow high\;L_s \rightarrow high\;\gamma_{sv}$$

35

Surface energy for high or irrational {hkl} index

Closer surface packing → smaller number of broken bond → lower surface energy
# of broken bonds will increase through the series {111} {200} {220} → γ_{SV} will increase along the same series (if different entropy term is ignored)

A crystal plane at an angle θ to the close-packed plane will contain broken bonds in excess of the close-packed plane due to the atoms at the steps.
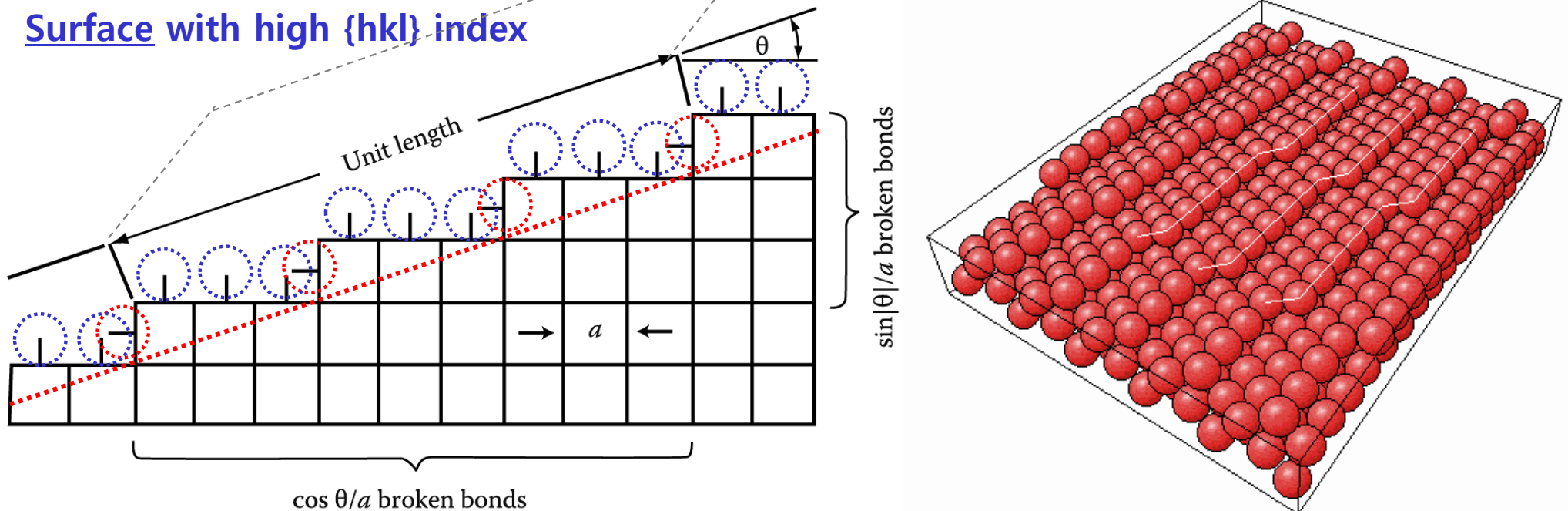
Surface with high {hkl} index

Fig. 3.3 The 'broken-bond' model for surface energy.

$(\cos\theta/a)(1/a)$: broken bonds from the atoms on the steps

$(\sin|\theta|/a)(1/a)$: additional broken bonds from the atoms on the steps

Surface energy for high or irrational {hkl} index

(cosθ/a)(1/a) : broken bonds from the atoms on the steps

(sin|θ|/a)(1/a) : additional broken bonds from the atoms on the steps

Attributing ε/2 energy to each broken bond,

$$E_{SV} = \frac{1}{1 \times a} \frac{\varepsilon}{2} \left(\frac{\cos\theta}{a} + \frac{\sin|\theta|}{a} \right)$$

$$= \frac{\varepsilon(\cos\theta + \sin(|\theta|))}{2a^2}$$

E-θ plot $E_{SV} = 3\,\varepsilon/2 = 0.25\,L_S/N_a$

Fig. 3.4 Variation of surface energy as a function of θ

- **The close-packed orientation (θ = 0) lies at a cusped minimum in the E plot.**

- Similar arguments can be applied to any crystal structure
  for rotations about any axis from any reasonably close-packed plane.

- **All low-index planes should therefore be located at low-energy cusps.**

- If γ is plotted versus θ similar cusps are found (γ-θ plot), but as a result of
 <u>entropy effects</u> they are <u>less prominent than in the E-θ plot</u>, and for the higher
  index planes they can even disappear.

37

Q: Free surface (solid/vapor interface)?

(a) E_{SV} vs γ ?

Extra energy per atom on surface

• The measured γ values for pure metals near the melting temperature

$$E_{SV} = 3\,\varepsilon/2 = 0.25\,L_S\,/N_a \quad\Longrightarrow\quad \gamma_{SV} = 0.15\,L_S\,/N_a \quad \text{J / surface atom}$$

($\because$ surface free E averaged over many surface plane, S effect at high T)

(b) Equilibrium shape: Wulff surface

: Polyhedron with the largest facets having the lowest interfacial free energy

Equilibrium shape: Wulff surface

* A convenient method for plotting the variation of γ with surface orientation in 3 dimensions

* Distance from center : γ_{sv}

→ Construct the surface using γ_{sv} value as a distance between the surface and the origin when measured along the normal to the plane

Wulff plane

Several plane A_1, A_2 etc. with energy γ_1 , γ_2

Total surface energy : $A_1\gamma_1 + A_2\gamma_2$ ....

$= \sum A_i \gamma_i \rightarrow$ minimum

$\rightarrow$ equilibrium morphology

: can predict the equilibrium shape of

an isolated single crystal

How is the equilibrium shape determined?

$$\sum_{i=1}^{n} A_i \gamma_j = Minimum$$

crystal shape

γ-θ **plot**

Due to entropy effects the plot are less prominent than in the E_{SV}-θ plot, and for the higher index planes they can even disappear

Process of Wulff shape intersection for two cubic Wulff shapes
: Polyhedron with the largest facets having the lowest interfacial free energy
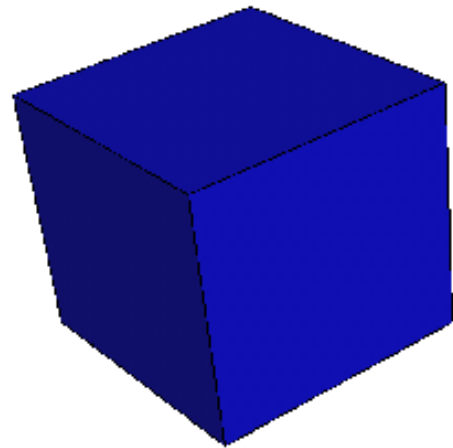
(a) Wulff Shape I
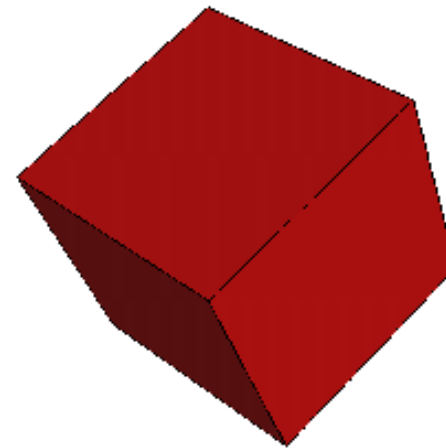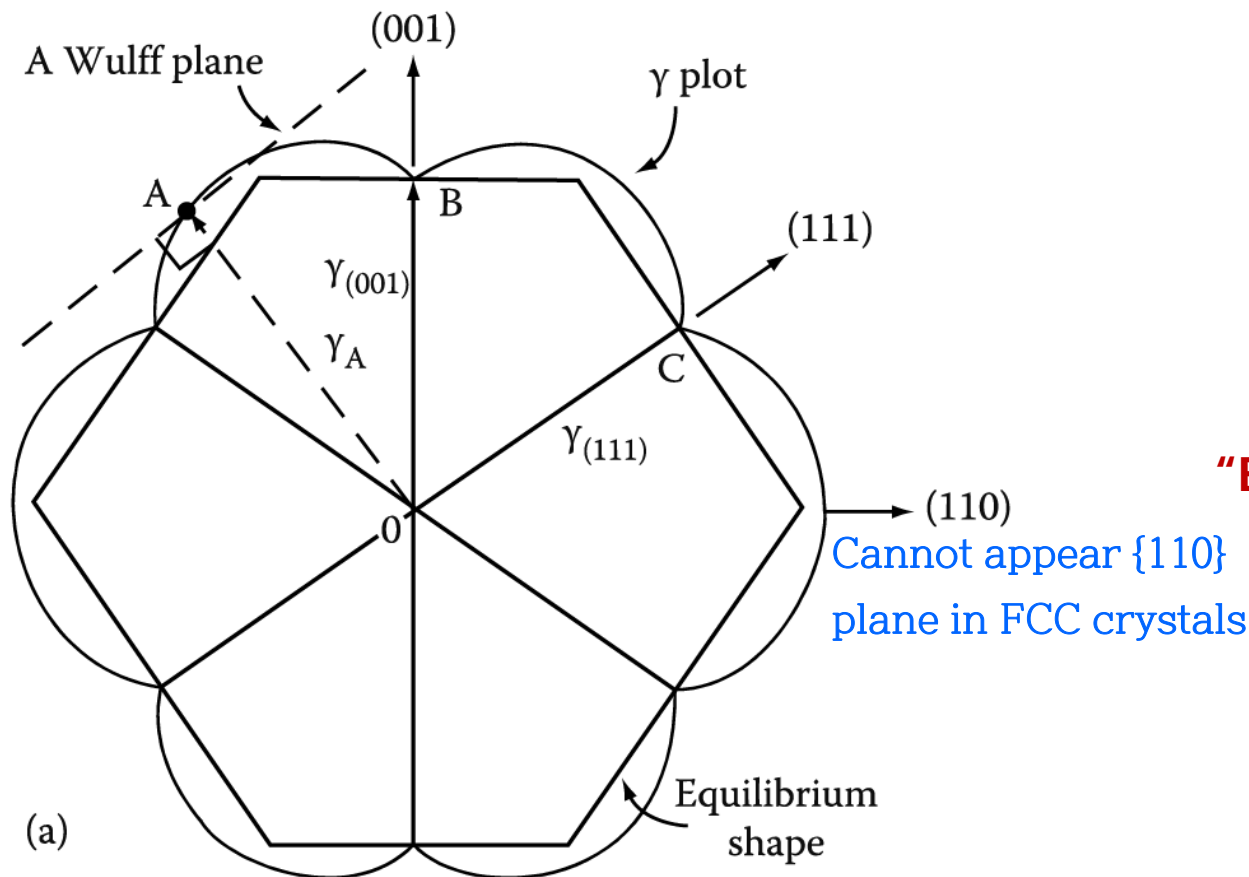
(b) Wulff Shape II
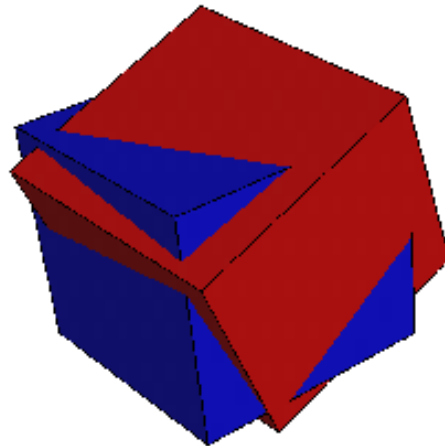
(c) Union of I and II
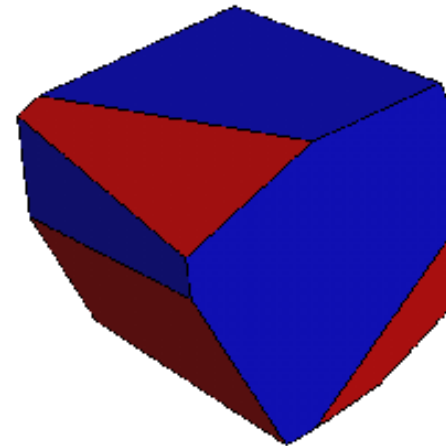
(d) Intersection of I and II

Figure 1: The process of Wulff shape intersection for two cubic Wulff shapes with displaced origins and rotated coordinate systems. Each individual shape has cubic symmetry *m3m* and **[100]** facets.

Equilibrium shape: Wulff surface

Equilibrium shape can be determined experimentally by annealing small single crystals at high temperatures in an inert atmosphere, or by annealing small voids inside a crystal.

Of course **when γ is isotropic**, as for liquid droplets, both the γ-plots and equilibrium shapes are **spheres**.

A possible (1̄10) section through the γ-plot of an fcc crystal

Cannot appear {110} plane in FCC crystals

"Equilibrium shape of FCC crystals"

1) Square faces {100} and

2) Hexagonal faces {111}

The length OA represents the free energy of a surface plane whose normal lies in the direction OA.

Q: Free surface (solid/liquid interface)?

- Faceted interface vs Diffusion interface (non-faceted)

- $\gamma_{SL} \approx 0.45\ \gamma_b (= 0.15\gamma_{SV})$ for the most metals
  (fcc & hcp~0.55 γ_b / bcc~0.3 γ_b)

$\Rightarrow$ $\gamma_{SV} > \gamma_{SL} + \gamma_{LV}$

3.3 Solid /Liquid Interfaces: consequences for the structure and energy of the interface

Faceted interface **Rather narrow transition zone** approximately one atom layer thick
~ same as solid/vapor interfaces, i.e., atomically flat close-packed interface

: some intermetallic compounds, elements such as Si, Ge, Sb, and most nonmetals

Fig. 3.6 Solid/liquid interfaces: (a) atomically smooth, (b) and (c) atomically rough, or diffuse interfaces.

In figure (a): Liquid / Solid, $L_f/T_m > 4R$, Liquid / Solid

Diffusion interface (non-faceted) **Rather wide transition zone** over several atom layers
: most metals, $L_f/T_m \sim R$ (gas constant) ~automatically **rough & diffuse interface**

43
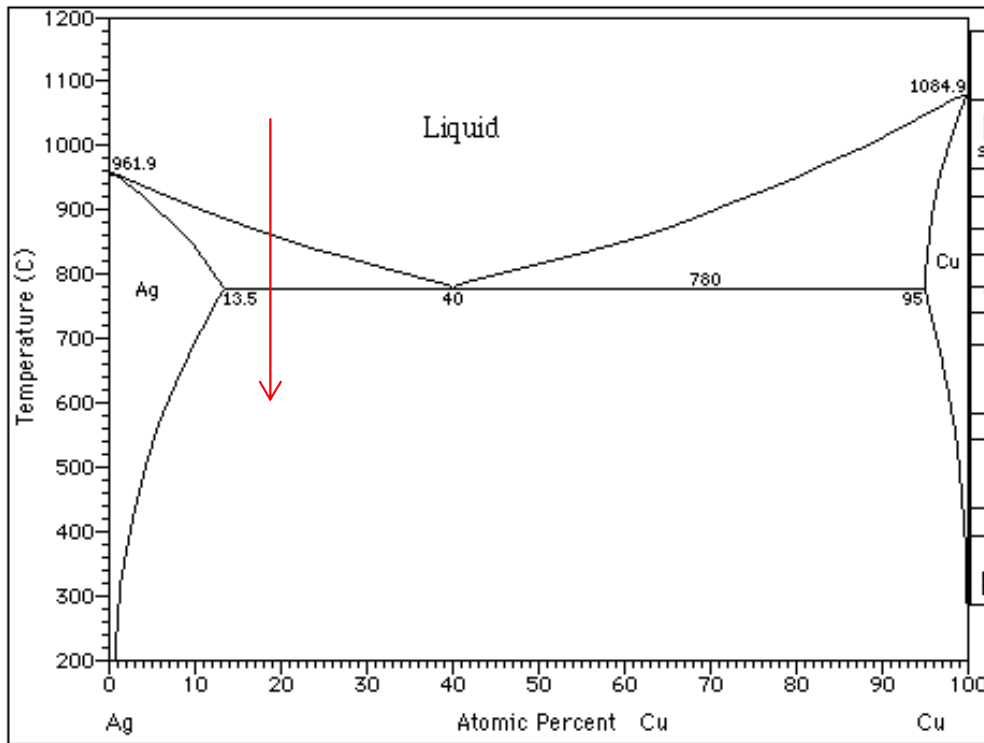
Primary Ag dendrite
in Cu-Ag eutectic matrix

β′-SnSb intermetallic compound
in Sn(Sb) solid solution
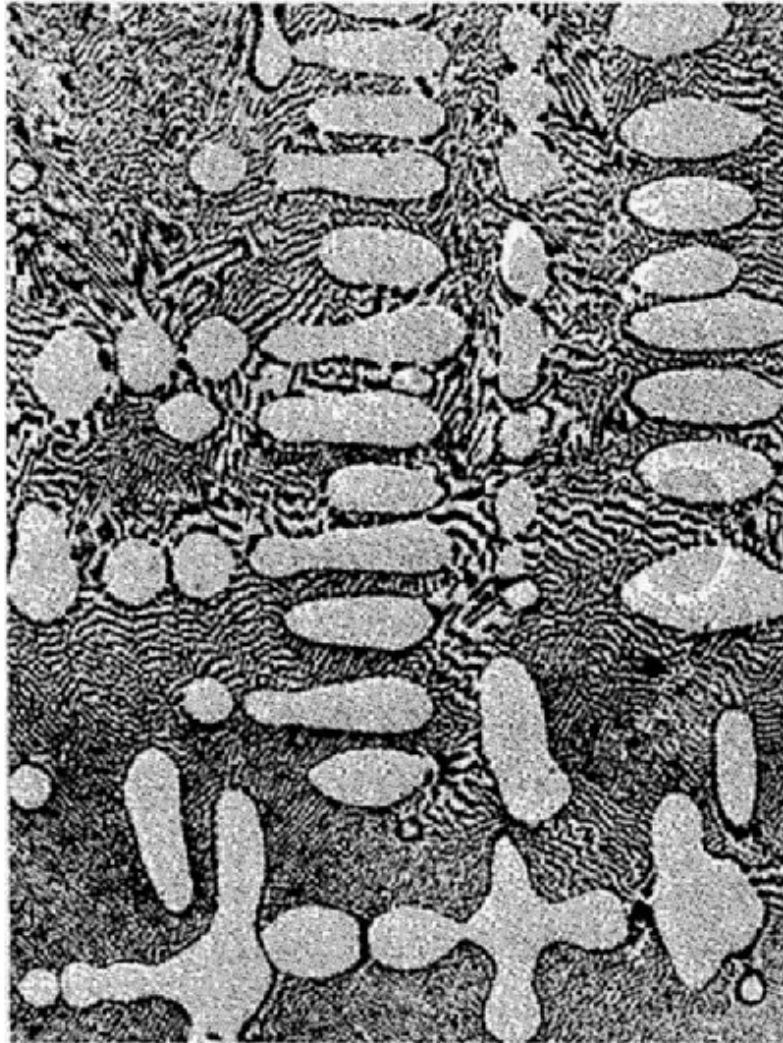
(a) **Non-faceted**
  - **Free E ~do not vary with**
    crystallographic orientation
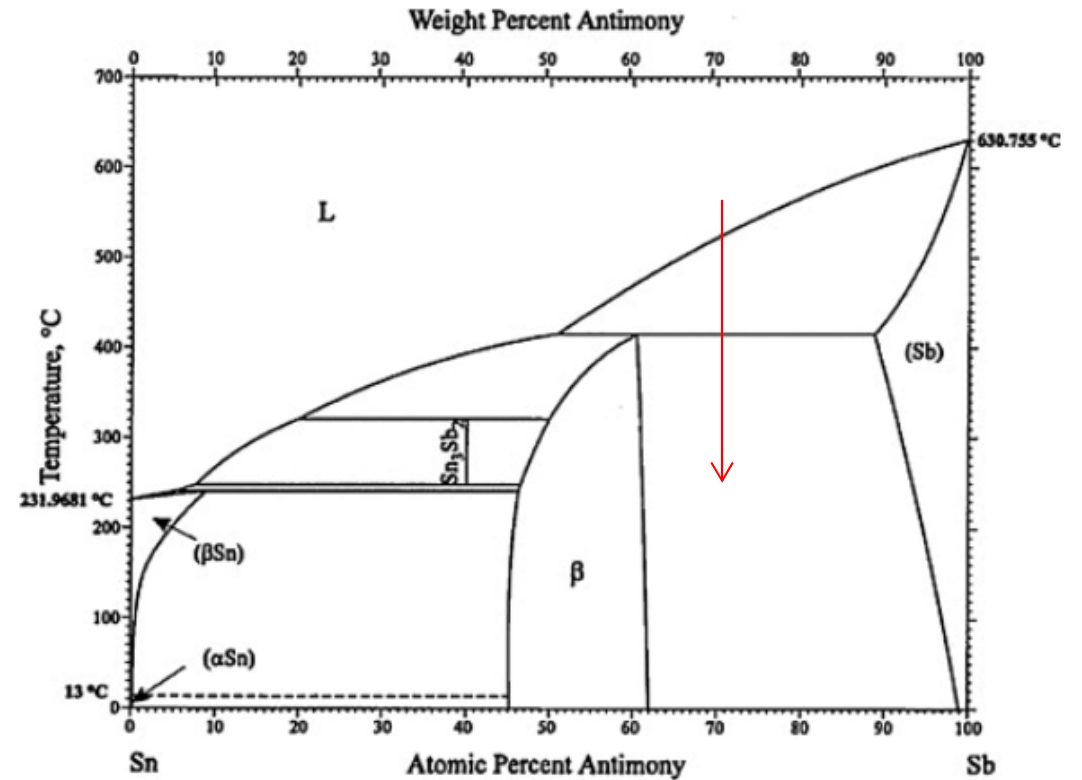 - **γ-plot ~ spherical**
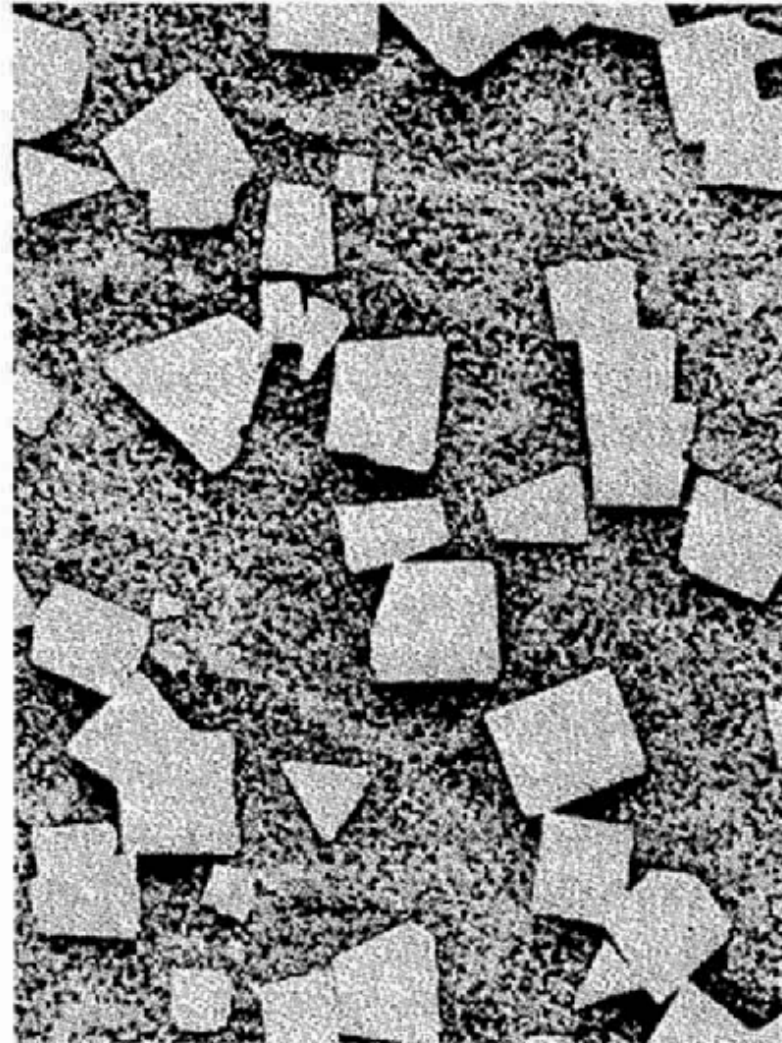
(b) **Faceted**
  - **Strong crystallographic effects**
  - **Solidify with low-index close-packed facets**

44

**Primary Ag dendrite
in Cu-Ag eutectic matrix**

**β′-SnSb intermetallic compound
in Sn(Sb) solid solution**

* Broken bond model → calculation of the E of solid/ liquid interface

$0.5L_f / N_a \rightarrow 0.45L_f / N_a$ (엔트로피 효과로 감소)

at equilibrium melting temp.

Table 3.1. Relationship between Maximum Supercooling, Solid-Liquid Interfacial Energy and Heat of Fusion[a]

Metal	Interfacial Energy σ (ergs/cm²)	σ_g (cal/mole)	σ_g/L	ΔT_{MAX} (deg)
Mercury	24.4	296	0.53	77
Gallium	55.9	581	0.44	76
Tin	54.5	720	0.42	118
Bismuth	54.4	825	0.33	90
Lead	33.3	479	0.39	80
Antimony	101	1430	0.30	135
Germanium	181	2120	0.35	227
Silver	126	1240	0.46	227
Gold	132	1320	0.44	230
Copper	177	1360	0.44	236
Manganese	206	1660	0.48	308
Nickel	255	1860	0.44	319
Cobalt	234	1800	0.49	330
Iron	204	1580	0.45	295
Palladium	209	1850	0.45	332
Platinum	240	2140	0.45	370

[a] Data from D. Turnbull, *J. Appl. Phys.*, **21**, 1022 (1950) and Ref. 3.

$\gamma_{SL} \approx 0.45\ L_f/N_a$ (= $0.15\gamma_{SV}$)
for the most metals
(fcc & hcp~0.55 L_f/N_a / bcc~0.3 L_f/N_a)

$\gamma_{SV} > \gamma_{SL} + \gamma_{LV}$

Distance across interface
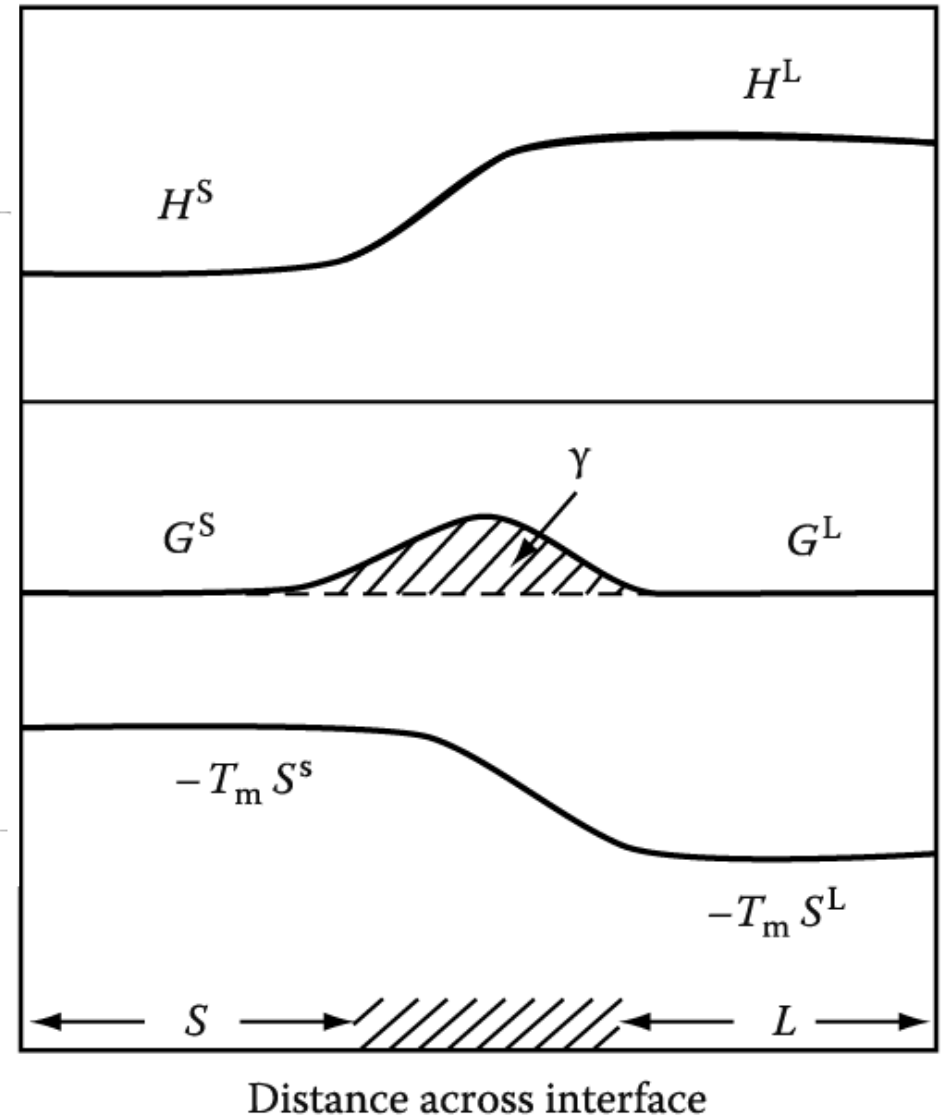
Showing the origin of the solid/ liquid interfacial energy, γ
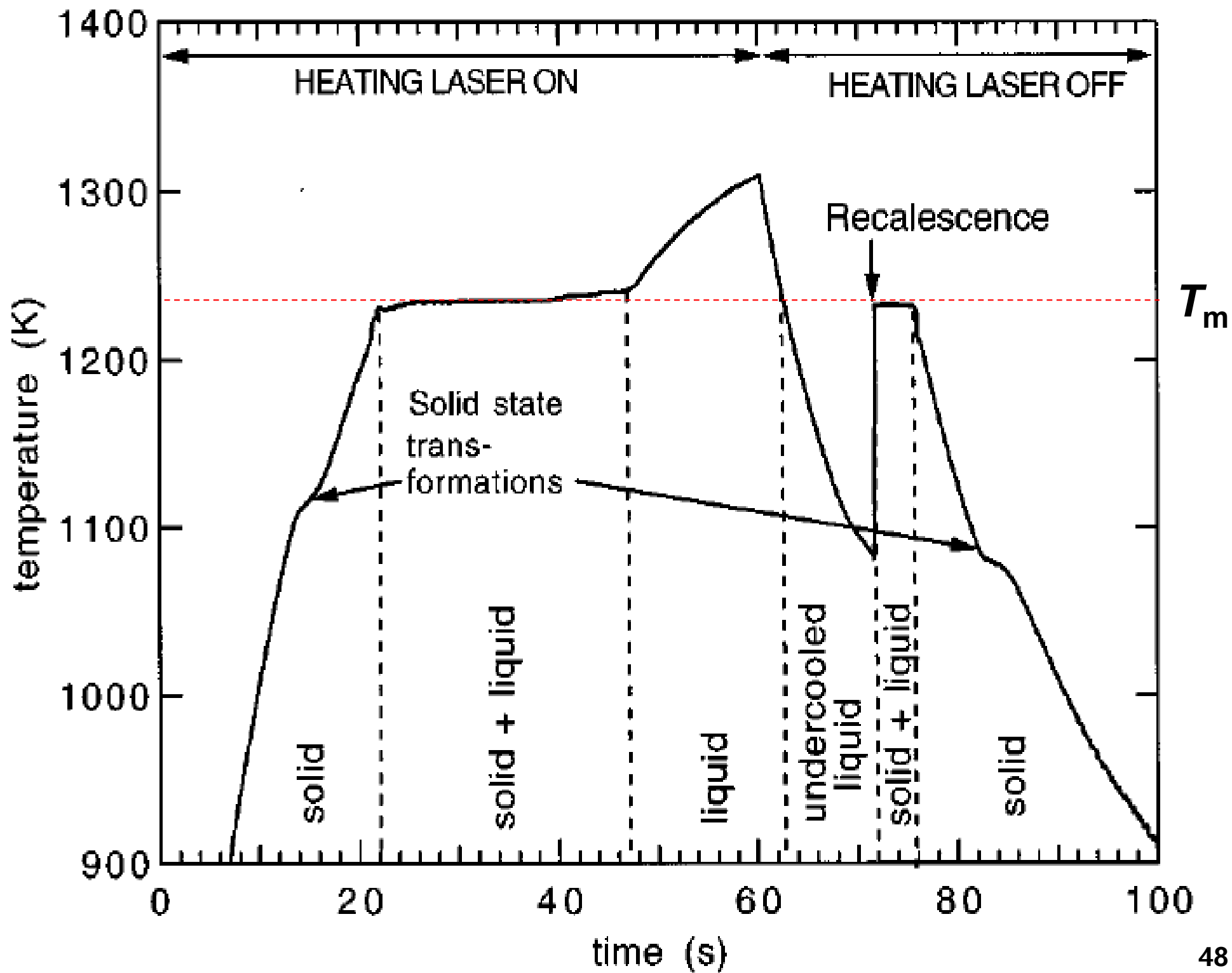
46

4.1.4. Nucleation of melting

Although nucleation during solidification usually requires some undercooling, melting invariably occurs at the equilibrium melting temperature even at relatively high rates of heating.

Why?
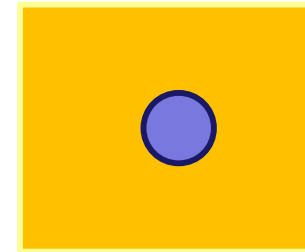
$$\gamma_{SL} + \gamma_{LV} < \gamma_{SV}$$ **(commonly)**

In general, wetting angle = 0 $\implies$ **No superheating required!**

48

Melting and Crystallization are Thermodynamic Transitions

Solidification: **Liquid** ⟶ **Solid**

<Thermodynamic>

- **Interfacial energy** ⟹ ΔT_{N}

T_{m} **Undercooled Liquid**

Liquid   **Solid**

No superheating required!

- **Interfacial energy** ⟹ **No ΔT_{N}**

$$\gamma_{SL} + \gamma_{LV} < \gamma_{SV}$$

vapor

Melting: **Liquid** ⟵ **Solid**

(a) E_{SV} vs γ ?

Extra energy per atom on surface: 표면 에너지

Interfacial energy (γ : J/m^2)

$\rightarrow$ **Gibbs free energy of a system containing an interface of area A**

$\rightarrow$ **G_{bulk} + $G_{interface}$**

vapor
solid

$\rightarrow$ **$G = G_0 + \boxed{\gamma A}$**　(excess free E arising from the fact that some material lies in or close to the interface)

"**Approximated value**" due to assumptions, 1) 2nd nearest neighbors have been ignored and 2) strengths of the remaining bonds in the surface are unchanged from the bulk values.

γ interfacial energy = surface free energy $\leftarrow$ Gibb's free energy (J/m^2)

$\rightarrow$ **$\gamma = E_{sv} - TS_{sv}$** (**$S_{sv}$** thermal entropy, configurational entropy) (**$E_{SV} \uparrow \rightarrow \gamma \uparrow$**)

Surface > Bulk　　　Extra configurational entropy due to vacancies

$\rightarrow$ **$\boxed{\partial \gamma / \partial T = -S}$** : **surface free energy decreases with increasing T**

$0 < S < 3$ (mJ/m^{-2}K^{-1}) due to increased contribution of entropy

• The measured γ values for pure metals near the melting temperature

$E_{SV} = 3\,\varepsilon/2 = 0.25\,L_S/N_a$ $\Longrightarrow$ **$\gamma_{SV} = 0.15\,L_S/N_a$** J / surface atom

(∵ surface free E averaged over many surface plane, S effect at high T)

50

Surface energy for high or irrational {hkl} index

(cosθ/a)(1/a) : <u>broken bonds</u> from the atoms on the steps

(sin|θ|/a)(1/a) : additional broken bonds from the atoms on the steps

Attributing ε/2 energy to each broken bond,

$$E_{SV} = \frac{1}{1 \times a} \frac{\varepsilon}{2} \left(\frac{\cos\theta}{a} + \frac{\sin|\theta|}{a} \right)$$

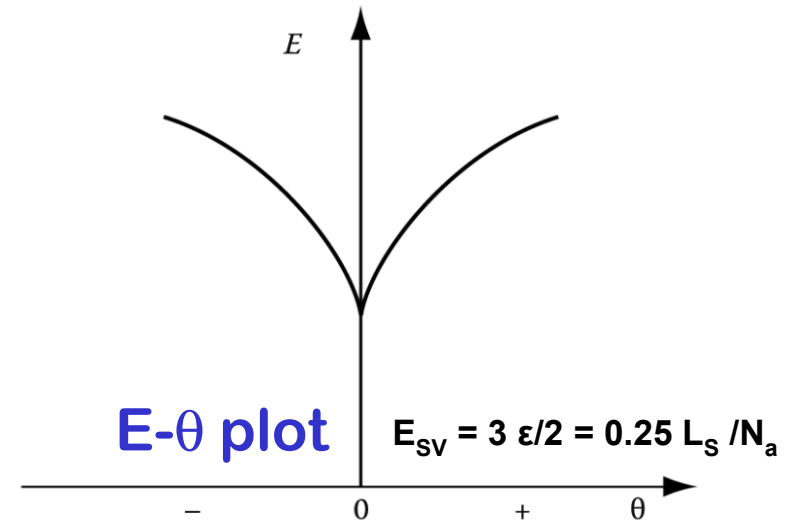$$= \frac{\varepsilon(\cos\theta + \sin(|\theta|))}{2a^2}$$

E-θ plot $E_{SV} = 3\,\varepsilon/2 = 0.25\,L_S\,/N_a$

Fig. 3.4 Variation of surface energy as a function of θ

- **The close-packed orientation (θ = 0) lies at a cusped minimum in the E plot.**

- Similar arguments can be applied to any crystal structure for rotations about any axis from any reasonably close-packed plane.

- **All low-index planes should therefore be located at low-energy cusps.**

- If γ is plotted versus θ similar cusps are found (γ-θ plot), but as a result of <u>entropy effects</u> they are <u>less prominent than in the E-θ plot</u>, and for the higher index planes they can even disappear.

51

Equilibrium shape: Wulff surface

 * A convenient method for plotting the variation of γ with surface orientation in 3 dimensions

 * Distance from center : γ_{sv}

→ Construct the surface using γ_{sv} value as a distance between the surface and the origin when measured along the normal to the plane

Several plane A_1, A_2 etc. with energy γ_1 , γ_2
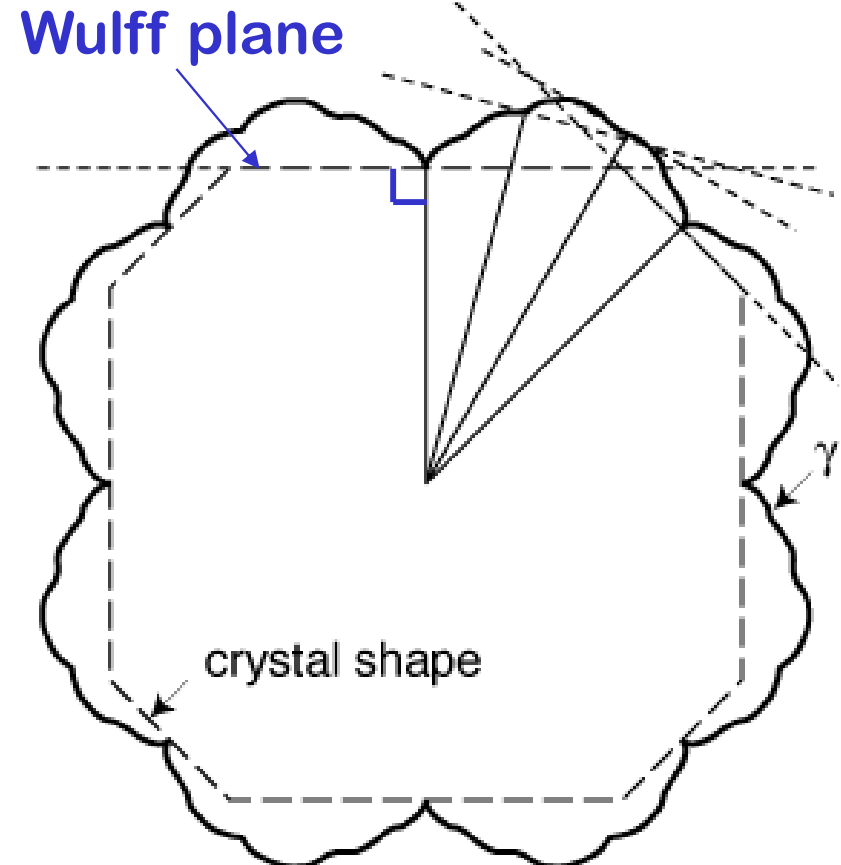
Total surface energy : $A_1\gamma_1 + A_2\gamma_2 \ldots$

$= \sum A_i \gamma_i \rightarrow$ minimum

$\rightarrow$ equilibrium morphology

   : can predict the equilibrium shape of

     an isolated single crystal

How is the equilibrium shape determined?

$$\sum_{i=1}^{n} A_i \gamma_j = Minimum$$

Wulff plane

crystal shape

γ

γ-θ plot

Due to entropy effects the plot are less prominent than in the E_{SV}-θ plot, and for the higher index planes they can even disappear

3.3 Solid /Liquid Interfaces: consequences for the structure and energy of the interface

Faceted interface **Rather narrow transition zone** approximately one atom layer thick
~ same as solid/vapor interfaces, i.e., atomically flat close-packed interface

: some intermetallic compounds, elements such as Si, Ge, Sb, and most nonmetals

Liquid

Solid

(a) $L_f/T_m > 4R$

Liquid

Solid

(c)

Liquid

(b)

Solid

Fig. 3.6 Solid/liquid interfaces: (a) atomically smooth, (b) and (c) atomically rough, or diffuse interfaces.

Diffusion interface (non-faceted) **Rather wide transition zone** over several atom layers
: most metals, L_f/T_m ~ R (gas constant) ~automatically rough & diffuse interface

53

"Phase Transformation *in* Materials"

10. 11. 2023

Eun Soo Park

Office: 33-313
Telephone: 880-7221
Email: espark@snu.ac.kr
Office hours: by an appointment

Chapter 3 Crystal Interfaces and Microstructure

1) Interfacial Free Energy

2) Solid/Vapor Interfaces

3) Solid/Liquid Interfaces

4) Boundaries in Single-Phase Solids

5) Interphase Interfaces in Solid (α/β)

6) Interface migration

(a) E_{SV} vs γ ?

Extra energy per atom on surface: 표면 에너지

Interfacial energy (γ : J/m^2)

$\rightarrow$ **Gibbs free energy of a system containing an interface of area A**

$\rightarrow$ **$G_{bulk} + G_{interface}$**

vapor

solid

$\rightarrow$ **$G = G_0 + \gamma A$**

(excess free E arising from the fact that some material lies in or close to the interface)

"Approximated value" due to assumptions, 1) 2nd nearest neighbors have been ignored and 2) strengths of the remaining bonds in the surface are unchanged from the bulk values.

γ interfacial energy = surface free energy $\leftarrow$ Gibb's free energy (J/m^2)

$\rightarrow$ $\gamma = E_{sv} - TS_{sv}$ (S_{sv} thermal entropy, configurational entropy) ($E_{SV} \uparrow \rightarrow \gamma \uparrow$)

Surface > Bulk   Extra configurational entropy due to vacancies

$\rightarrow$ $\partial\gamma /\partial T = -S$: **surface free energy decreases with increasing T**

$0 < S < 3$ (mJ/m^{-2}K^{-1}) due to increased contribution of entropy

• The measured γ values for pure metals near the melting temperature

$E_{SV} = 3 \varepsilon/2 = 0.25 L_S /N_a$ $\Rightarrow$ $\gamma_{SV} = 0.15 L_S /N_a$ J / surface atom

3

($\because$ surface free E averaged over many surface plane, S effect at high T)

Surface energy for high or irrational {hkl} index

(cosθ/a)(1/a) : <u>broken bonds</u> from the atoms on the steps

(sin|θ|/a)(1/a) : additional broken bonds from the atoms on the steps

Attributing ε/2 energy to each broken bond,

$$E_{SV} = \frac{1}{1 \times a} \frac{\varepsilon}{2} \left(\frac{\cos\theta}{a} + \frac{\sin|\theta|}{a} \right)$$

$$= \frac{\varepsilon\left(\cos\theta + \sin(|\theta|)\right)}{2a^2}$$

E-θ plot $E_{SV} = 3\,\varepsilon/2 = 0.25\, L_S\,/N_a$

Fig. 3.4 Variation of surface energy as a function of θ

- **The close-packed orientation (θ = 0) lies at a cusped minimum in the E plot.**

- Similar arguments can be applied to any crystal structure for rotations about any axis from any reasonably close-packed plane.

- **All low-index planes should therefore be located at low-energy cusps.**

- If γ is plotted versus θ similar cusps are found (γ-θ plot), but as a result of <u>entropy effects</u> they are <u>less prominent than in the E-θ plot</u>, and for the higher index planes they can even disappear.

4

Equilibrium shape: Wulff surface

* A convenient method for plotting the variation of γ with surface orientation in 3 dimensions

* Distance from center : γ_{sv}

→ Construct the surface using γ_{sv} value as a distance between the surface and the origin when measured along the normal to the plane

Several plane A_1, A_2 etc. with energy γ_1 , γ_2

Total surface energy : $A_1\gamma_1 + A_2\gamma_2 \ldots$

$= \sum A_i \gamma_i \rightarrow$ minimum

→ equilibrium morphology

: can predict the equilibrium shape of
an isolated single crystal

How is the equilibrium shape determined?

$$\sum_{i=1}^{n} A_i \gamma_j = Minimum$$

Wulff plane

crystal shape

γ

γ-θ plot

Due to entropy effects the plot are less prominent than in the E_{SV}-θ plot, and for the higher index planes they can even disappear

3.3 Solid /Liquid Interfaces: consequences for the structure and energy of the interface

Faceted interface **Rather narrow transition zone** approximately one atom layer thick
~ same as solid/vapor interfaces, i.e., atomically flat close-packed interface

: some intermetallic compounds, elements such as Si, Ge, Sb, and most nonmetals

Liquid

Solid

(a) $L_f/T_m > 4R$

Liquid

Solid

(c)

Liquid

(b)

Solid

Fig. 3.6 Solid/liquid interfaces: (a) atomically smooth, (b) and (c) atomically rough, or diffuse interfaces.

Diffusion interface (non-faceted) Rather wide transition zone over several atom layers
: most metals, $L_f/T_m \sim R$ (gas constant) ~automatically rough & diffuse interface

6

Contents for today's class

Chapter 3 Crystal Interfaces and Microstructure

1) Interfacial Free Energy

2) Solid/Vapor Interfaces

3) Solid/Liquid Interfaces

4) Boundaries in Single-Phase Solids

5) Interphase Interfaces in Solid (α/β)

6) Interface migration

Q: Grain boundary (α/ α interfaces)

= Boundaries in Single-Phase Solids

(a) Low-Angle and High-Angle Boundaries

(b) Special High-Angle Grain Boundaries

(c) Equilibrium in Polycrystalline Materials

3.4 Boundaries in Single-Phase Solids: definition

Grain boundary (α/α interfaces)   **Single phase - Poly grain**

L → (six circles with dots) → (hkl) (polygrain diagram)
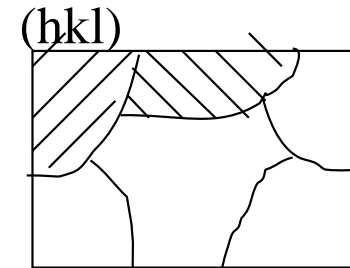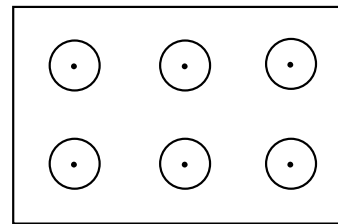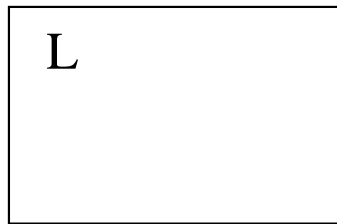
> **same composition, same crystal structure**

> **different orientation (axis-angle pair)**

(hkl)

G.B.
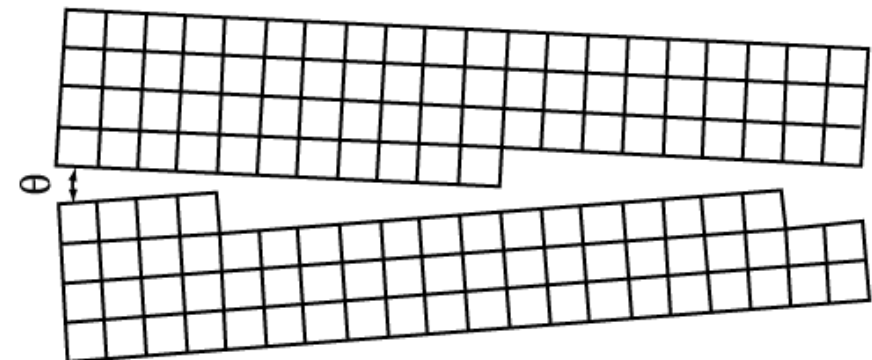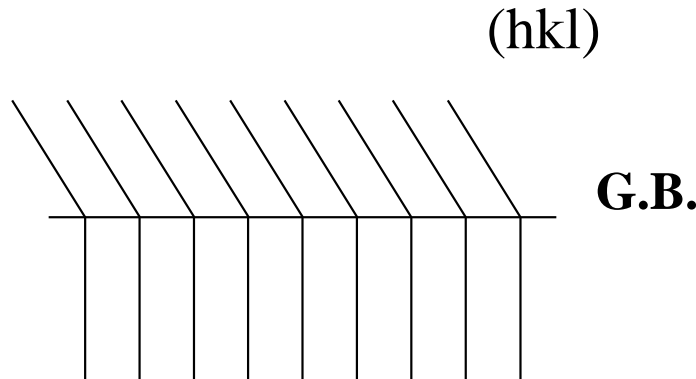
1) misorientation of the two adjoining grains   **2) orientation of the boundary plane**

두 개 인접한 결정립간 방위차이 *cf.* 두 조밀면 만남   인접 결정립과 입계면의 방위관계   **9**

3.4 Boundaries in Single-Phase Solids

: The lattices of any two grains can be made to coincide by rotating one of them through a suitable angle about a single axis.

* Relatively simple boundary: relative orientation of the crystals and the boundary
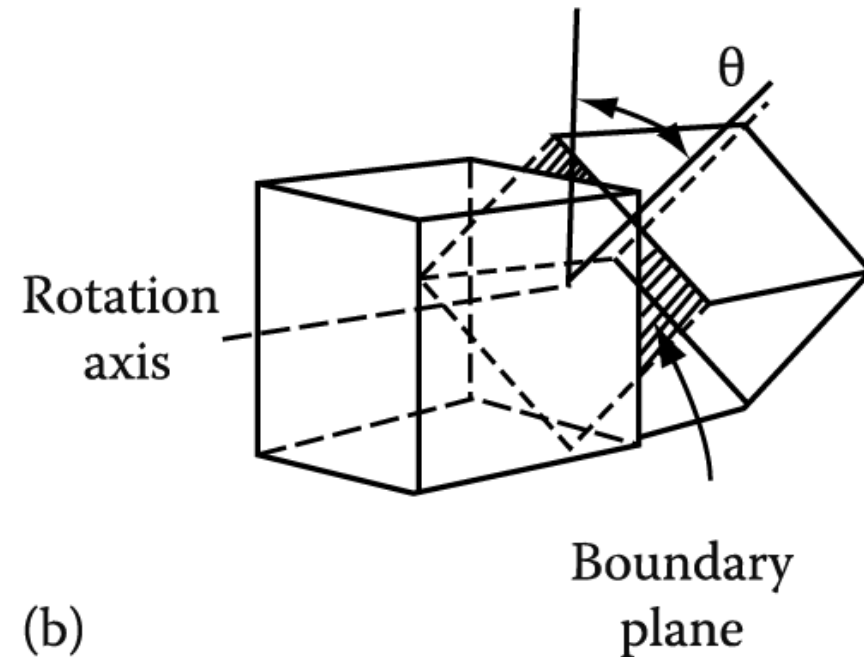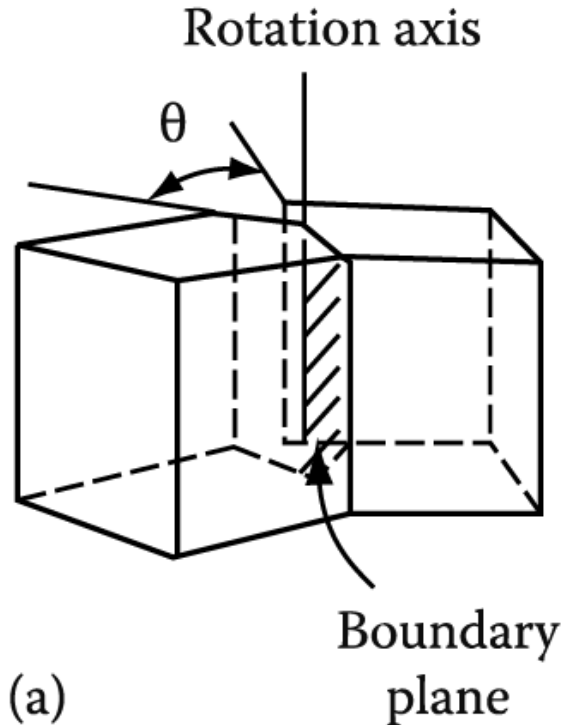
Fig. 3.9   (a)

tilt boundary

$\theta \rightarrow$ **misorientation**
$\rightarrow$ **tilt angle**

Axis of rotation: parallel to the plane of the boundary

twist boundary

$\theta \rightarrow$ **misorientation**
$\rightarrow$ **twist angle**

Perpendicular to the boundary

⎡ **symmetric tilt or twist boundary**
⎣ **non-symmetric tilt or twist boundary**

3.4.1 Low-Angle and High-Angle Boundaries

Low-Angle Boundaries

Symmetrical low-angle tilt boundary   Symmetrical low-angle twist boundary
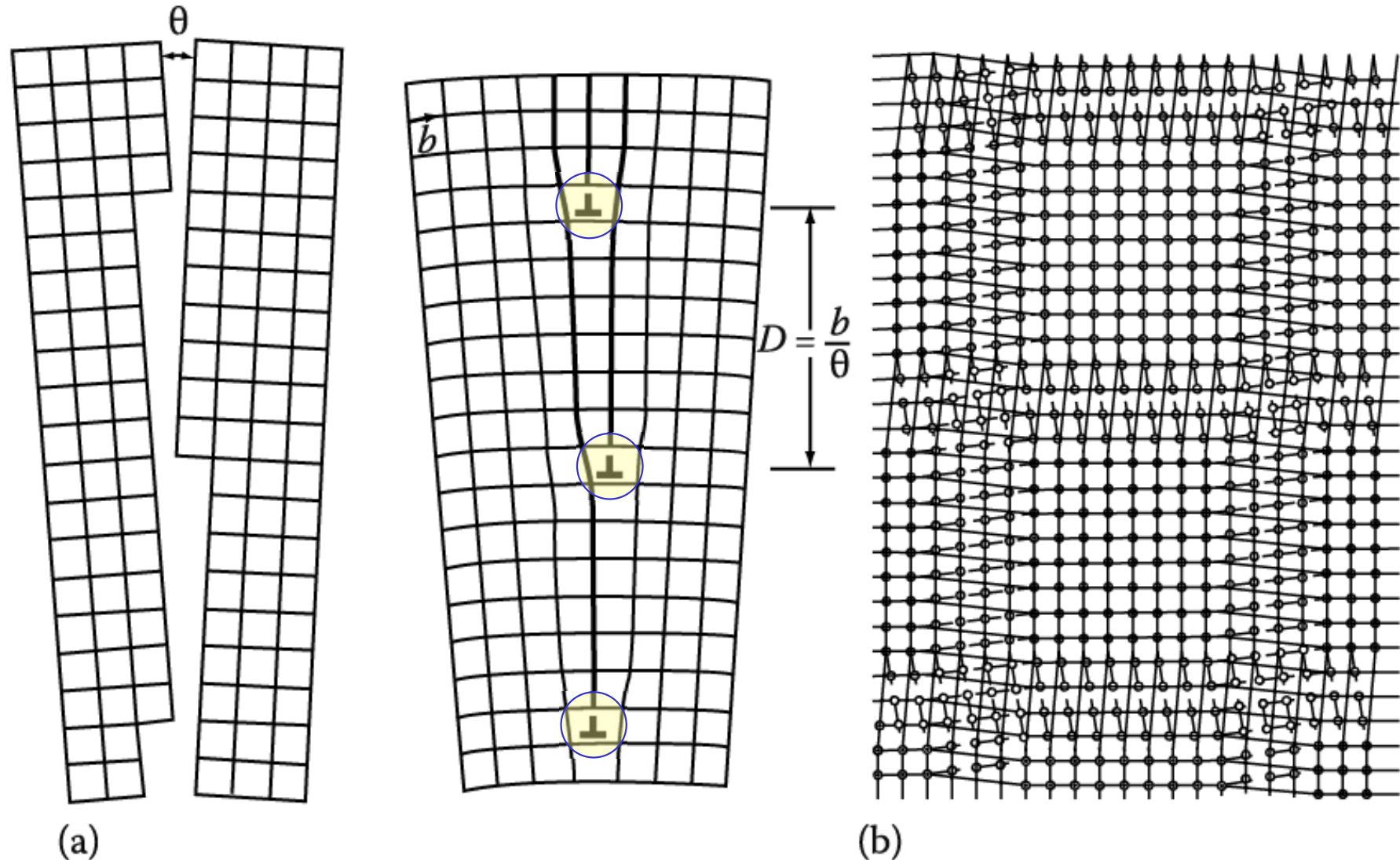
Fig. 3.10 (a) Low-angle tilt boundary, (b) low-angle twist boundary: ○ atoms in crystal below, ● atoms in crystal above boundary.

An array of parallel edge dislocation   **Cross-grid of two sets of screw dislocations**

tilt Boundaries
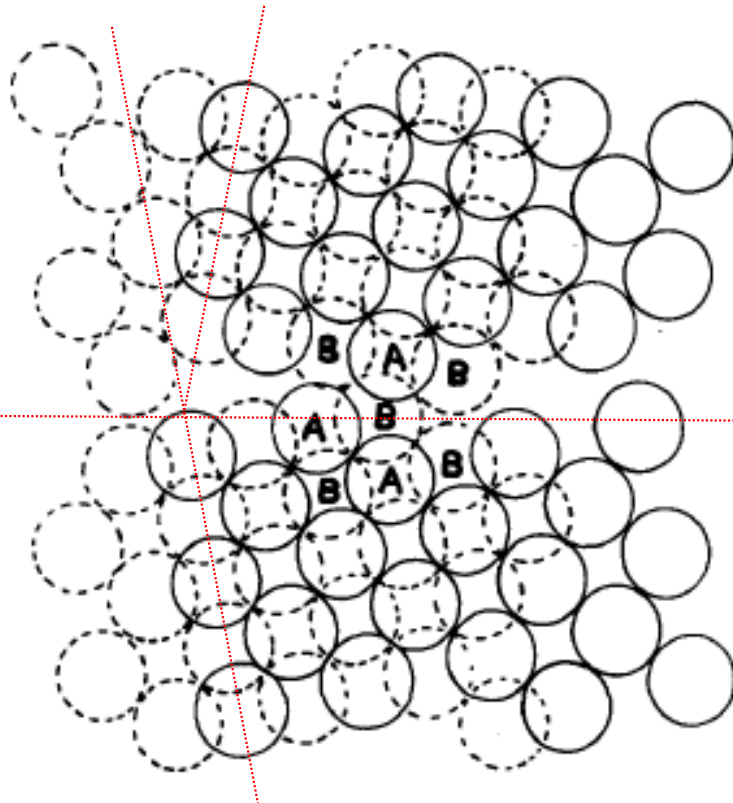
Figure 1 - 23° symmetric tilt boundary about a <001> axis. The circles with dashed lines represent one layer and the circles with solid lines the other layer of the AB....stacked {001} planes. The atoms labelled A and B denote the structural unit.

Figure 2 - 23° symmetric tilt boundary about a <001> axis. Δ represent one layer and 0 represent the other layer of the AB..... stacked {001} planes. The ledge like character of the boundary is shown by the dashed lines.

Dislocations

dislocation wall

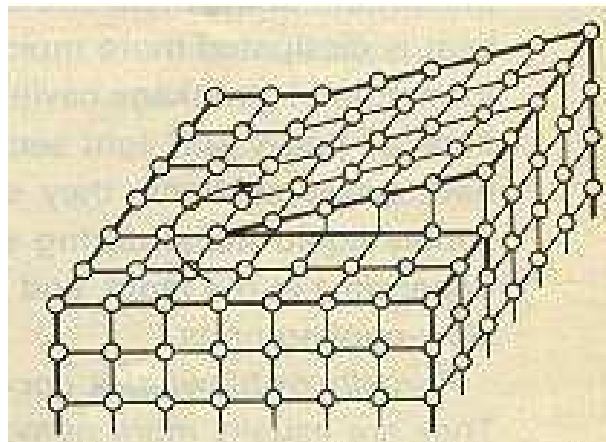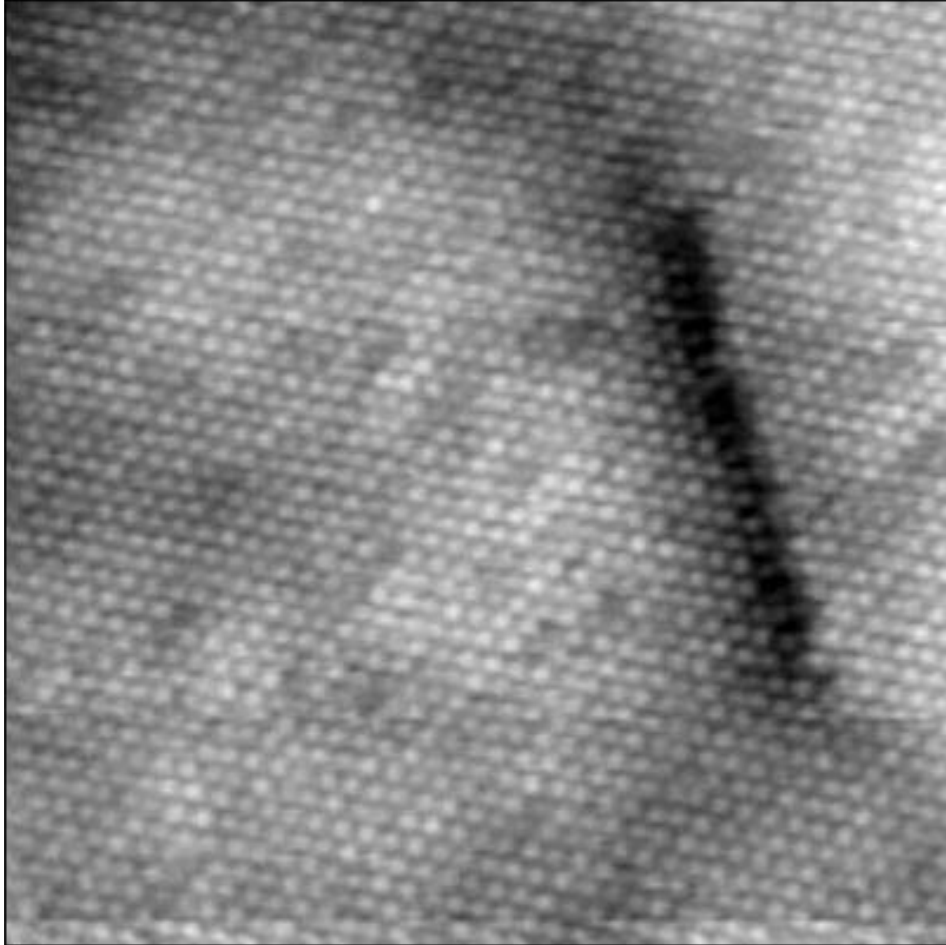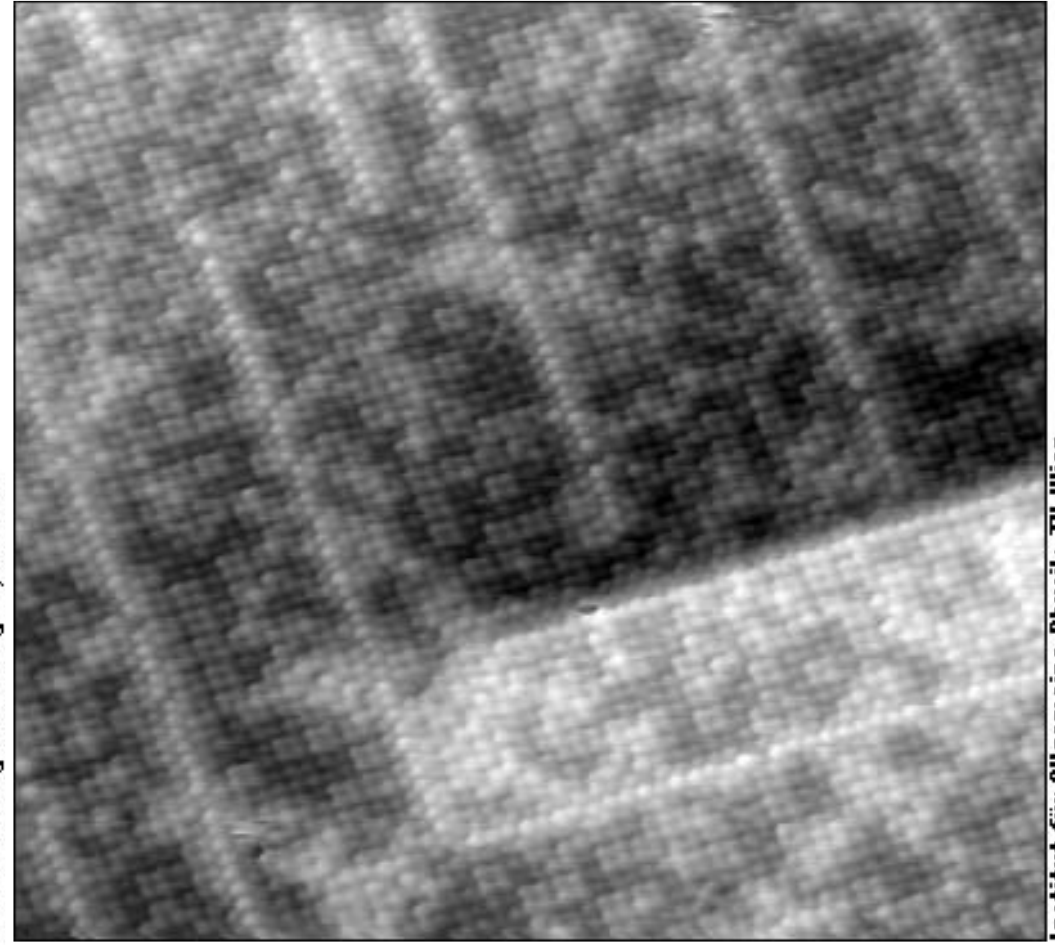sub-grains

0.5 μm
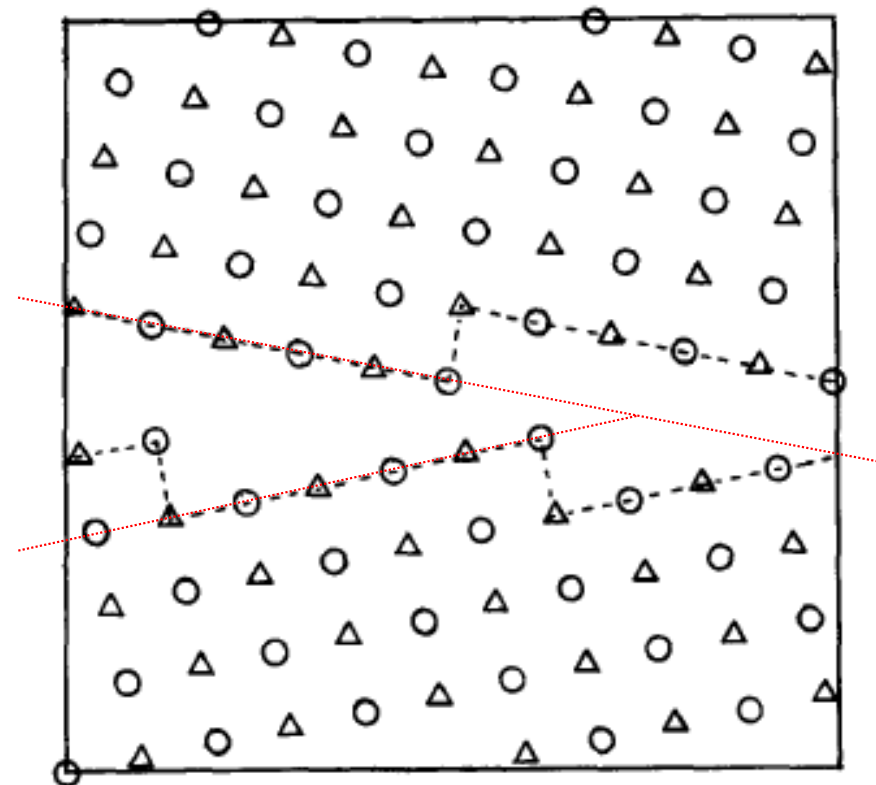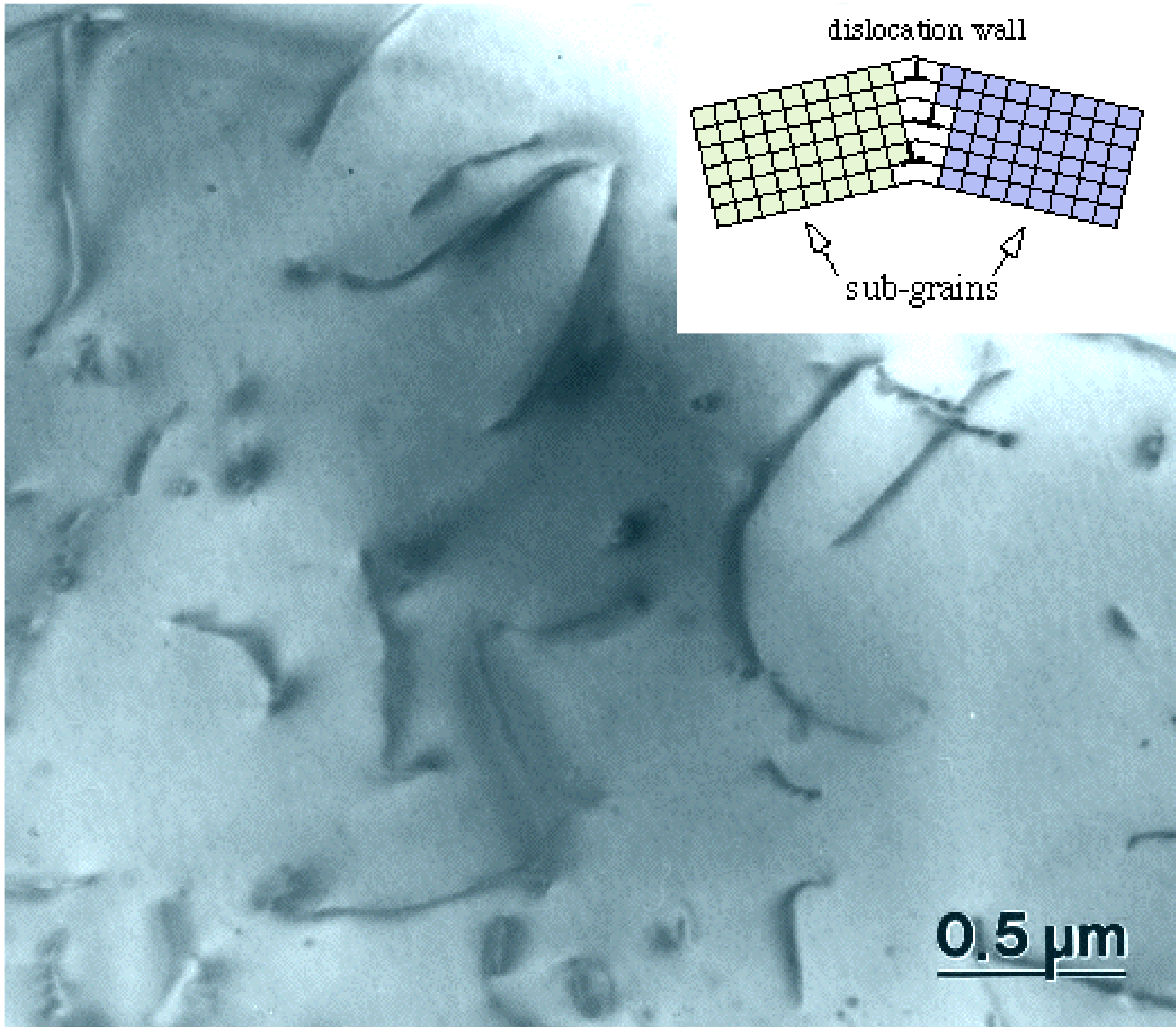
twist Boundaries
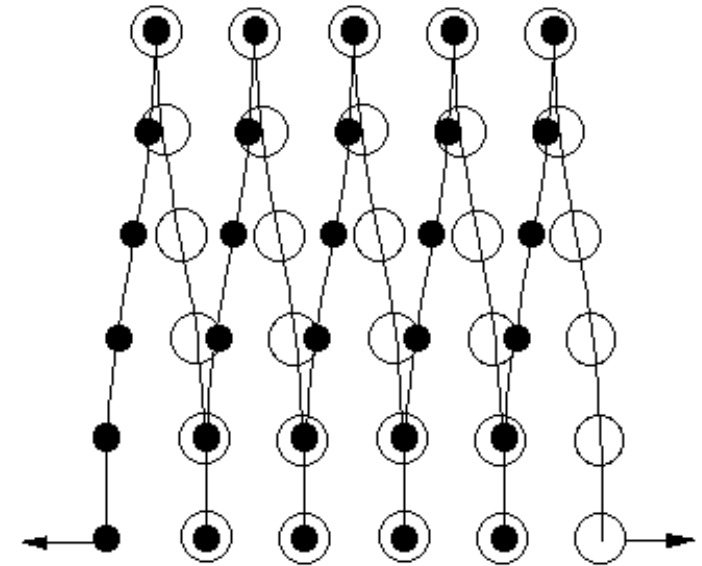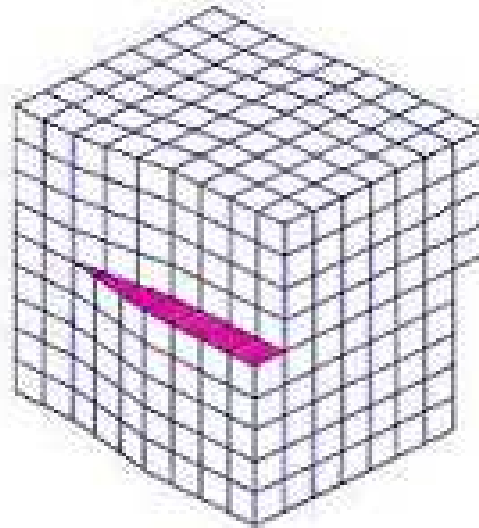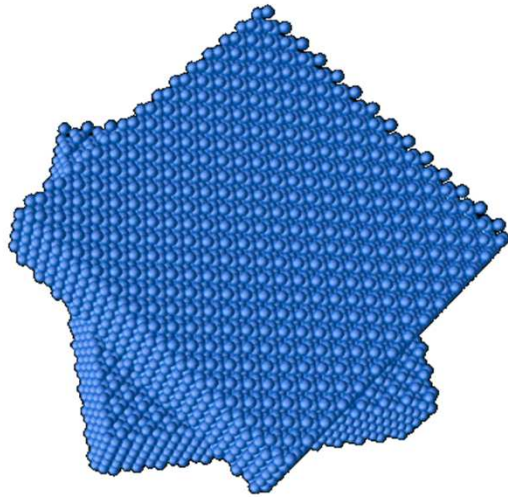
Figure 2. A screw dislocation; note the screw-like 'slip' of atoms in the upper part of the lattice
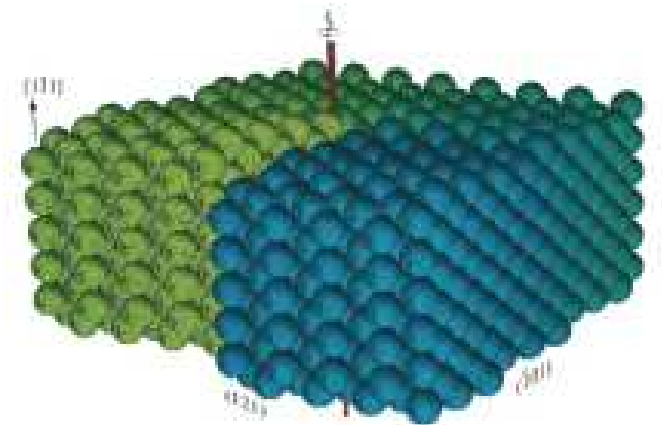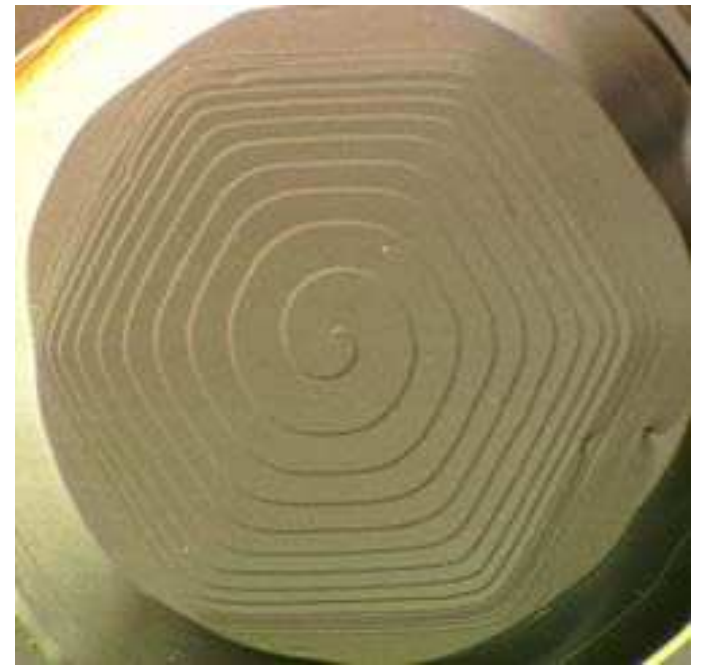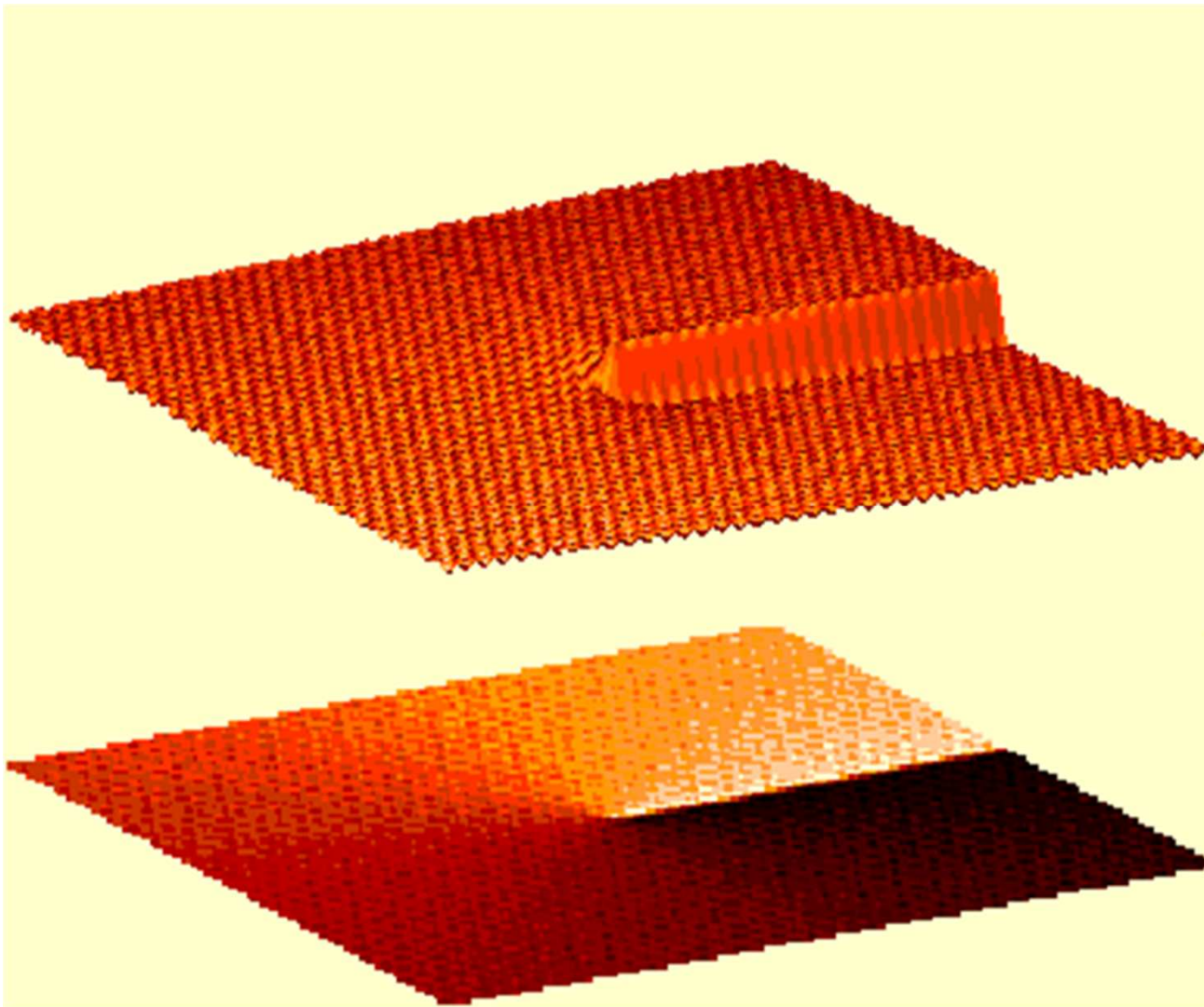
Screw dislocation

Institut für Allgemeine Physik, TU Wien

Institut für Allgemeine Physik, TU Wien

Growth of Screw dislocation

**In general boundaries of a mixture of the tilt and twist type,
→ several sets of different edges and screw dislocations.**

**If the boundary is unsymmetrical, dislocations with different
burgers vectors are required to accommodate the "misfit".**
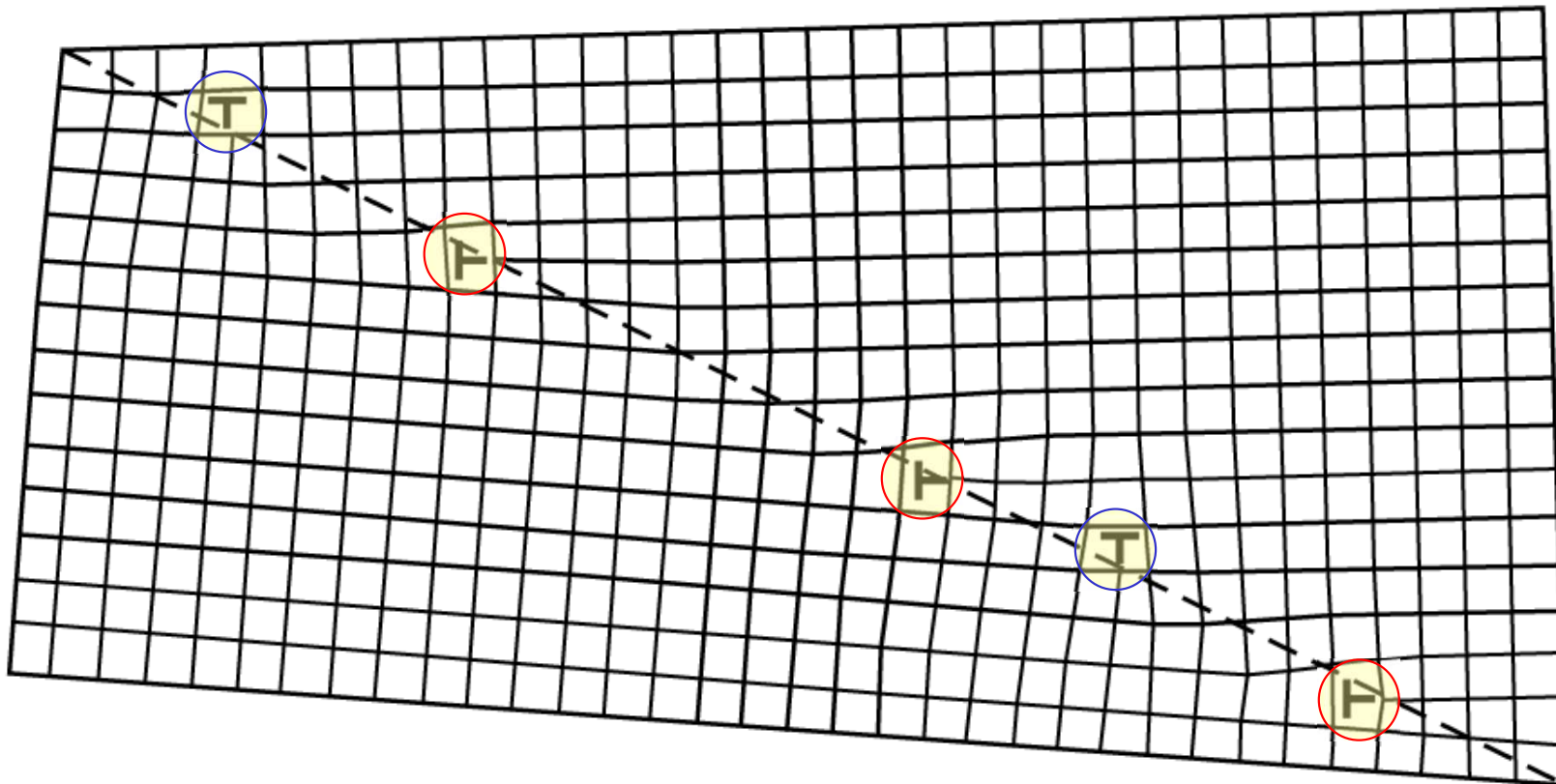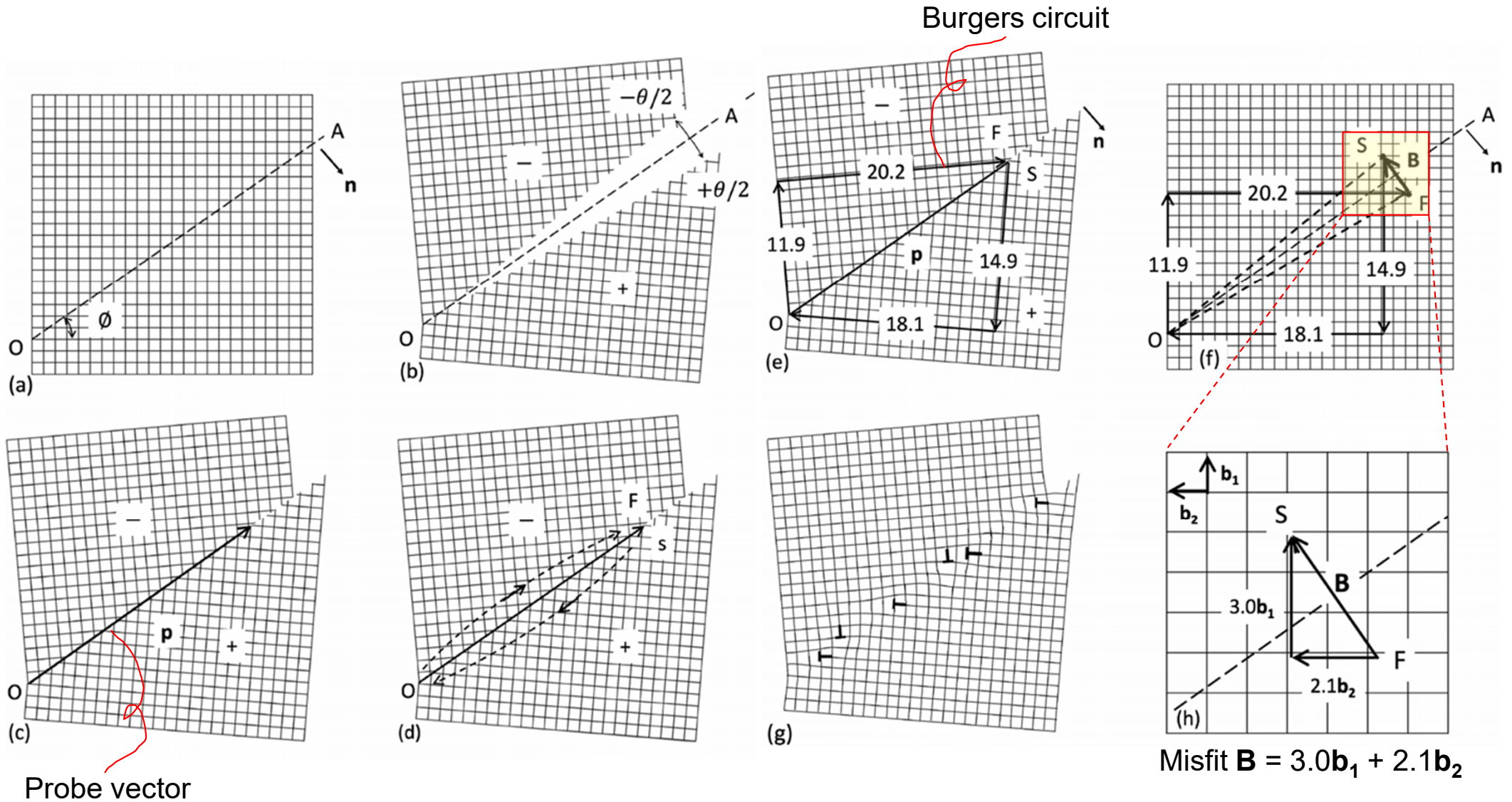
Non-symmetric Tilt Boundary

Fig. An unsymmetrical tilt boundary. Dislocations with two different Burgers vectors are present.

17

# Fig. 3.11 The formation and dislocation content of an asymmetric tilt boundary.

Burgers circuit

Probe vector

Misfit $\mathbf{B} = 3.0\mathbf{b_1} + 2.1\mathbf{b_2}$

Boundary crossed by $\mathbf{P}$ contains three dislocation with burgers vector $\mathbf{b_1}$ and two dislocation with $\mathbf{b_2}$.
→ A vector $10\mathbf{P}$ will be intersected by 51 dislocations.

$$\mathbf{B} = |\mathbf{p}| \cdot 2\sin\left(\frac{\theta}{2}\right) \cong |\mathbf{p}| \cdot \theta \text{ (for small value of } \theta) \quad \text{or} \quad \mathbf{B} = \sum_i n_i b_i$$

18

3.4.1 Low-Angle and High-Angle Boundaries

Low-Angle Tilt Boundaries
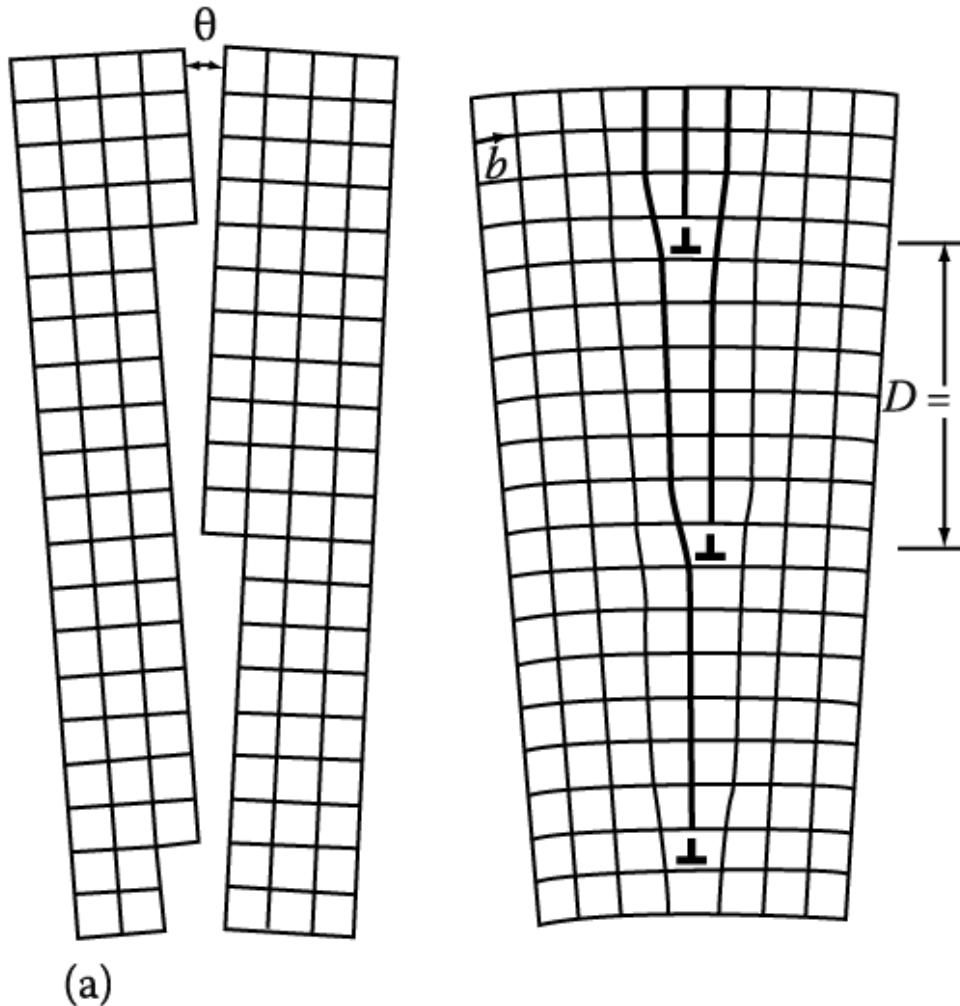
→ **around edge dislocation : strain ↑**

but, LATB ~ almost perfect matching

Burgers vector of the dislocations

$$\sin \frac{\theta}{2} = \frac{b/2}{D}$$

$$\sin \frac{\theta}{2} \approx \frac{\theta}{2}$$

Angular mis-orientation across the boundary

$$D \cong \frac{\vec{b}}{\theta}$$

(a)

Energy of LATB ~ Total E of the dislocations within unit area of boundary

~ depends on the spacing of the dislocations (D)

(For brevity, the distinction between internal E and free E will usually not be made from now)

3.4.1 Low-Angle and High-Angle Boundaries

Low-Angle Tilt Boundaries

(a)
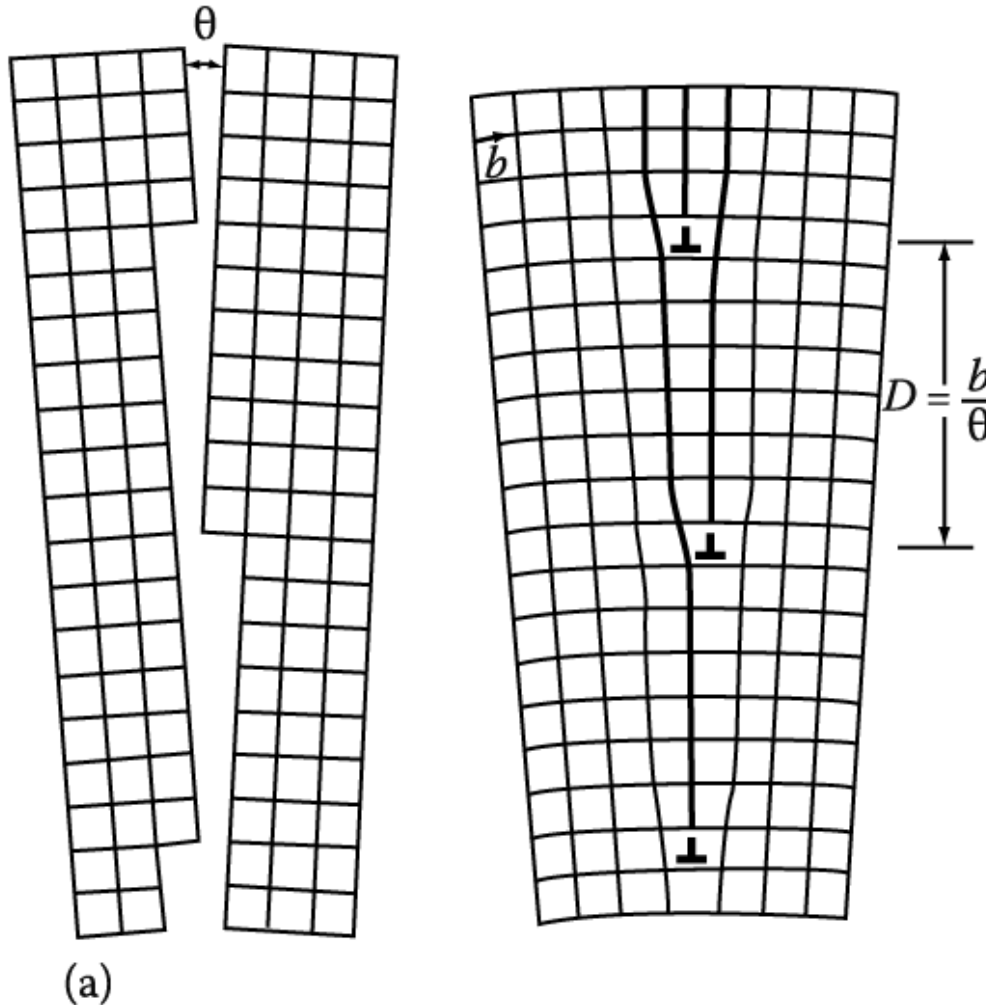
→ **around edge dislocation : strain ↑**

but, LATB ~ almost perfect matching

→ **g.b. energy : $\gamma_{g.b.}$ → E /unit area**

(energy induced from dis.)

* Relation between D and γ ?

Sinθ = $\overrightarrow{b}$/D , at low angle Very small θ →
Very large D

→ **D=$\overrightarrow{b}$/θ → $\gamma_{g.b.}$ is proportional to 1/D**

→ **Density of edge dislocation in low**
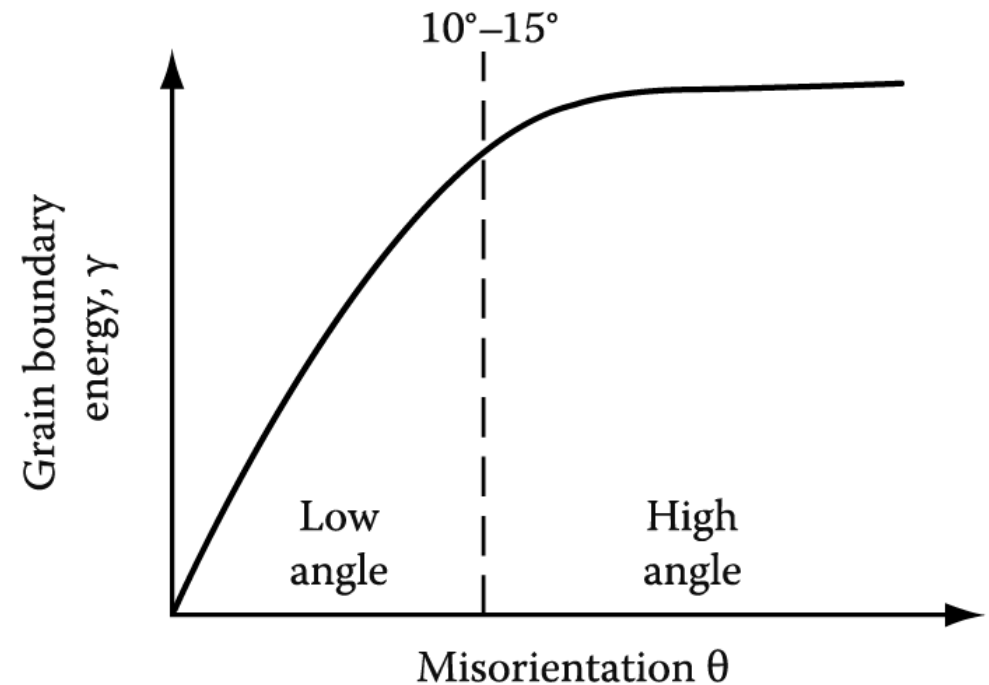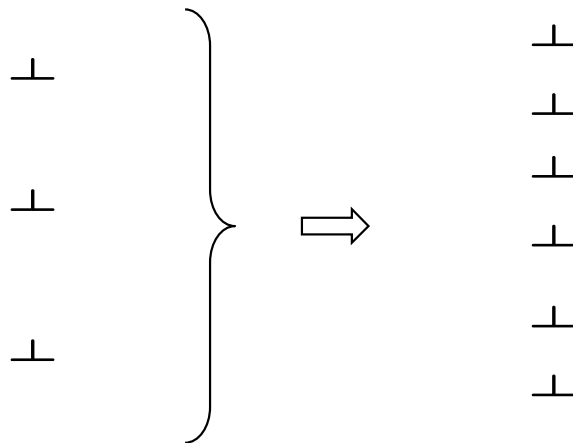
angle tilt boundary $\boxed{\gamma \propto \theta}$

(cf. low angle twist boundary → screw dis.)

Energy of LATB ~ total energy of the dislocations within unit area of boundary

~ depends on the spacing of the dislocation (D)

Low-Angle tilt Boundaries

$\boxed{\gamma \propto \theta}$

$\Longrightarrow$ **1) As θ increases, $\gamma_{g.b.}$ ↑**

Grain boundary energy, γ vs Misorientation θ — 10°–15°, Low angle, High angle

Strain field overlap

→ cancel out

→ **2) $\gamma_{g.b.}$ increases and the increasing rate of γ (=d γ/d θ) decreases.**

→ **3) if θ increases further, it is impossible to physically identify the individual dislocations**

→ **4) When θ > 10°-15°, increasing rate of $\gamma_{g.b.}$ ~ 0**

5) When θ > 10°-15°, Grain-boundary energy ~ almost independent of misorientation

Soap Bubble Model Structural difference between low-angle and high angle grain boundary
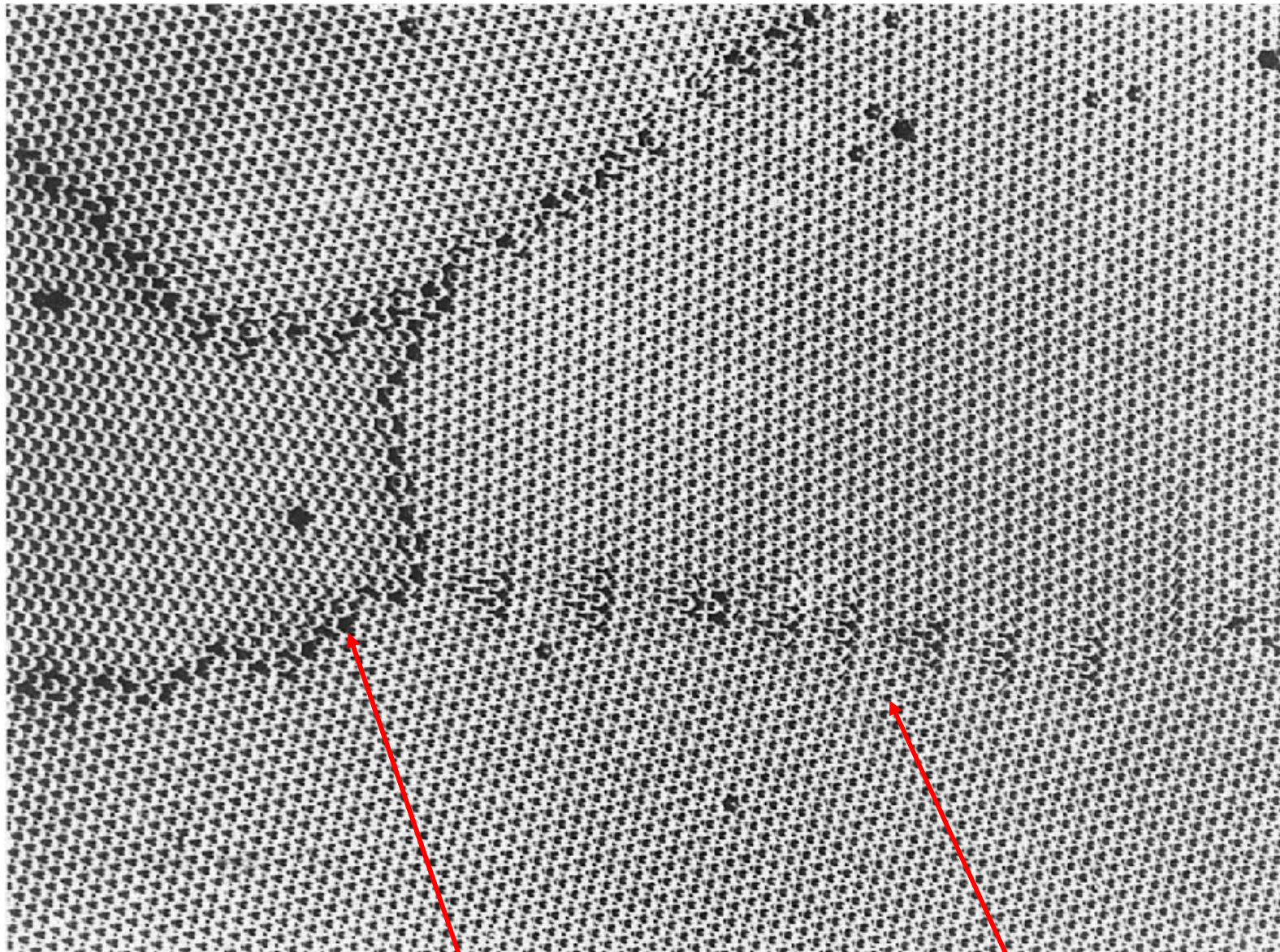

Fig. 3.12 Rafts of soap bubbles showing several grains of varying misorientation. Note that the boundary with the smallest misorientation is made up of a row of dislocations, whereas the high-angle boundaries have a disordered structure in which individual dislocations cannot be identified.

Fit very well/ very little free volume/ slightly distorted

Large area of poor fit/relatively open structure/highly distorted

22

High Angle Grain Boundary: θ > 10°-15°

Grain-
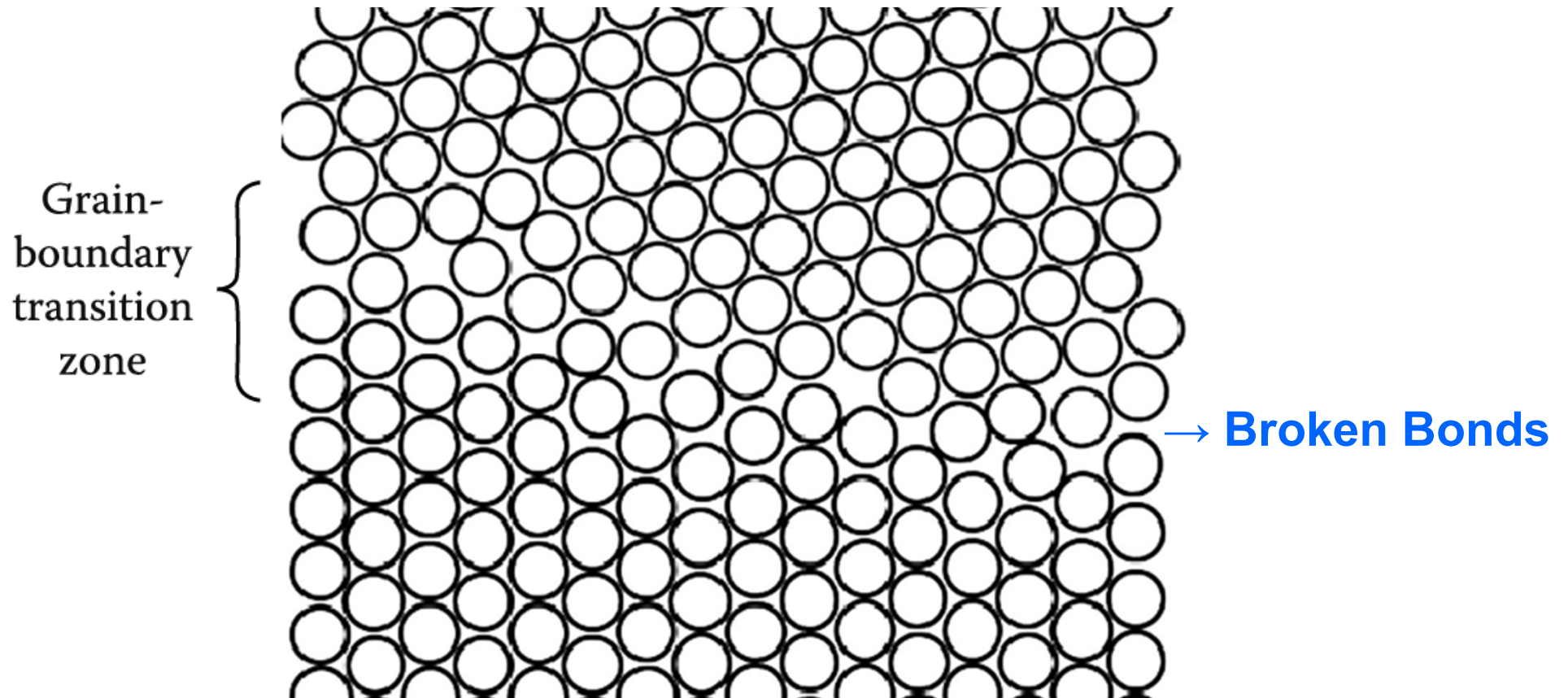boundary
transition
zone

→ **Broken Bonds**

Fig. 3.13 Disordered grain boundary structure (schematic). Misorientation 17°.

High angle boundaries contain large areas of poor fit and have a relatively open structure.

→ high energy, high diffusivity, high mobility (**cf. gb segregation**)

High Angle Grain Boundary

Low angle boundary

→ almost perfect matching (except dislocation part)

High angle boundary (almost)

→ open structure, large free volume

* low and high angle boundary

high angle $\gamma_{g.b.} \approx 1/3 \, \gamma_{S/V.}$ → Broken Bonds

Measured high-angle grain boundary energies

Crystal	γ (mJ m^{-2})	T (°C)	γ_b/γ_{sv}
Sn	164	223	0.24
Al	324	450	0.30
Ag	375	950	0.33
Au	378	1000	0.27
Cu	625	925	0.36
γ-Fe	756	1350	0.40
δ-Fe	468	1450	0.23
Pt	660	1300	0.29
W	1080	2000	0.41

* Like $\gamma_{S/V}$, γ_b is temperature dependent decreasing somewhat with increasing temperature.

Q: Grain boundary (α/ α interfaces)

= Boundaries in Single-Phase Solids

(a) Low-Angle and High-Angle Boundaries

(b) Special High-Angle Grain Boundaries

(c) Equilibrium in Polycrystalline Materials

<u>Not all high-angle grain boundaries have a disordered atomic structure.</u>
For certain axis-angle pairs and grain boundary planes, it is possible to have grain boundaries with fewer broken bonds and a less open structure.

⟹ **Special high angle grain boundary = formation of CLS** (coincident site lattice)

• symmetrical tilt boundary

   ~38.2 °

• a small group of

   atoms are repeated

   regular intervals

   along the boundary.
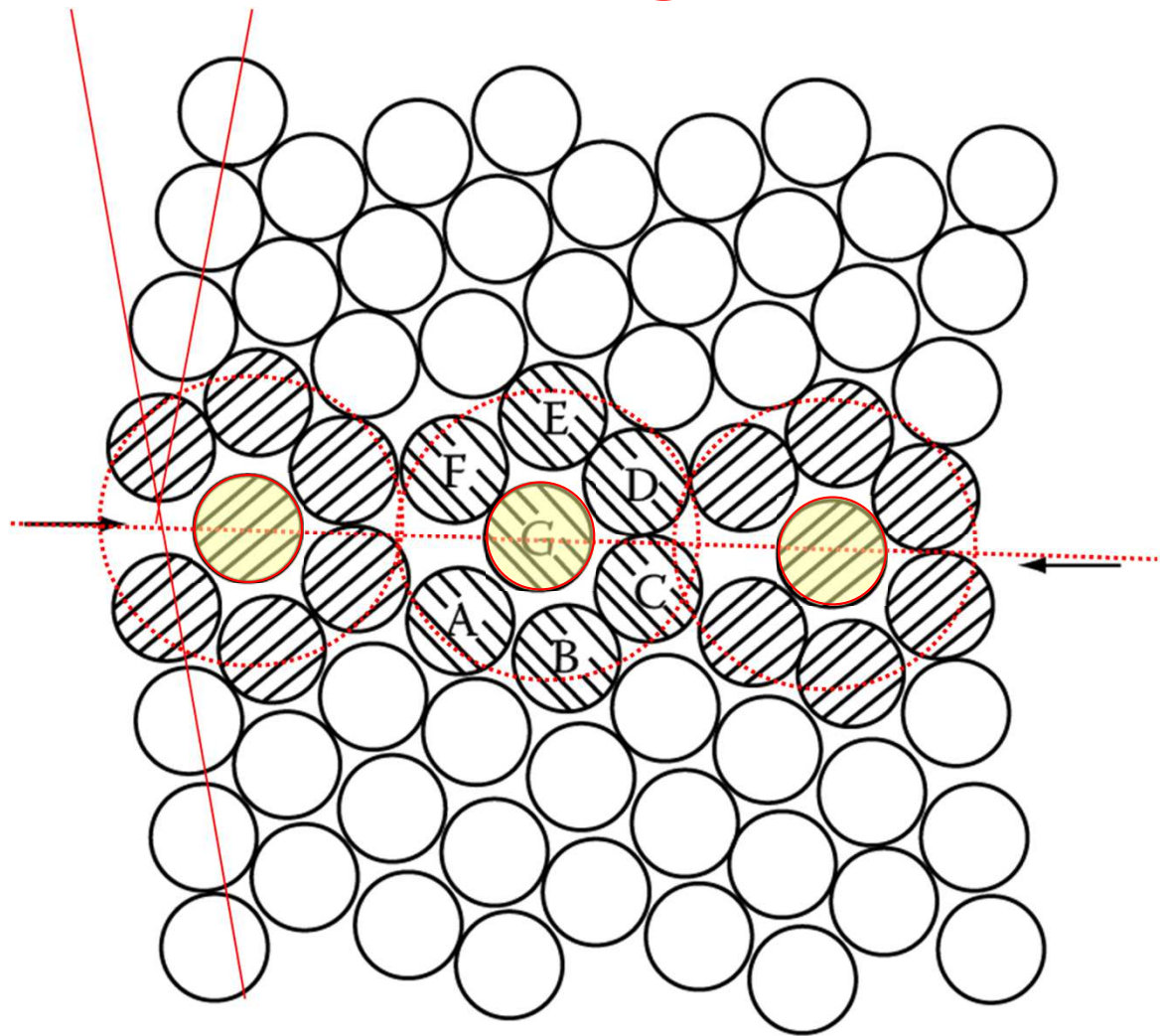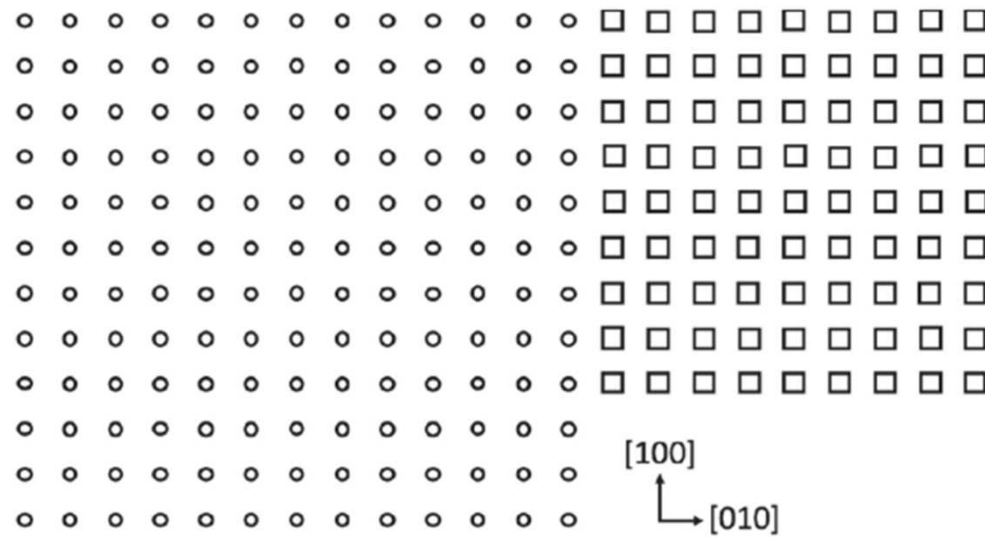
   ~relatively little free volume

Fig. Special grain boundary: two dimensional example.

입계의 원자구조가 주위의 격자와 폭넓게 잘 일치 됨

26

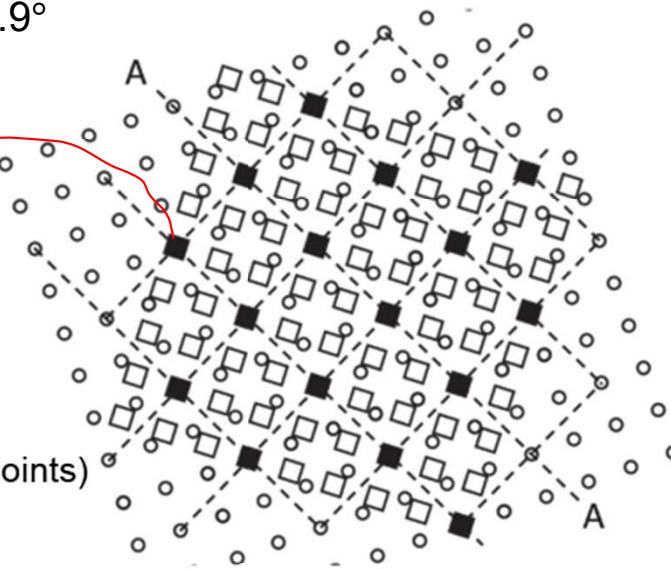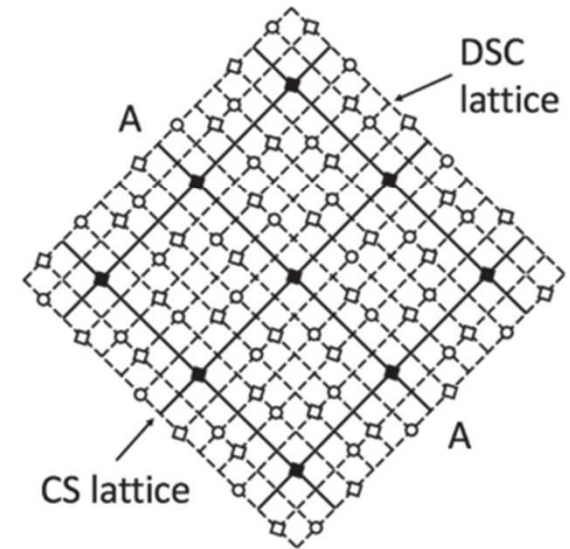Two cubic crystal lattices with the same lattice parameter

[100]

[010]

(a)

Rotated by 36.9°

CLS
(coincident site lattice)

One CSL point out of a total of five lattice points for either lattice = Greek uppercase sigma $\Sigma = 5$ (inverse of the relative density of CSL points)

A

A

(b)

DSC lattice

A

A

CS lattice

(c)

FIGURE 3.14 (a) Two-dimensional section perpendicular to [001] through two cubic crystal lattices with the same lattice parameter. Lattice points are identified by circles and squares to aid their identification. (b) The lattices have been rotated by 36.9° with respect to each other and superimposed to form a dichromatic pattern. The filled squares mark the positions where the lattice points coincide. The dashed lines mark the square $\Sigma 5$ CSL. (c) An enlarged detail of four CSL unit cells with the square DSC lattice marked by dashed lines.

27

The CSL just describes the orientation relationship between the lattices of the two grains.

The CSL points are positioned on the grain boundary depends on the orientation of the boundary with respect to the CSL.

For $\Sigma = 5$, highest possible density of CSL points
~ along the line AA

Referring to the unit cell of the simple cubic lattice Denoted by the open circles, the line AA corresponds to the plane (210).

To specify the crystallography of a special grain boundary: to give **CSL and axis-angle pair** concerned together with the orientation of the grain boundary plain in each grain

$$\Sigma = 5 \,(210)36.9°/[001]$$

Displacement shift complete

DSC lattice
(Dotted line)

A

CS lattice
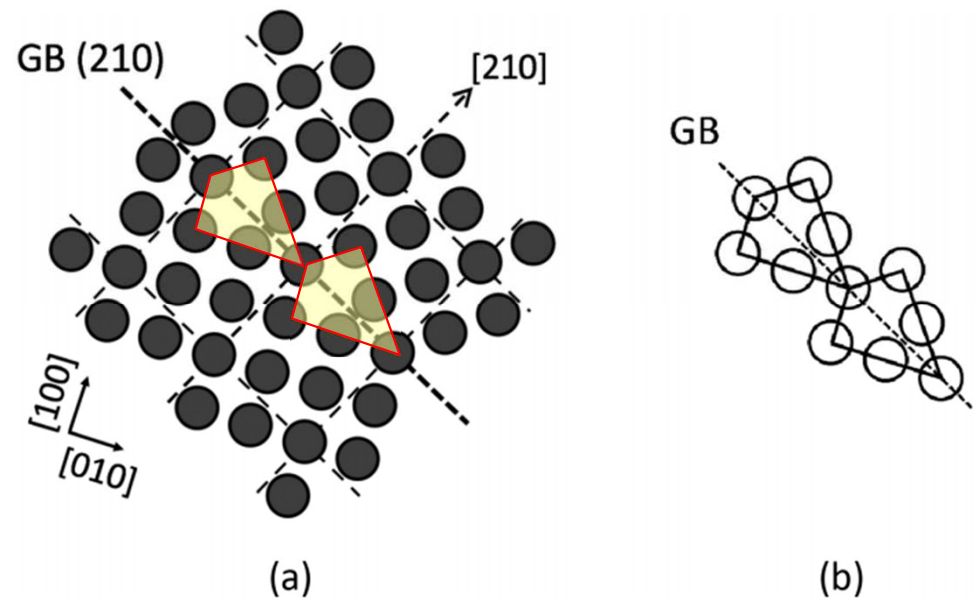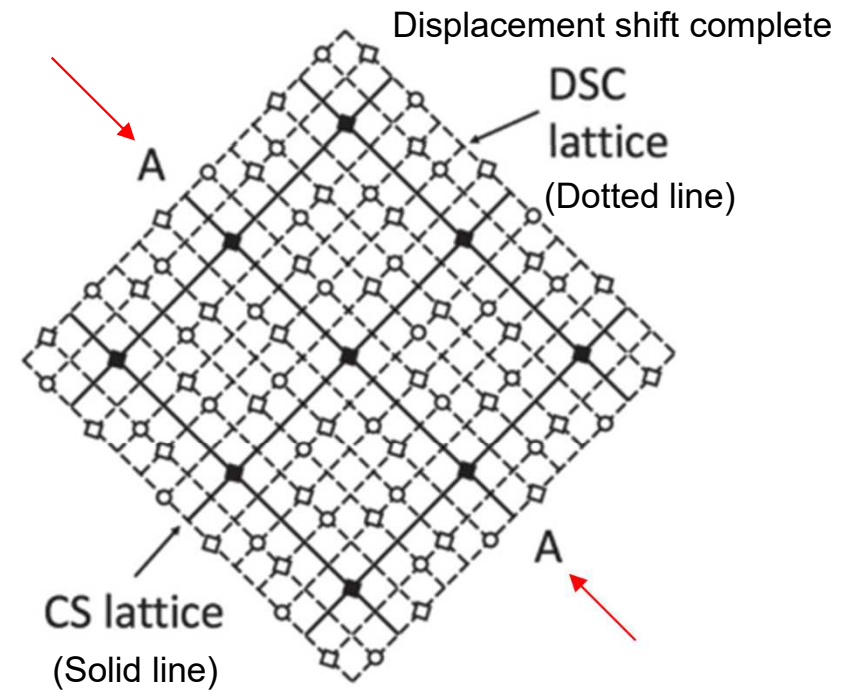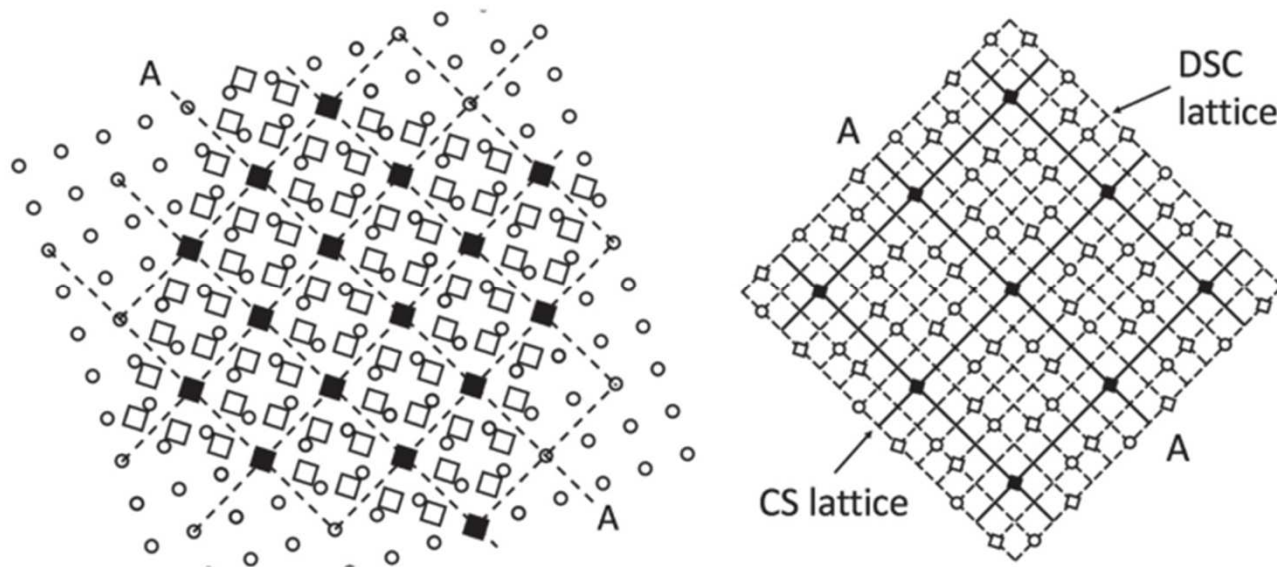(Solid line)

A

GB (210)

[210]

GB

[100]

[010]

(a)

(b)

FIGURE 3.15 (a) The atomic structure of a grain boundary formed by dividing the lattices in Figure 3.14 along the line AA, i.e., the (210) plane of the lower grain, and locating one atom at each lattice point in both grains. (b) A detail showing a possible atomic structural unit that repeats itself along the boundary concerned.

- The dislocations that take up the deviation from a perfect CSL orientation can have **very small Burgers vectors** when compared to dislocation in the lattice of the grains.
  = magnitudes equal to the length of the sides of the fine square mesh $(=\frac{1}{5}[\bar{1}20])$ in Fig 3.14(c)

- Small angle grain boundary ~ showing small angular deviations from a $\Sigma 1$

The CSL and DSC lattice correspond to the crystal lattices, and the Burgers vectors of the grain boundary dislocations have the same magnitudes as the crystal lattice vectors.

- In the case of low angle grain boundaries, the dislocations are known as **primary dislocations**, while the dislocations taking up the deviation from the perfect CSL are called **secondary dislocations**. In the case of the CSLs with $\Sigma > 1$, the primary dislocation are so close as to be indistinguishable from each other.

- Σ is always an odd number.

$\Sigma = 1$ means that the two lattices are in the same orientation.

$\Sigma = 3$, two twin-oriented grains with fcc lattices give the next highest density of coincident lattice points.

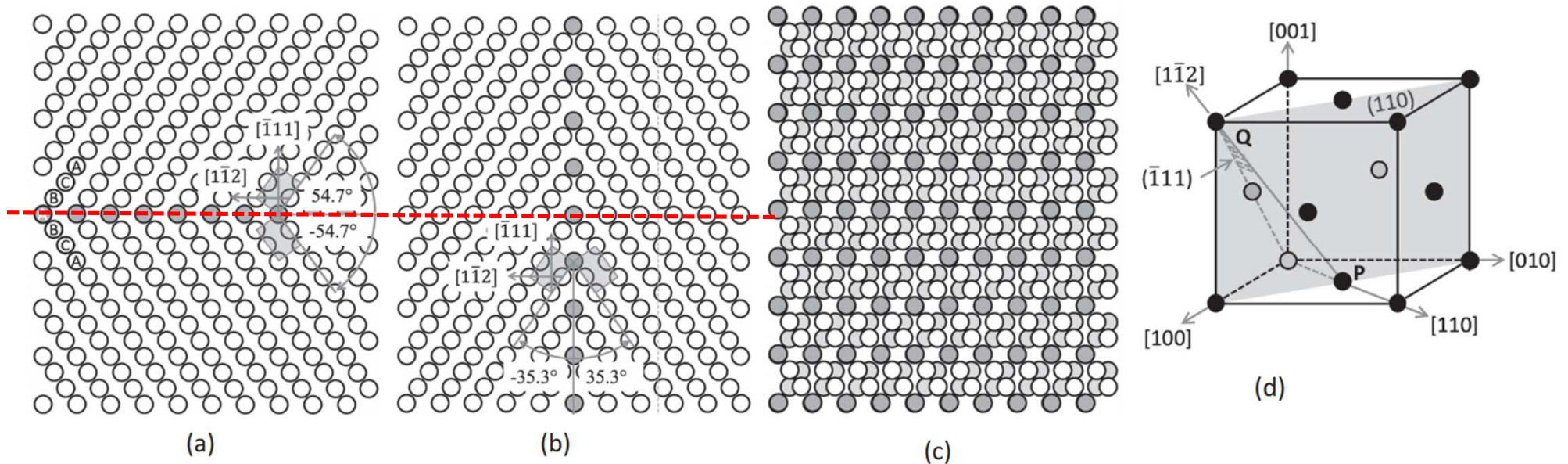Twins are commonly seen in annealed fcc metals and alloys!

FIGURE 3.18 Boundaries in twin-related fcc metals. (a) Coherent twin boundary parallel to $(\bar{1}11)$ as seen from the [110] direction. All atoms in the boundary plane are on coincident lattice sites. Stacking sequence ABCA in each twin is marked. (110) sections through the fcc unit cells of each twin are indicated in grey. (b) Incoherent twin boundary parallel to $(1\bar{1}2)$ as seen from the [110] direction. Only every third boundary site is coincident to both lattices. (c) The dichromatic pattern formed by the two twin lattices. Sites on every third $(\bar{1}11)$ plane are coincident, i.e., $\Sigma = 3$. (d) An fcc unit cell showing relevant planes and directions. Line PQ is the intersection of the planes $(\bar{1}11)$ and (110) and lies in the direction $[1\bar{1}2]$.
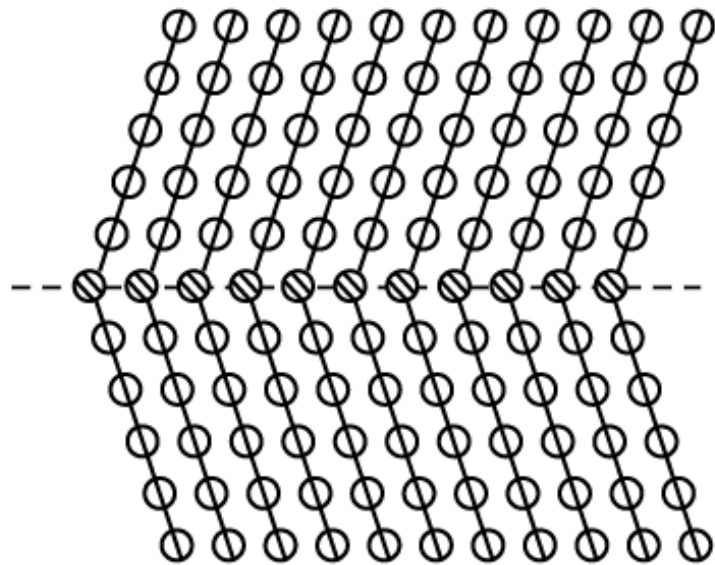
① $\Sigma 3$ CSL from (c)

② coherent vs incoherent twin boundary

30

(b) Special High-Angle Grain Boundaries

: high angle boundary but with low $\gamma_{g.b.}$.

Twin boundary ≠ coherent twinning plane

a) **Coherent twin boundary**
symmetric twin boundary

$\rightarrow$ **low** $\gamma_{g.b.}$.

**Atoms in the boundary
are essentially in
undistorted positions**
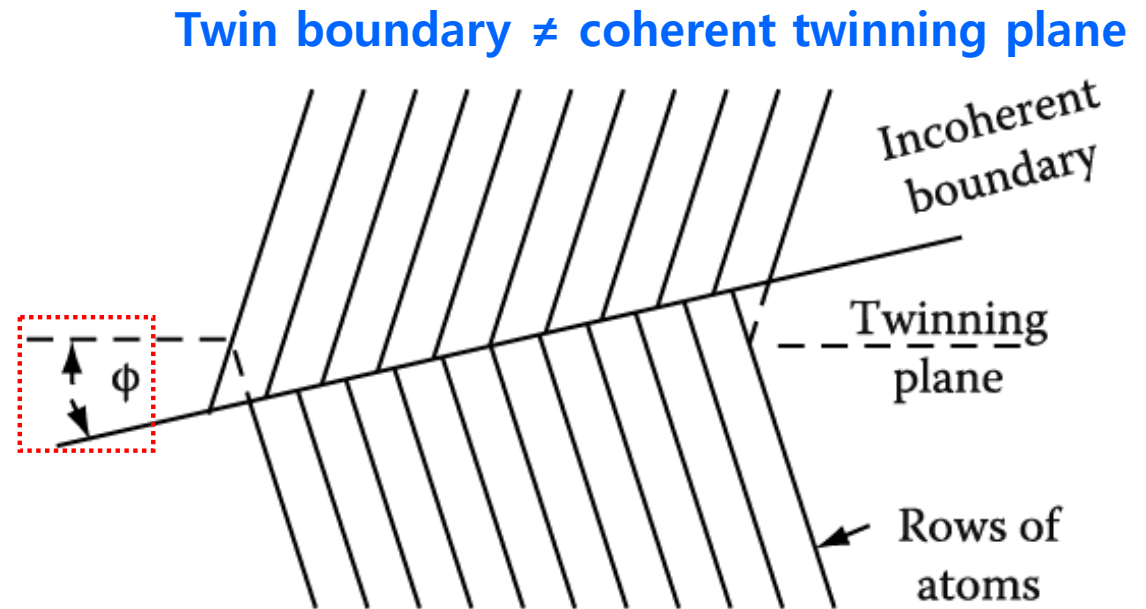
b) **Incoherent twin boundary**
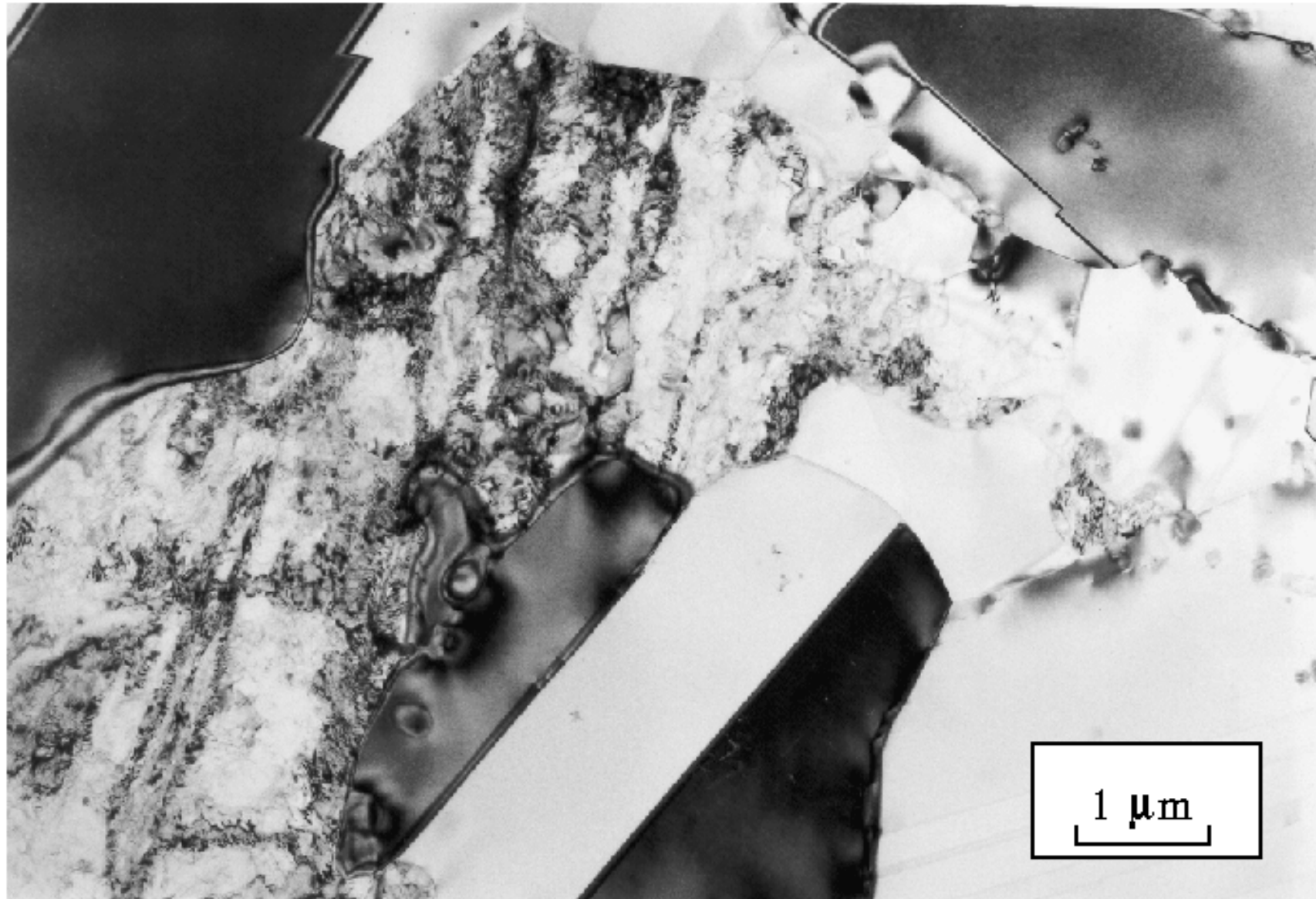**asymmetric twin boundary**

$\rightarrow$ **low** $\gamma_{g.b.}$.

**Energy of twin boundary~
very sensitive to the orienta-
tion φ of the boundary plane**

31

Twin boundary

200 nm
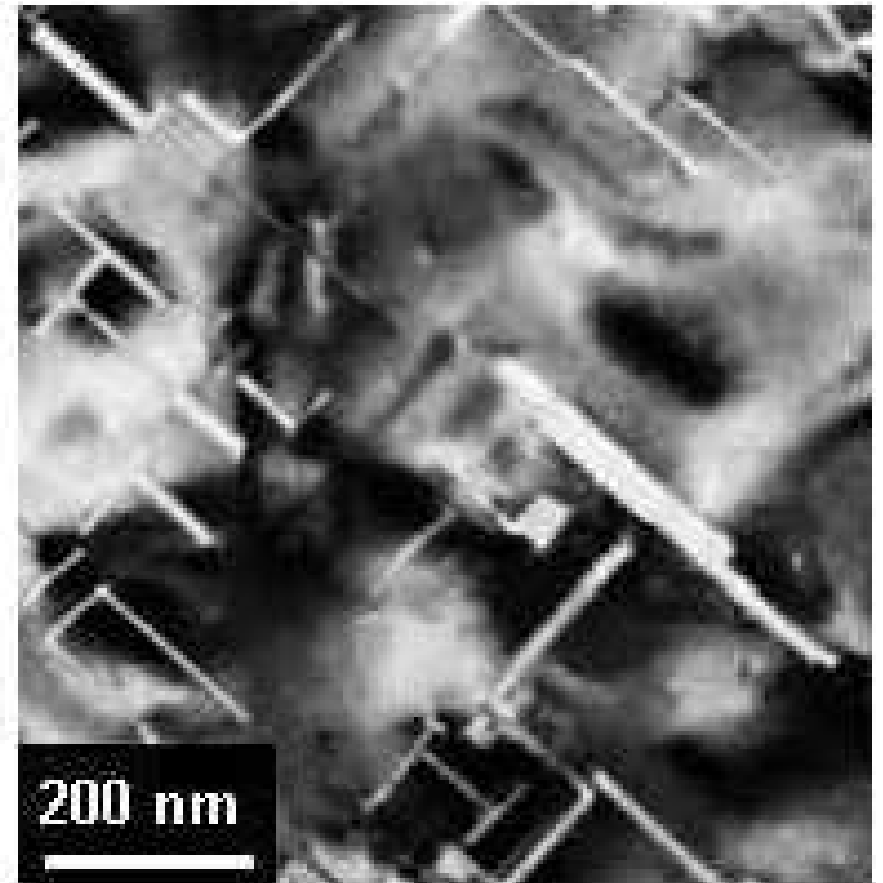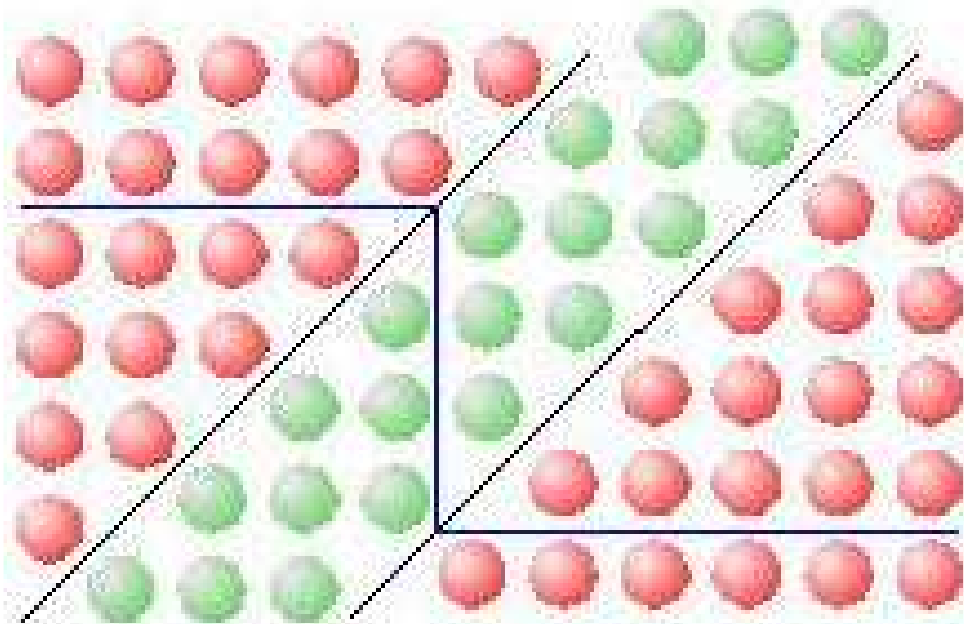
Twin boundary

Twin boundary
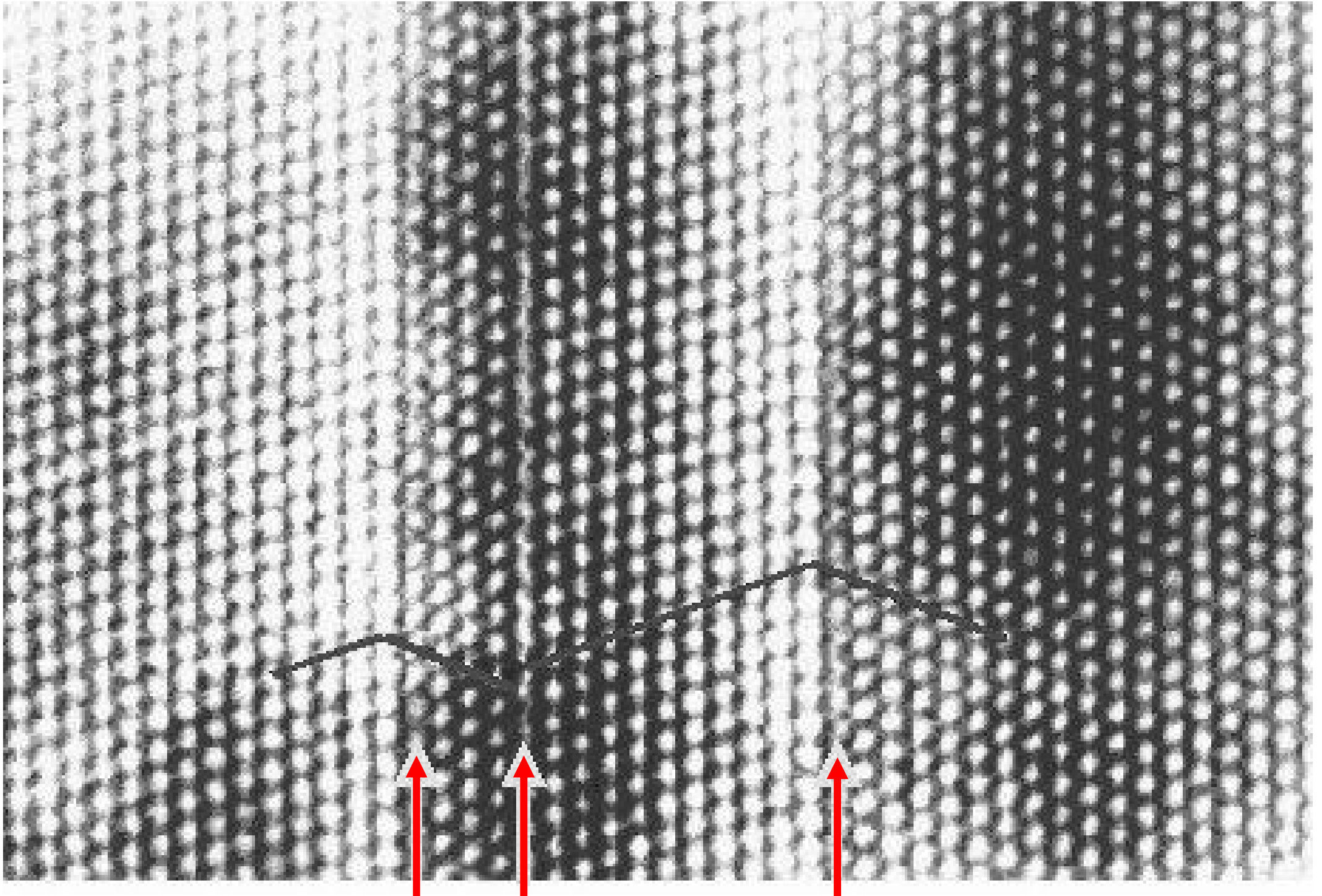
(b) Special High-Angle Grain Boundaries

c) Twin boundary energy as a function of the grain boundary orientation

(c)

Table 3.3 Measured Boundary Free Energies for Crystals in Twin Relationships

(Units mJ/m^2)

Crystal	Coherent Twin-Boundary Energy		Incoherent Twin-Boundary Energy		Grain-Boundary Energy
Cu	21		498		623
Ag	8	<<	126	<	377
Fe-Cr-Ni (stainless steel type 304)	19		209		835

3.4.3 Grain Boundary Energy of Pure Metals

① $\boxed{\gamma \propto \theta}$ & Most high angle GB~ same E
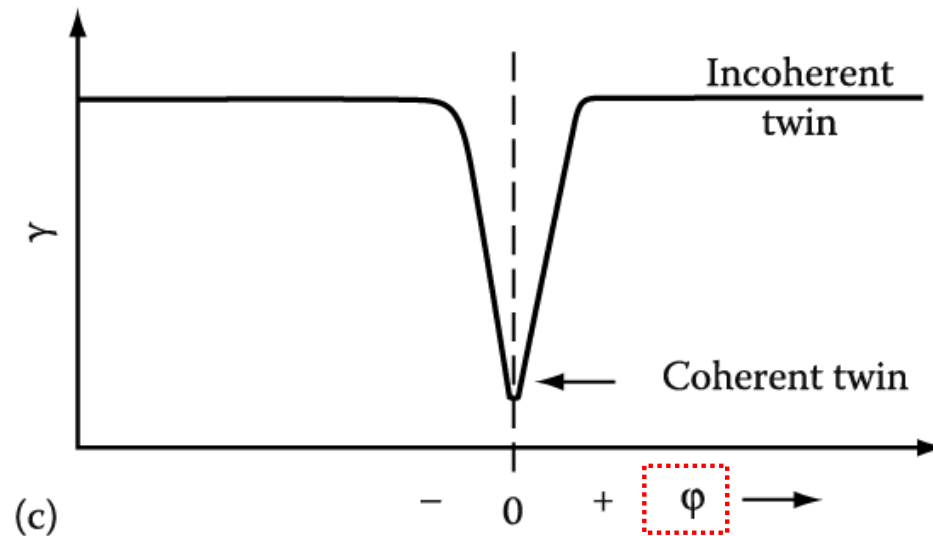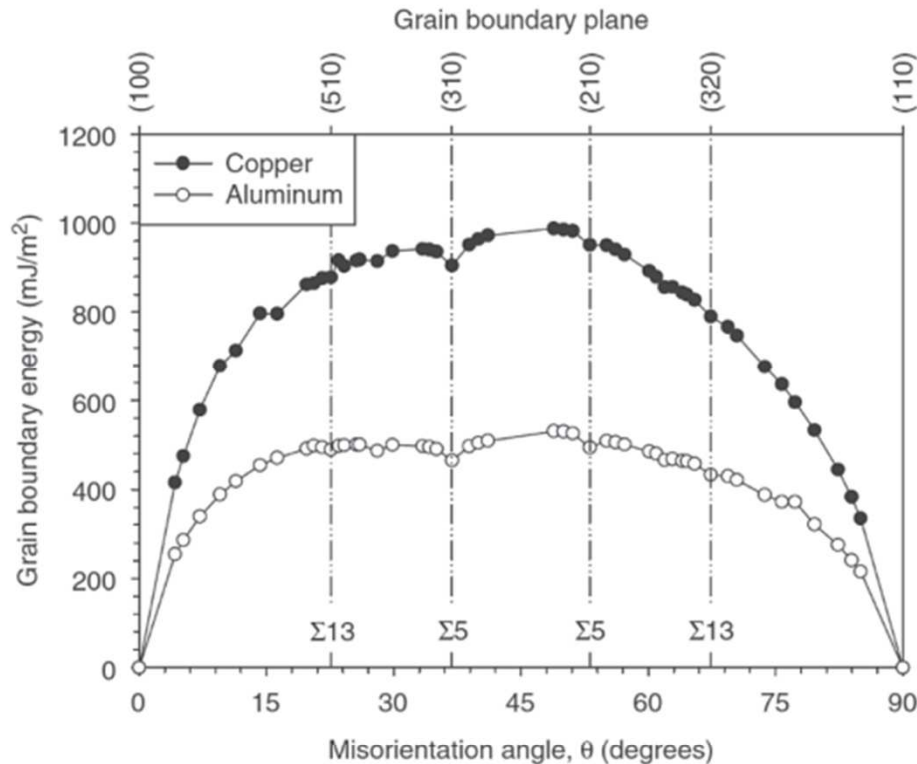
Coherent twin boundary: $\Sigma 3$ boundary at the misorientation angle of $109.5°(=2\times54.74°)$

② $\gamma_{Cu} > \gamma_{Al} (\because T_{m,Cu}(strong\ bond\ E) > T_{m,Al})$ **vs** $\gamma_{Cu} \approx \gamma_{Al}$ at $\Sigma 3 (\because SFE_{Cu} < SFE_{,Al})$
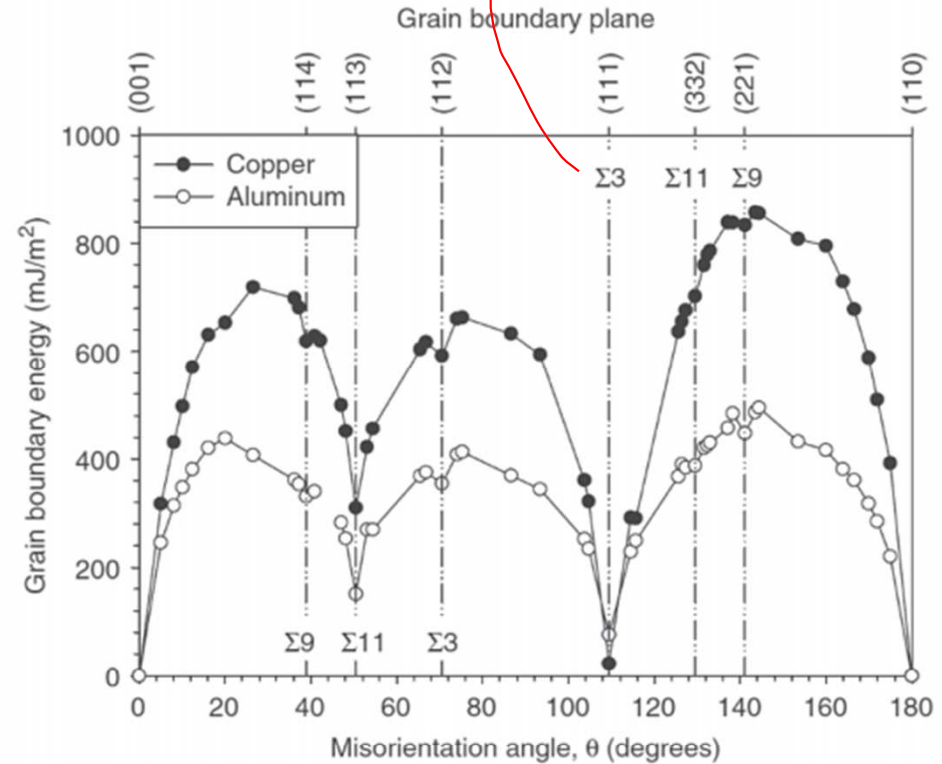
FIGURE 3.19 Energies of symmetric tilt boundaries in aluminum and copper at 0 K calculated using interatomic energies. (a) Rotation axis [001], (b) rotation axis $[1\bar{1}0]$. (Reprinted from M. A. Tschopp & D. L. McDowell, Asymmetric tilt grain boundary structure and energy in copper and aluminium, *Philosophical Magazine*, 87:3871–3892 (2007) with permission from Taylor and Francis.)

Asymmetrical Incoherent Twin Boundary (AITB)

"Stepped structure"

= Step of SITB and terrace of CTB

$$\gamma_{AITB} = \gamma_{CTB} \cdot cos\emptyset + \gamma_{SITB} \cdot sin\emptyset$$

~ relatively low γ
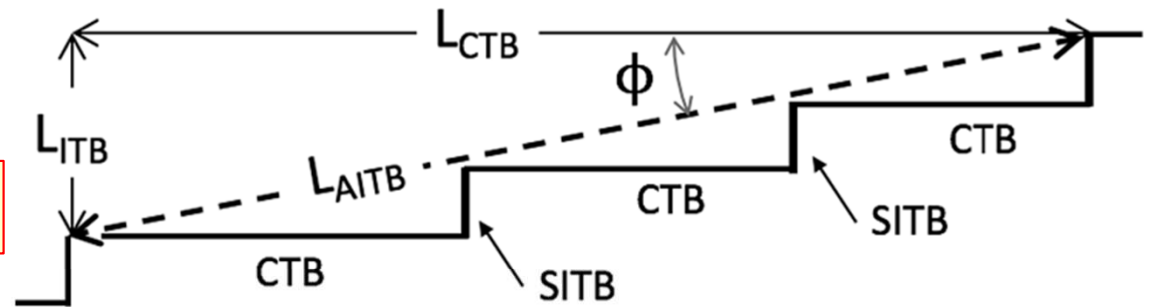
FIGURE 3.20   The step and terrace structure of an incoherent twin boundary inclined at an angle $\emptyset$ to the CTB. SITB, symmetrical twin boundary; AITB asymmetric twin boundary.

SITB = symmetrical incoherent twin boundary **CTB** = symmetrical twin boundary
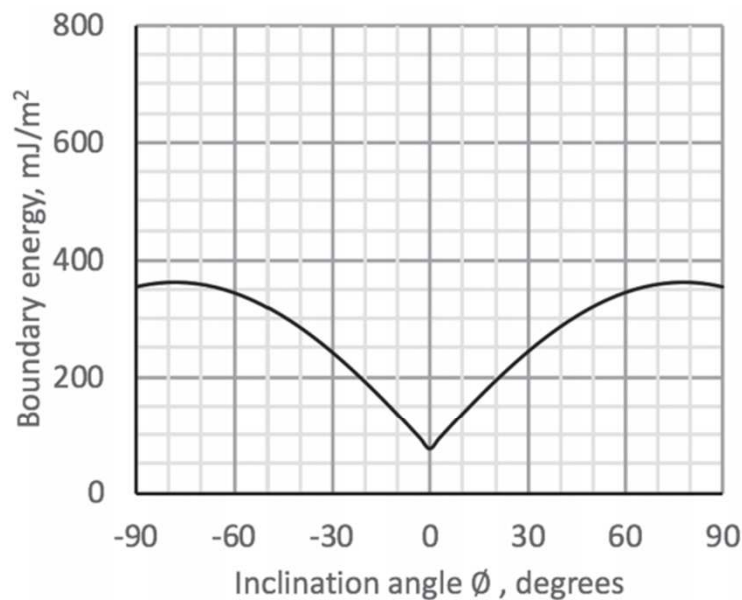
(a)
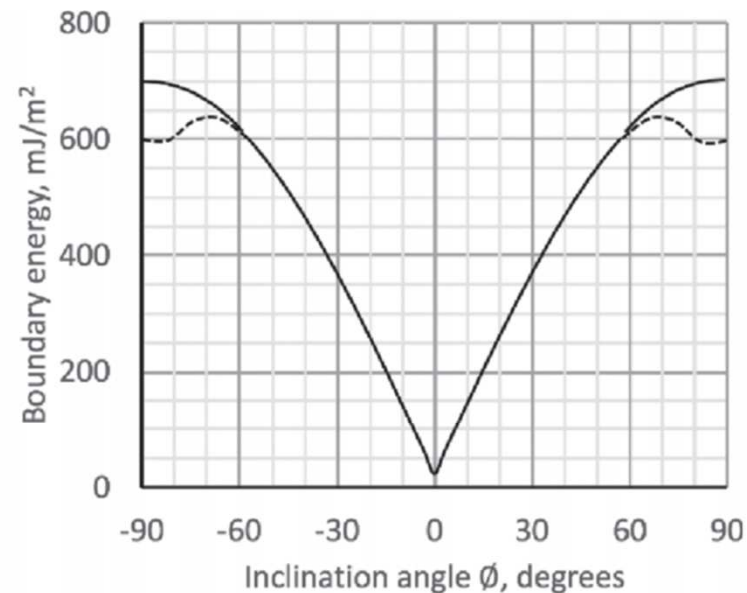
(b)

FIGURE 3.21   Asymmetric tilt boundary energies at 0 K predicted using Equation 3.16. (a) Aluminum with $\gamma_{CTB} = 75.2 \, mJ/m^2$ and $\gamma_{SITB} = 354.4 \, mJ/m^2$. (b) Copper $\gamma_{CTB} = 22.2 \, mJ/m^2$ and $\gamma_{SITB} = 700 \, mJ/m^2$ as given in reference. In the case of copper above 60° inclination, atomic model-ling (*ab initio*) calculations indicate a deviation from Equation 3.16 as shown by the dashed line.

37

- **Special high-angle grain boundaries with relatively low energies ~ associated with CSL orientations btw grains**/ not correlate with CSL density along the boundary

- **GB free energy (~H) decrease with increasing temperature due to entropy effect.**

  Atomic calculations show that the energy of a grain boundary decrease by **about two-thirds between 0 K and the melting point**.

- **Width of the grain boundary (~activation energy for grain boundary diffusion) changes depending on temperature.**

- **Grain boundary energies** scale in proportion to the shear modulus multiplied by the lattice parameter. (∵ Grain boundaries ~ comprising various dislocation networks – the line energy of dislocations scales as the shear modulus) & Grain boundary energy correlates with the melting temperature (~bond strength).

3.4.4 Grain boundary energy of dilute binary alloys

- **Grain boundary energy can be expected to change on alloying.**
  There will be a higher concentration of solute at the GBs, and the interaction of the strain files of the solute and boundary will lower the GB energy.

  A simple way to modelling GB segregation is to treat the boundary as a separate phase.

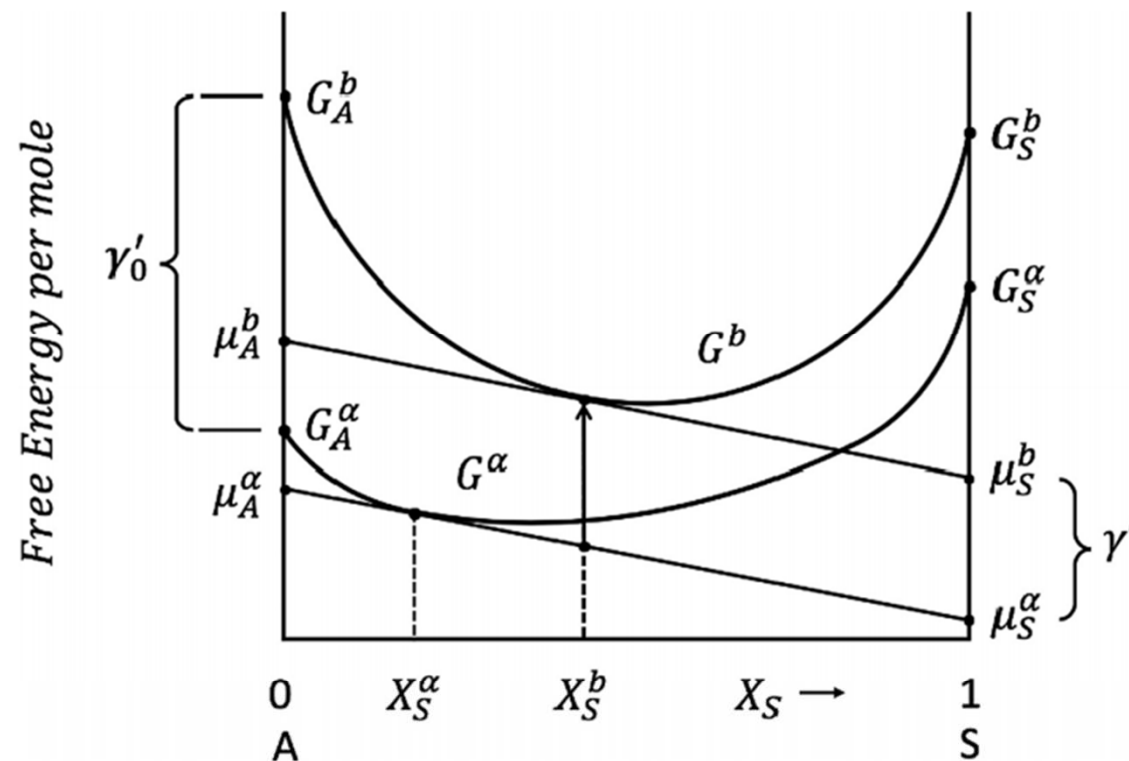**FIGURE 3.22** Free energy diagram for solid α phase and grain boundary phase b for a binary alloy of A containing solute S. X_S^α is the mole fraction of solute in the α grain and X_S^b is the content in the grain boundary. γ_0' is the grain boundary energy of pure A and the length of the vertical arrow (distance between the tangents), γ', the grain boundary energy of the alloy.

A grain phase α and a boundary phase b,
If we transfer dN_A moles of solvent A and dN_S moles of solute S from the grain to the GB,

(3.17) $dG' = (\mu_A^b - \mu_A^\alpha)dN_A - (\mu_S^b - \mu_S^\alpha)dN_S = 0$ ($\because$ Metastable equilibrium btw grain and GB)

If total quantity of atoms in the boundary is constant, $\qquad dN_A + dN_S = 0$

(3.18) $\therefore (\mu_A^b - \mu_A^\alpha) = (\mu_S^b - \mu_S^\alpha)$

If we assume that the grain and boundary phase follow the regular solution model,

(3.19) $\mu_A^\alpha = G_A^\alpha + \Omega^\alpha (1 - X_A^\alpha)^2 + RT \ln X_A^\alpha$ $\qquad \mu_A^b = G_A^b + \Omega^b (1 - X_A^b)^2 + RT \ln X_A^b$

$\mu_S^\alpha = G_S^\alpha + \Omega^\alpha (1 - X_S^\alpha)^2 + RT \ln X_S^\alpha$ $\qquad \mu_S^b = G_S^b + \Omega^b (1 - X_S^b)^2 + RT \ln X_S^b$

where, Ω^α and Ω^b : the difference in A-A and A-S bond energies in the grain and GB,
and $X_A + X_S = 1$ for each phase.

(3.20) $\Delta G_b = (G_S^b - G_S^\alpha) - (G_A^b - G_A^\alpha) + (\Omega^b - \Omega^\alpha)$ $\Rightarrow$ (3.21) $\dfrac{X_S^b}{(1 - X_S^b)} = \dfrac{X_S^\alpha}{(1 - X_S^\alpha)} exp\left\{\dfrac{-\Delta G_b}{RT}\right\}$

then substituting Equations (3.19) into Equation (3.18)
and ignoring small terms:

If X_S^α and X_S^b are small, the terms $(1 - X_S^\alpha)$ and $(1 - X_S^b)$ can be ignored:

(3.22) $\boxed{X_S^b \approx \dfrac{X_S^\alpha exp\{-\Delta G_b/RT\}}{1 + X_S^\alpha exp\{-\Delta G_b/RT\}}}$

Here, ΔG_b=Gibbs energy of segregation
~usually negative (In regular solution, strong A-S bonding in the GB, week A-S bonding in the α phase, In real solution, increasing size misfit btw solute and matrix; varies with temp. and atomic structure (misorientation btw the grains and the orientation of the GB plane)

Solute tends to segregate to the boundary to reduce the overall free energy of the system

$$\text{(3.21)} \quad \frac{X_S^b}{(1 - X_S^b)} = \frac{X_S^\alpha}{(1 - X_S^\alpha)} exp\left\{\frac{-\Delta G_b}{RT}\right\}$$

If X_S^α and X_S^b are small, the terms $(1 - X_S^\alpha)$ and $(1 - X_S^b)$ can be ignored:

$$\text{(3.22)} \quad X_S^b \approx \frac{X_S^\alpha exp\{-\Delta G_b/RT\}}{1 + X_S^\alpha exp\{-\Delta G_b/RT\}}$$

Here, ΔG_b=Gibbs energy of segregation
~usually negative (In regular solution, strong A-S bonding in the GB, week A-S bonding in the α phase, In real solution, increasing size misfit btw solute and matrix; varies with temp. and atomic structure (misorientation btw the grains and the orientation of the GB plane)

Solute tends to segregate to the boundary to reduce the overall free energy of the system

- Equations (3.21) and (3.22) show how **grain boundary segregation decreases as temperature increases**, i.e., the solute 'evaporates' into the matrix.

- **A large size misfit btw the solute and matrix** leads to a low solubility of the solute in the matrix → ΔG_b becomes more negative and GB segregation becomes stronger as the solubility of the solute decreases

- GB enrichment ratio, X_S^b/X_S^α tends to increase as the solubility of the solute in the matrix decrease. In the case of low solubilities, X_S^b/X_S^α can be several orders of magnitude in size reaching even 10^4 for example in the case of carbon and boron in bcc ferritic iron.

Derive an expression for how GB segregation affects the GB energy.

: the GB energy is the decrease in free energy that occurs if the atoms in the boundary rearrange themselves into the crystal structure of the α phase $((\mu_A^b \text{ and } \mu_S^b) \rightarrow (\mu_A^\alpha \text{ and } \mu_S^\alpha))$

If there are n_A^b moles of A atoms and n_S^b moles of S atoms in the boundary, the decrease in free energy is:

$$n_A^b(\mu_A^b - \mu_A^\alpha) + n_S^b(\mu_S^b - \mu_S^\alpha) = (n_A^b + n_S^b)(\mu_A^b - \mu_A^\alpha) = n^b(\mu_A^b - \mu_A^\alpha)$$

where, n^b is the total number of moles of boundary $(n_A^b + n_S^b)$

$\therefore$ GB energy per mole : $(\mu_A^b - \mu_A^\alpha) = (\mu_S^b - \mu_S^\alpha) = \gamma'$

GB energy per unit area $\boxed{\gamma = (\mu_A^b - \mu_A^\alpha)\delta/V_m^b \quad \text{J/m}^2}$ (3.23)

Fig. 3.22

where, δ is the thickness of the boundary phase and V_m^b is the molar volume of the boundary, assumed to be independent of the boundary composition. V_m^b/δ is the area of GB containing 1 mole.

In a similar way,
GB energy per mole for pure A is γ_0', i.e., $G_A^b - G_A^\alpha$ and per unit area $\boxed{\gamma_0 = (G_A^b - G_A^\alpha)\delta/V_m^b \quad \text{J/m}^2}$

(3.24)

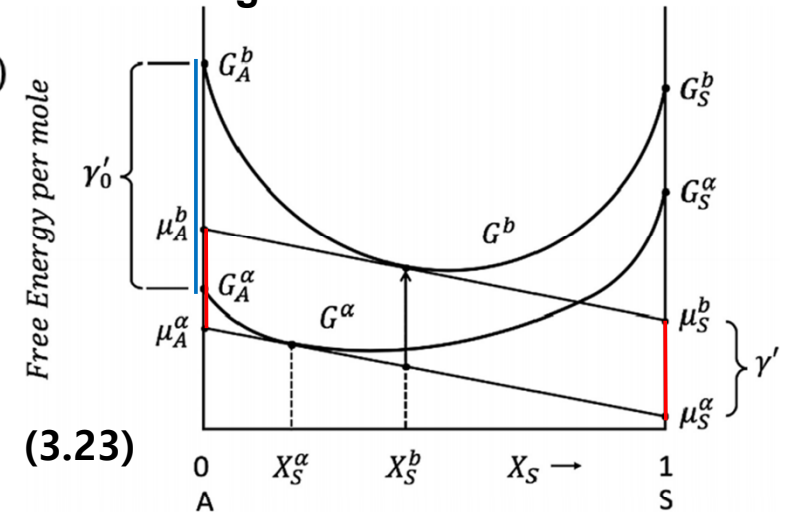**GB energy for binary alloys** $\gamma = \gamma_0 - \dfrac{\delta RT}{V_m^b} \ln\{1 + X_S^\alpha \exp(-\Delta G_b/RT)\}$ (3.25)

Since $\ln(1+x) \rightarrow x$ as $x \rightarrow 0$, for very dilute solutions, i.e., metals containing impurities
The rate of change of GB energy with increasing X_S^α is given by

$$\frac{\partial \gamma}{\partial X_S^\alpha} = -\frac{\delta RT}{V_m^b} \exp(-\Delta G_b/RT)\}$$ (3.26)

42

GB energy for binary alloys $\gamma = \gamma_0 - \dfrac{\delta RT}{V_m^b} \ln \{1 + X_S^\alpha \exp(-\Delta G_b/RT)\}$ (3.25)

Since $\ln (1+x) \rightarrow x$ as $x \rightarrow 0$, for very dilute solutions, i.e., metals containing impurities
The rate of change of GB energy with increasing X_S^α is given by

$$\frac{\partial \gamma}{\partial X_S^\alpha} = -\frac{\delta RT}{V_m^b} \exp(-\Delta G_b/RT)\}$$ (3.26)

- **The stronger the tendency for solute or impurities to segregate to the grain boundary, the greater is the reduction in the GB energy.** Note that, in the case of impurity contents, is essential the same as the total impurity content in the alloy.

For example, Putting δ=0.75 nm, V_m^b=7 cm³, R =8.314 J/mol·K and T=773 K (500 ℃) gives X_S^α = 1,650 J/m² for ΔG_b= -50 kJ/mol, which is a strong free energy of segregation.

In such a case, **an addition of just 0.0001 mole fraction (0.01 atomic %) would reduce the GB energy by 165 mJ/m², which is an appreciable effect considering that random high-angle GB energies are typically of the order of 1,000 mJ/m².**

Putting the same value of ΔG_b into Equation (3.22) predicts that the enrichment ratio X_S^b / X_S^α is 2,000 giving the mole fraction of solute in the boundary as 0.2.

Contents for today's class

3) Boundaries in Single-Phase Solids
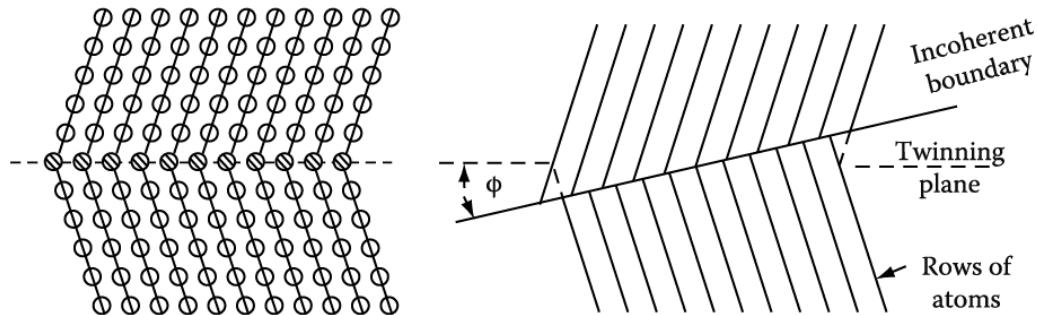
(a) Low-Angle and High-Angle Boundaries

Θ < 15° : **total energy of the dislocations within unit area of boundary**

Θ > 15° : **impossible to physically identify the individual dislocations → strain field overlap → cancel out**

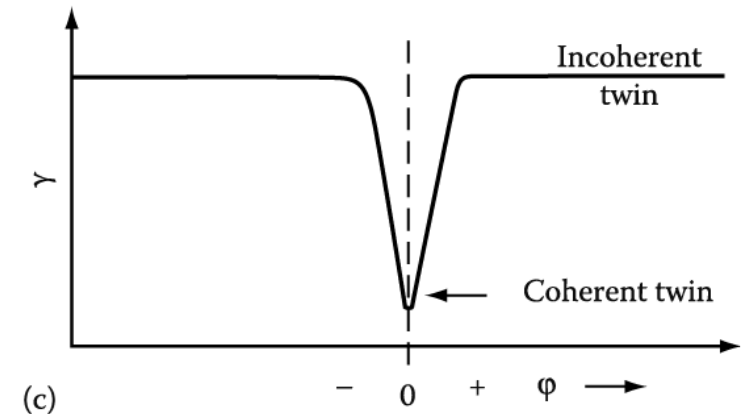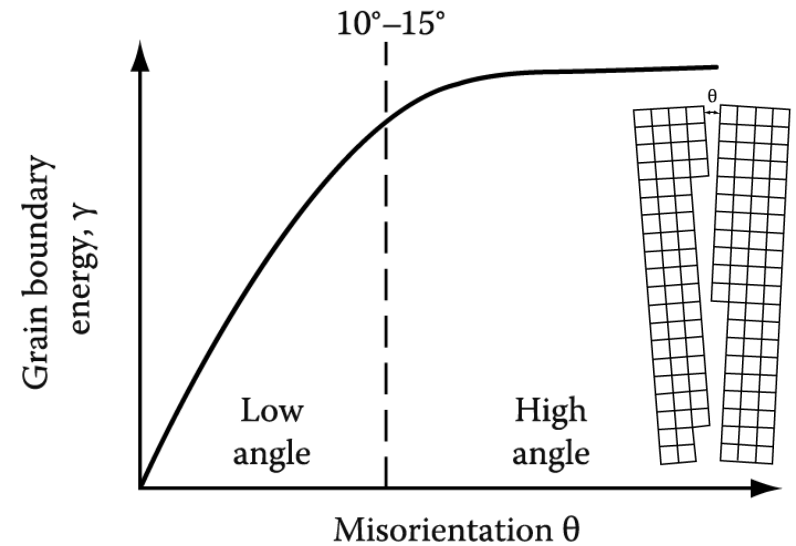**Broken Bonds → high angle $\gamma_{g.b.} \approx 1/3 \; \gamma_{S/V.}$**

(b) Special High-Angle Grain Boundaries

: high angle boundary but with low $\gamma_{g.b.}$

→ **twin boundary**

Atoms in the boundary are essentially in undistorted positions ~relatively little free volume

3.4.4 Grain boundary energy of dilute binary alloys

Solute tends to segregate to the boundary to reduce the overall free energy of the system

$$X_S^b \approx \frac{X_S^\alpha exp\{-\Delta G_b/RT\}}{1 + X_S^\alpha exp\{-\Delta G_b/RT\}}$$

Here, ΔG_b=Gibbs energy of segregation

~usually negative (In regular solution, strong A-S bonding in the GB, week A-S bonding in the α phase, In real solution, increasing size misfit btw solute and matrix; varies with temp. and atomic structure (misorientation btw the grains and the orientation of the GB plane)

GB energy for binary alloys $\gamma = \gamma_0 - \frac{\delta RT}{V_m^b} \ln \{1 + X_S^\alpha exp(-\Delta G_b/RT)\}$ (3.25)

Since $\ln(1+x) \rightarrow x$ as $x \rightarrow 0$, for very dilute solutions, i.e., metals containing impurities
The rate of change of GB energy with increasing X_S^α is given by

$$\frac{\partial \gamma}{\partial X_S^\alpha} = -\frac{\delta RT}{V_m^b} exp(-\Delta G_b/RT)\}$$ (3.26)

- **The stronger the tendency for solute or impurities to segregate to the grain boundary, the greater is the reduction in the GB energy.** Note that, in the case of impurity contents, is essential the same as the total impurity content in the alloy.

For example, Putting δ=0.75 nm, V_m^b=7 cm³, R =8.314 J/mol·K and T=773 K (500 ℃) gives X_S^α = 1,650 J/m² for ΔG_b= -50 kJ/mol, which is a strong free energy of segregation.

In such a case, an addition of just 0.0001 mole fraction (0.01 atomic %) would reduce the GB energy by 165 mJ/m², which is an appreciable effect considering that random **high-angle GB energies are typically of the order of 1,000 mJ/m².**